Protein fibrillization: preparation, mechanism and application

Promotoren:

Prof. dr. ir. R.M. Boom
Hoogleraar Levensmiddelenproceskunde, Wageningen Universiteit

Prof. dr. E. Van der Linden
Hoogleraar Fysica en Fysische Chemie van Levensmiddelen, Wageningen Universiteit

Co-promotoren:

Dr. ir. A.J. Van der Goot
Universitair docent, leerstoelgroep Levensmiddelenproceskunde, Wageningen Universiteit

Dr. P. Venema
Universitair docent, leerstoelgroep Fysica en Fysische Chemie van Levensmiddelen, Wageningen Universiteit

Promotiecommissie:

Prof. dr. A.C.M. Van Hooijdonk (Wageningen Universiteit, Nederland)

Prof. dr. A.M. Hermansson (Swedish Institute for Food and Biotechnology, SIK, Göteborg, Zweden)

Prof. dr. P. Dejmek (Food Engineering, Lund University, Zweden)

Dr. T. Jongsma (Friesland Foods Corporate Research, Deventer, Nederland)

Dit onderzoek is uitgevoerd binnen de onderzoeksschool VLAG.

C. Akkermans

Protein fibrillization: preparation, mechanism and application

Proefschrift
ter verkrijging van de graad van doctor
op gezag van de rector magnificus
van Wageningen Universiteit,
Prof. dr. M.J. Kropff,
in het openbaar te verdedigen
op vrijdag 6 juni 2008
des namiddags te vier uur in de Aula

Cynthia Akkermans
Protein fibrillization: preparation, mechanism and application
Thesis Wageningen University, The Netherlands, 2008 – with Dutch summary

ISBN 978-90-8504-879-4

Contents

Introduction

Chapter 1

PROTEIN FIBRILS

Protein fibrils are a special type of aggregates originating from globular protein molecules. These aggregates have a length in the order of 1 μm and a diameter of 1-10 nm, which means that they are highly anisotropic. Due to their large aspect ratio, protein fibrils could be used as food ingredients to improve the textural properties. Their presence results in an increase in viscosity, shear thinning behaviour, and gelation with a low amount of protein.[1-3]

Many globular proteins of animal and human origin have shown the ability to form these fibrils. Some of these proteins are related to diseases, such as amylin (related to diabetes)[4] and β-amyloid (related to Alzheimer).[5] Examples of food proteins that can form these long fibrils are β-lactoglobulin,[6,7] lysozyme,[8] ovalbumin,[9] and BSA.[10]

APPLICATION OF PROTEIN FIBRILS

There is a need for the development of new functional food ingredients that can be used to modify the textural properties of food products. For many applications, it is desirable to make these new ingredients protein based. Possible applications for the protein fibrils are elucidated by the examples described below.

High protein foods

Protein fibrils might be used to improve the textural properties of high protein foods (foods with a protein content above 10%). High protein foods are developed because protein consumption is associated with a higher satiety level. Therefore, high protein foods can help in body weight reduction.[11,12] Furthermore, many elderly people suffer from increased muscle loss. To prevent this, they need to consume higher amounts of protein.[13]

Properties that can be affected using protein fibrils as ingredients are the viscosity, flow behaviour and gelation. However, the behaviour of protein fibrils in concentrated protein solutions is at this moment relatively unexplored.

Meat replacement products

A second possible application of these protein fibrils can be found in meat replacement products. Meat production requires many natural resources (energy, land and water),[14,15] and results in high emissions of greenhouse gases.[16] Developing fibrous products from plant proteins (e.g. soy, rapeseed and peas) could contribute to a more sustainable production, because the direct conversion of plants into meat replacement products is much more efficient than the conversion of plants into meat.[17] For example, 6 kg of peas is necessary to obtain 1 kg of protein that can be used in meat replacement products, while 42 kg of plants (tapioca and soy) is necessary to produce 1 kg of protein in meat (pork).[18]

Most existing meat replacement products do not have the same anisotropic texture as meat, and therefore their sensorial quality is inferior to that of meat. The main difficulty in mimicking the texture of meat is the hierarchical anisotropic structure present in meat, which starts at a nanoscale with collagen, myosin and actin, and ends at a macroscale with muscle fibres. Protein fibrils are highly anisotropic structures of a few nanometers thick, and they arrange themselves into mesoscopic phases at sufficient high concentrations.[19] Furthermore, they are easy to align in a flow field. Therefore, they could be used as nanoscale fibers for new meat replacement products. In view of this application, it useful to study the ability of plant proteins (for instance soy proteins) to form fibrils.

Low-calorie products

A final possible application for the protein fibrils can be found in low-calorie products. In these products, the original ingredients are replaced by other ingredients, which results in a decrease of the energy content (e.g. replacement of sugar by artificial sweeteners, or skim yoghurt). The challenge for some of these products is to keep the textural properties similar to the properties of the original products, for instance by increasing the thickness of skim yoghurt by adding thickening agents. Mostly, polysaccharides (e.g. xanthan gum, locust bean gum or starch) are used as thickening agents. Protein fibrils could be an interesting alternative, because due to their length, they can increase the viscosity and form gels on a weight-efficient basis.[3]

PREPARATION AND MECHANISM

Fibrillization of the whey protein β-lactoglobulin has been the subject of many studies. Fibrils of β-lactoglobulin can be obtained by heating the protein above 80 °C for several hours (5-24 h) under acidic conditions and low ionic strength,[6,7,20,21] or by adding a denaturing agent like urea.[22] The fibrils can have a length up to 10 μm,[6,7,21,23] while their thickness is around 4 nm.[20] Fibrils with similar morphology as β-lactoglobulin fibrils can be obtained by heating whey protein isolate (WPI) at low ionic strength and acidic pH. β-Lactoglobulin was found to be the only protein that is incorporated into these WPI fibrils.[19] The amount of WPI that is assembled into fibrils varies between 1 and 40%, depending on the conditions used.[1] This means that full conversion of β-lactoglobulin or WPI into fibrils has never been reported.

The protein molecules inside β-lactoglobulin fibrils are held together by intermolecular β-sheets, which extend over the length of the fibril. Hydrogen bonds are present between the atoms of the β-strands.[24] The bonds between the proteins are initially weak, and become stronger in time.[20] It is not known yet which effect the heat treatment under acidic conditions has on the molecular structure of β-lactoglobulin.

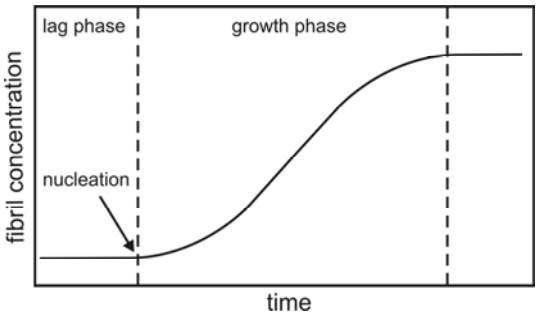

Figure 1. *Different stages of fibril formation: lag phase, nucleation and growth phase.*

Different stages are generally observed during the formation of fibrils, which are shown in Figure 1. First, a lag time is observed during which no fibrils are formed. After a certain lag time, nucleation occurs, and fibrils start to form (growth phase). Eventually, the growth rate decreases and becomes zero, indicating either a limitation in monomer supply or a thermodynamic equilibrium.[25,26] Factors that can influence the kinetics of fibril formation are protein concentration,[1] addition of pre-formed fibrils (seeding),[22,25] and mixing/stirring during heating.[1,25] Although stirring enhances the fibril formation, it is not known yet how the flow field influences the kinetics of fibril formation.

MOTIVATION, OBJECTIVES AND OUTLINE

The overall goal of this project was to study the application possibilities of protein fibrils in food systems by obtaining more knowledge about the process and mechanism of fibril formation, and studying the behaviour of these fibrils in the presence of other proteins. Therefore, the research can be divided into three objectives, relating to *preparation*, *mechanism* and *application*. β-Lactoglobulin and WPI were mainly used as protein sources, because β-lactoglobulin has been the subject of many previous studies, and WPI is an industrially relevant protein mixture. Figure 2 gives a schematic overview of the contents of this thesis.

The first objective was to gain more insight into the *preparation* of the fibrils. Stirring enhances the fibril formation of WPI,[1] but it is not clear yet how the flow influences the kinetics of fibril formation. Therefore, the effect of a well-defined flow field (shear flow) was studied to gain more insight into the effect of flow on the fibril formation, and to have more control over the process of fibril formation. In **Chapter 2**, we studied the effect of shear flow on the nucleation of the fibril formation. To decouple nucleation and fibril growth, a short heat treatment was applied during which no fibril growth took place, followed by nucleation of the fibril growth at room temperature. In **Chapter 3**, we studied the effect of shear flow during heating on the fibril formation and the fibril properties (fibril concentration, fibril length and flow behaviour). A shearing device was developed to apply shear flow during the heat treatment. The results were compared with a

model describing the effect of shear rate on fibril growth.

Preparing these fibrils from proteins that are plant based instead of animal based will contribute to the development of more sustainable products. Therefore, the possibility to make these fibrils from soy protein was studied in **Chapter 4**. The physical properties of the soy protein fibrils were compared to the properties of WPI and β-lactoglobulin fibrils.

To obtain fibrils from β-lactoglobulin, heating at acidic pH can be used. However, the reason behind this treatment at these specific conditions is not clear yet, and the same holds for the limited conversion of protein into fibrils. To find an explanation for the necessity of heating at low pH and the limited conversion of protein into fibrils, the second objective was to gain more insight into the *mechanism* of fibril formation. Therefore, the chemical composition of β-lactoglobulin fibrils was studied, and these results are shown in **Chapter 5**. Based on the results of Chapter 5, we developed an alternative method to obtain protein fibrils (enzymatic hydrolysis), and these results are described in **Chapter 6**.

Previous research has shown that the presence of fibrils can result in an increase of viscosity, shear thinning behaviour, and gels with a low protein concentration.[1-3] However, for the application in food products, it is necessary to study the behaviour of fibrils in the presence of other ingredients. Therefore, the final objective of this thesis was studying the *application* possibilities of protein fibrils in order to modify the structural properties of concentrated WPI solutions. Concentrated WPI solutions were chosen as a model system for high protein foods. These results are described in **Chapter 7**.

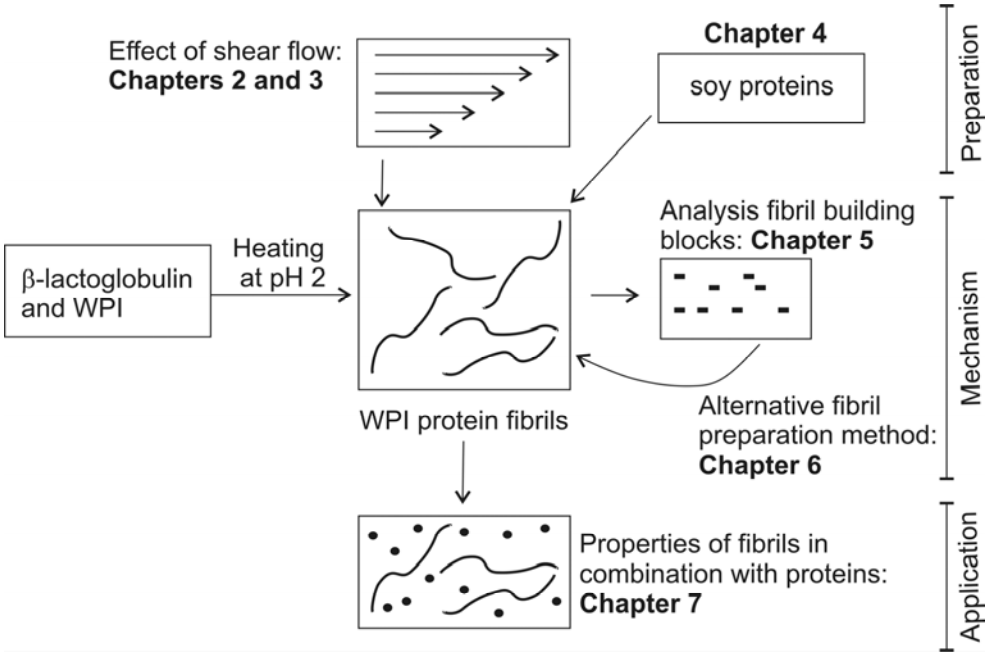

***Figure 2**. Schematic overview of the thesis "Protein fibrillization: preparation, mechanism and application" based on the different chapters in this thesis.*

REFERENCES

1. Bolder, S.G.; Sagis, L.M.C.; Venema, P.; Van der Linden, E. Effect of stirring and seeding on whey protein fibril formation. *Journal of Agricultural and Food Chemistry* **2007**, 55, 5661-5669.

2. Bolder, S.G.; Hendrickx, H.; Sagis, L.M.C.; Van der Linden, E. Ca^{2+}-induced cold-set gelation of whey protein isolate fibrils. *Applied Rheology* **2006**, 16, 258-264.

3. Veerman, C.; Baptist, H.; Sagis, L.M.C.; Van der Linden, E. A new multistep Ca^{2+}-induced cold gelation process for β-lactoglobulin. *Journal of Agricultural and Food Chemistry* **2003**, 51, 3880-3885.

4. Cooper, G.J.S.; Willis, A.C.; Clark, A.; Turner, R.C.; Sim, R.B.; Reid, K.B.M. Purification and characterization of a peptide from amyloid-rich pancreases of type 2 diabetic patients *Proceedings of the National Academy of Science of the United States of America* **1987**, 84, 8628-8632.

5. Tanzi, R.E.; Gusella, J.F.; Watkins, P.C.; Bruns, G.A.P.; St George-Hyslop, P.; Van Keuren, M.L.; Patterson, D.; Pagan, S.; Kurnit, D.M.; Neve, R.L. Amyloid beta

protein gene: cDNA, mRNA distribution, and genetic linkage near the Alzheimer locus. *Science* **1987**, 235, 880-884.

6. Gosal, W.S.; Clark, A.H.; Pudney, P.D.A.; Ross-Murphy, S.B. Novel amyloid fibrillar networks derived from a globular protein: β-lactoglobulin. *Langmuir* **2002**, 18, 7174-7181.

7. Durand, D.; Gimel, J.C.; Nicolai, T. Aggregation, gelation and phase separation of heat denatured globular proteins. *Physica A* **2002**, 304, 253 - 265.

8. Arnaudov, L.N.; De Vries, R. Thermally induced fibrillar aggregation of hen egg white lysozyme. *Biophysical Journal* **2005**, 88, 515-526.

9. Veerman, C.; De Schiffart, G.; Sagis, L.M.C.; Van der Linden, E. Irreversible self-assembly of ovalbumin into fibrils and the resulting network rheology. *International Journal of Biological Macromolecules* **2003**, 33, 121-127.

10. Veerman, C.; Sagis, L.M.C.; Heck, J.; Van der Linden, E. Mesostructure of fibrillar bovine serum albumin gels. *International Journal of Biological Macromolecules* **2003**, 31, 139-146.

11. Westerterp-Plantenga, M.S.; Rolland, V.; Wilson, S.A.J.; Westerterp, K.R. Satiety related to 24 h diet-induced thermogenesis during high protein/ carbohydrate vs high fat diets measured in a respiration chamber. *European Journal of Clinical Nutrition* **1999**, 53, 495-502.

12. Anderson, G.H.; Moore, S.E. Dietary proteins in the regulation of food intake and body weight in humans. *The Journal of Nutrition* **2004**, 134, 974S-979S.

13. Evans, W.J. Protein nutrition, exercise and aging. *Journal of the American College of Nutrition* **2004**, 23, 601S-609S.

14. Pimentel, D.; Pimentel, M. Sustainability of meat-based and plant-based diets and the environment. *American Journal of Clinical Nutrition* **2003**, 78, 660S-663S.

15. White, T. Diet and the distribution of environmental impact. *Ecological Economics* **2000**, 34, 145-153.

16. Carlsson-Kanyama, A. Climate change and dietary choices - how can emissions of greenhouse gases from food consumption be reduced? *Food Policy* **1998**, 23, 277-293.

17. Smil, V. Worldwide transformation of diets, burdens of meat production and opportunities for novel food proteins. *Enzyme and Microbial Technology* **2002**, 30, 305-311.

18. Aiking, H.; Helms, M.; Niemeijer, D.; Zhu, X. The protein chains: pork vs. pea-based NPFs. In *Sustainable protein production and consumption: pigs or peas?* Aiking, H.; De Boer, J.; Vereijken, J.M. Eds. Springer: Dordrecht, **2006**.

19. Bolder, S.G.; Hendrickx, H.; Sagis, L.M.C.; Van der Linden, E. Fibril assemblies

in aqueous whey protein mixtures. *Journal of Agricultural and Food Chemistry* **2006**, 54, 4229-4234.

20. Arnaudov, L.N.; De Vries, R.; Ippel, H.; Van Mierlo, C.P.M. Multiple steps during the formation of β-lactoglobulin fibrils. *Biomacromolecules* **2003**, 4, 1614-1622.

21. Veerman, C.; Ruis, H.; Sagis, L.M.C.; Van der Linden, E. Effect of electrostatic interactions on the percolation concentration of fibrillar β-lactoglobulin gels. *Biomacromolecules* **2002**, 3, 869-873.

22. Hamada, D.; Dobson, C.M. A kinetic study of β-lactoglobulin amyloid fibril formation promoted by urea. *Protein Science* **2002**, 11, 2417-2426.

23. Rogers, S.S.; Venema, P.; Sagis, L.M.C.; Van der Linden, E.; Donald, A.M. Measuring the length distribution of amyloid fibrils: a flow birefringence technique. *Macromolecules* **2005**, 38, 2948-2958.

24. Bromley, E.H.C.; Krebs, M.R.H.; Donald, A.M. Aggregation across the length-scales in β-lactoglobulin. *Faraday Discussions* **2005**, 128, 13-27.

25. Nielsen, L.; Khurana, R.; Coats, A.; Frokjear, S.; Brange, J.; Vyas, S.; Uversky, V.N.; Fink, A.L. Effect of environmental factors on the kinetics of insulin fibril formation: elucidation of the molecular mechanism. *Biochemistry* **2001**, 40, 6036-6046.

26. Rochet, J.C.; Lansbury Jr, P.T. Amyloid fibrillogenesis: theme and variations. *Current Opinion in Structural Biology* **2000**, 10, 60-68.

Shear pulses nucleate fibril aggregation

Chapter 2

This chapter has been published as: C. Akkermans, P. Venema, S.S. Rogers, A.J. Van der Goot, R.M. Boom, E. Van der Linden. Shear pulses nucleate fibril aggregation. Food Biophysics ***2006****, 1, 144-150.*

ABSTRACT

We have studied the effect of shear flow on the formation of amyloid fibrils of the whey protein β-lactoglobulin. β-Lactoglobulin aggregates into long, thin, and semi-flexible fibrils upon heating at low pH and low ionic strength. Solutions with a protein concentration of 0.5% (w/w) were used, and the formation of fibrils was quantified with flow-induced birefringence, a proportional measure of the length concentration of the fibrils. From the decay of the birefringence after cessation of the flow, a length distribution could be fitted. Pulsed and continuous shear treatment of the samples resulted in a comparable enhancement of the fibrillar growth as compared to the fibrillar growth under quiescent conditions. This indicates that the onset of shear flow is the key parameter for the enhancement of fibrillar growth and not the continuous shear flow itself. This behaviour is comparable to a nucleation-like process, during which pre-aggregates of the fibrils are induced during the onset of the flow and orthokinetic coagulation is absent. However, a difference was present in the length distribution between the pulsed and continuously sheared samples, which can be explained by the homogenizing effect of shear flow.

INTRODUCTION

The assembly of proteins into amyloid fibrils has received considerable attention in a variety of research fields, from medical[1-3] to materials science.[4,5] Recently, the assembly of proteins into fibrils has gained more attention in the field of food technology, mainly because of the potential utility in modifying the material properties of food products. Examples of food proteins that have shown the ability to aggregate into fibrils are β-lactoglobulin, bovine serum albumin, lysozyme, and ovalbumin.[6-10] An interesting protein on which to study the effect of process parameters on the fibril formation is β-lactoglobulin, because the fibrils formed by this protein have a large aspect ratio, are polydispers, and are semi-flexible. This enables us to picture them as rod-like particles. For these rod-like systems, a method has been developed recently, which links the decay of birefringence directly to the length distribution.[11]

The most common treatment of β-lactoglobulin solutions to induce the formation of fibrils consists of prolonged heating (6–24 h) at 80 °C at pH 2 and low ionic strength.[6,11-14] The average length of the fibrils depends on the conditions used (e.g., heating time, ionic strength, pH, concentration), but is typically found to be in the range of 1–8 μm.[6,11-14] The diameter of the fibrils is around 4 nm, which implies a thickness of 1 or 2 monomers.[13] The molecular mechanism of the formation of β-lactoglobulin fibrils is not yet clear. During the fibril formation, an increased amount of intermolecular β-sheets was detected with Fourier transform infrared spectroscopy; these β-sheets may bind the monomers together in the fibril.[14,15] Dynamic light scattering showed that after short heating times, the fibrils disintegrate during cooling, but after longer heating times, the fibrils do not disintegrate upon cooling.[13]

For the industrial application of fibrils in food products, an acceleration of the fibril formation would be advantageous. Enhanced formation of different protein fibril systems by addition of preformed fibrils (seeding) has previously been established.[16-18] Another possibility is inducing a mechanical disturbance in the system. In insulin solutions, continuous agitation enhanced the fibril formation.[17] Unfortunately, these experiments were not performed in a well-defined flow field.

Stathopulos et al.[18] found that sonication of a diverse group of proteins resulted in the formation of fibrils. However, these sonication experiments are characterized by an approximately 10^6-fold higher energy input than the energy input of the shear treatment used for our experiments.

To analyze the fibrils, transmission electron microscopy or atomic force microscopy can be used to determine the length distribution of the fibrils,[6,13,14] but these techniques are very laborious and often give only semi-quantitative information. Other methods that can be used to measure the fibril concentration include the binding of fluorescent dyes (e.g. Congo Red[19,20] and Thioflavin T[16,17]), but these methods give no information on the fibril length distribution. During this study, flow-induced birefringence was used to analyze the fibril solution. The major advantage of using flow-induced birefringence is that both the concentration and the length distribution of the fibrils can be measured quantitatively in-situ.[11] Apart from flow-induced birefringence, static light scattering was used to detect the presence of aggregates (in-situ) in the early stages of the aggregation process.

In this paper, we report on the effect of applying the mechanical disturbance of simple shear flow to the formation of β-lactoglobulin fibrils. We found that the onset of the shear flow is the key parameter for the enhancement of fibrillar growth, and we propose that this is caused by a nucleation-growth mechanism.

MATERIAL AND METHODS

Preparation of β-lactoglobulin stock solution

β-Lactoglobulin (18.3 kDa) was obtained from SIGMA and contained the genetic variants A and B. The stock solution of the protein was made by dissolving the protein in a HCl solution of pH 2. To remove traces of electrolytes, the solution was dialyzed (dialysis tube of 12-14 kDa from Visking) against an HCl solution of pH 2 until the pH and ionic strength of the protein solution were equal to the solvent. To remove traces of undissolved protein, the solution was centrifuged at 22,600 g for 30 min and, subsequently, filtered through a protein filter (FP 030/0.45 μm, Schleicher & Schuell). The concentration of the β-lactoglobulin

stock solution was determined with a UV spectrophotometer at a wavelength of 278 nm, using a calibration curve of known β-lactoglobulin concentrations.

Sample treatment

The β-lactoglobulin concentration of all samples in this study was 0.5% (w/w). This concentration is far below the minimum gelation concentration (under no shear condition) of 2.3% at an ionic strength of 0.01 M,[6] and this concentration resulted in isotropic fibril solutions. During the experiments, the solutions were kept at pH 2, and no electrolytes were added. Table 1 shows an overview of the treatment of different samples (A–I). As a pre-treatment, samples were heated at 90 °C in glass tubes, followed by cooling at room temperature for 1 h. The heating times of the samples were 0, 2, or 10 h. During the pre-treatment, no shear treatment was applied. After the pre-treatment, the following different treatments were applied: no shear, continuous shear (at a shear rate of 200 s^{-1}), or short shear pulses of 30 s at a shear rate of 200 s^{-1}. A shear rate of 200 s^{-1} was selected because we expected the effect of shear flow on the fibril formation to be more pronounced at high shear rates. This shear rate is close to the highest shear rate possible without the risk of expelling the sample from the Couette geometry.
Measurements of the non-sheared samples were performed on different samples. For measuring the flow-induced birefringence, shear flow needs to be applied, and after the measurement, the sample cannot be regarded as a non-sheared sample anymore. Therefore, the different non-sheared samples are numbered, and each number refers to a different sample.

Flow-induced birefringence

The samples were subjected to shear flow in a rheometer (ARES, Rheometric Scientific Ltd.) with Couette geometry (rotating cup with a diameter of 33.8 mm and a static bob with a diameter of 30.0 mm) at a shear rate of 200 s^{-1} for 30 s. During the shear treatment, the flow-induced birefringence was measured. A laser beam of wavelength 670 nm passed vertically through the gap between the cup and bob, and the birefringence was measured with a modified optical analysis module (OAM)[21]. The rheo-optical analysis was performed in a temperature-controlled

room at 20 °C. At complete alignment of the fibrils, the flow-induced birefringence (Δn) is proportional to the total length concentration of the fibrils:[11]

$$\Delta n = M \cdot \int c_L \cdot dL \qquad (1)$$

In Equation 1, c_L is the contribution to the total length per unit volume in the system as a result of the fibrils with a length between L and $L + dL$. The constant M is the contribution to the birefringence per unit length concentration, and was determined for β-lactoglobulin fibrils by Rogers et al.[11] The applied shear rate was 200 s^{-1} because this was the highest rate experimentally possible. At a higher shear rate, part of the sample would be expelled from the measuring cup. During the steady shear of 30 s, a constant birefringence was measured for all samples, indicating that the amount of fibrils did not change during the measurement. Furthermore, Rogers et al.[11] also performed birefringence measurements on β-lactoglobulin fibrils, and they showed that the fibrils did not break up during the shear treatment of the measurement up to shear rates of 200 s^{-1}.

Length distribution of the fibrils

To determine the length distribution of the fibrils, the samples were subjected to steady shear flow at a shear rate of 200 s^{-1} for 30 s. After cessation of the flow, the decay curve of the birefringence was measured. Rogers et al.[11] developed a method to deduce the length distribution of β-lactoglobulin fibrils from this decay curve, based on the Doi-Edwards-Marruci-Grizzuti (DEMG) theory.[22,23] A simplified version of this method was used: each decay curve was fitted by assuming a Gaussian distribution function for the length distribution. The mean and variance of this Gaussian were adjusted to provide the closest fit of the decay curve via the DEMG theory.

Static light scattering (SLS)

Static light scattering was measured with a Multi Angle DAWN®EOS™ laser photometer from Wyatt Technology. At room temperature, a β-lactoglobulin solution was injected into the flow cell. The sample was heated to 90 °C at a rate

of 1 °C/min. When this temperature was established, the solution was kept at this temperature for 2 h. After the heat treatment, the solution was cooled to 20 °C (1 °C/min). Because no angle dependency was found, the scattered intensity at an angle of 90° was used.

Table 1. *Overview of sample treatment.*

Sample	Heating time of pre-treatment (h)[a]	Treatment		Measurement time (h after pre-treatment)[b]
		Type	Time (h after pre-treatment)[b]	
A	0	no shear		0
B1	2	no shear		0
B2	2	no shear		5
B3	2	no shear		22.5
C1	10	no shear		0
C2	10	no shear		5
D	0	continuous shear[c]	5	0 – 5
E	2	continuous shear[c]	5	0 – 5
F	10	continuous shear[c]	5	0 – 5
G	2	shear pulses[d]	0, 1, 2, 3, 4	0, 1, 2 , 3, 4, 5
H	2	shear pulses[d]	0	0, 5
I	2	shear pulses[d]	5	5, 25

[a] The pre-treatment consisted of heating, followed by 1 h cooling at room temperature. During the pre-treatment, no shear treatment was applied.

[b] t = 0 refers to the time at which the shear treatment started.

[c] The shear rate of continuous shear treatment was 200 s^{-1}.

[d] Pulsed shear treatment comprised of a shear pulse of 30 s at a shear rate of 200 s^{-1}. The time refers to the time at which the shear pulse was given.

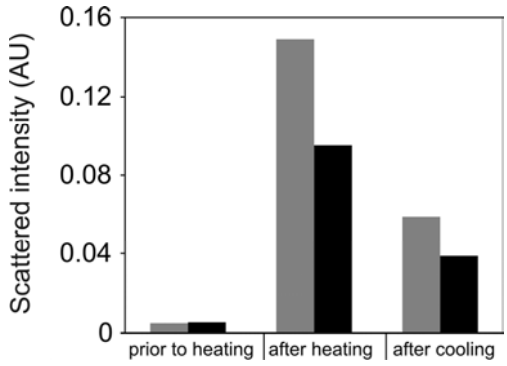

***Figure 1**. Scattered intensity of β-lactoglobulin solutions (0.5%) before heating, after heating for 2 h at 90 °C and after cooling to 20 °C (performed two times).*

RESULTS

Effect of pre-treatment (in absence of shear flow)

In this section, the effect of the pre-treatment (heating and subsequent cooling) on the fibril formation without applying shear treatment is described. These experiments will serve as a reference relative to which the different shear treatments are compared. Using static light scattering, the presence of aggregates was studied during a 2-h heat treatment and 1 h cooling.

In Figure 1, the scattering intensities (at an angle of 90°) are shown for duplicated experiments at three different moments: before heating, after heating for 2 h at 90 °C, and after cooling. Before heating, the scattered intensities corresponded to the intensity of native β-lactoglobulin molecules. Immediately after heating for 2 h, the scattered intensities were higher than the intensities before heating, implying that aggregates had formed during heating. After cooling, the scattered intensities decreased, meaning that aggregates disintegrated during cooling. The scattered intensities did not decrease to the same level as before heating, suggesting that a part of the aggregates formed during heating were still present after cooling. The size of the aggregates was estimated to be in the range of nanometers because no angle dependence was found for the scattered intensity. Because a low protein concentration was used and initial times of aggregation were studied, the scattered intensity resulting from a change in second virial coefficient was assumed to be

low compared to the scattered intensity of the aggregates. Arnaudov and de Vries[24] have used light scattering in a similar way for β-lactoglobulin aggregates at low protein concentration.

The presence of fibrils after heating was detected using flow birefringence at a shear rate of 200 s^{-1}. Different heating times (0, 2, and 10 h) were used, and the birefringence was measured at lag times that were comparable to those used for the shear treatments. Figure 2 shows the birefringence of the samples after different lag times (samples A, B1, B2, B3, C1, and C2; Table 1). The numbers after B and C indicate that different non-sheared samples were used for each measurement. For measuring the flow-induced birefringence, shear flow needed to be applied, meaning that for each measurement time, a "fresh" non-sheared sample was needed.

At t = 0 h (immediately after heating and cooling), a negligible flow birefringence was observed for all three heating times. After a lag time of 5 h, the sample heated for 2 h (B2) did not show an increase of flow birefringence, but the sample heated for 10 h (C2) gave a significant flow birefringence; an appreciable yield of fibrils was achieved after 10 h of heating and a 5-h lag time. After a 22.5-h lag time, the sample that was heated for 2 h (C3) also showed an increase of birefringence, meaning that the concentration of fibrils was significantly higher after a 22.5-h lag time than after a 5-h lag time.

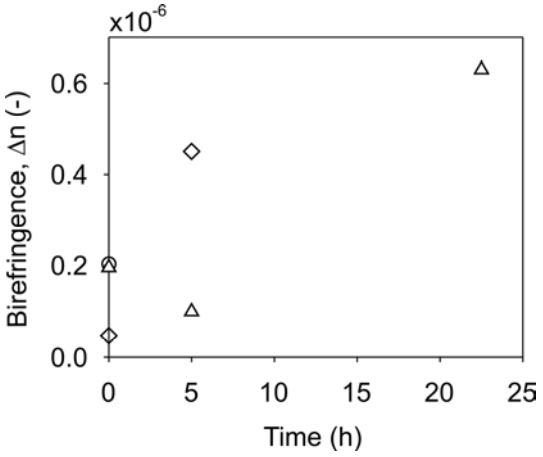

Figure 2*. Birefringence signals at different lag times after various heating times (samples A, B1, B2, B3, C1 and C2; Table 1): (○) 0 h, (△) 2 h, (◇) 10 h.*

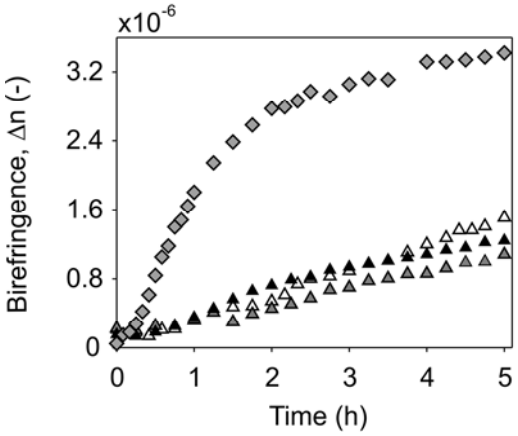

Figure 3*. Increase of birefringence during continuous shear treatment (samples E and F; Table 1): (△, ▲, ▲) 2 h heating, (◇) 10 h heating.*

Effect of continuous shear treatment

The effect of continuous shear flow on the formation of the β-lactoglobulin fibrils was determined by subjecting heated samples to continuous shear flow for 5 h (samples D, E, and F; Table 1). Shear treatment was applied at room temperature. Figure 3 shows the increase of birefringence during continuous shear treatment after heating for 2 and 10 h. The sample heated for 0 h (sample D) did not show any increase of birefringence during continuous shear treatment for 5 h and is not shown in Figure 3. Heating for 2 h followed by continuous shear treatment for 5 h (sample E) was performed three times to test the experimental variability, which turned out to be quite modest. The trends observed under different treatment conditions were much larger than this variability.

After 5 h of shear treatment, the birefringence signals of the sheared samples were significantly higher than the birefringence signals of the samples not subjected to shear flow, described above (Figure 2). At the start of the shear treatment (t = 0 h), no birefringence was observed for both samples (E and F), but after the start of the shear treatment, the birefringence of the samples started to increase. The increase of birefringence was faster after heating for 10 h than after heating for 2 h. The birefringence increased approximately linearly with time during the 5-h shear treatment for the sample heated for 2 h. The birefringence of the sample heated for

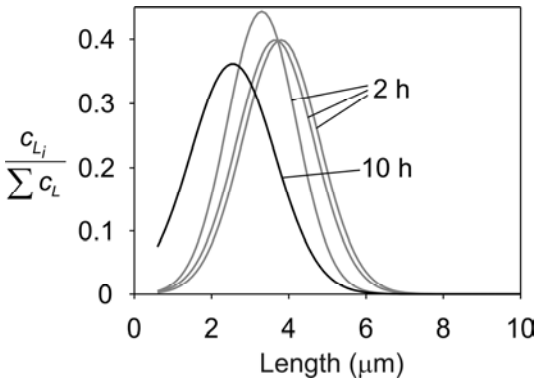

Figure 4*. Length distributions after 5 h of continuous shear treatment (samples E and F; Table 1): (grey) 2 h heating, and (black) 10 h heating.*

10 h increased very quickly during the first hour of shear treatment, but was approaching a plateau value after 5 h.

A length distribution was fitted to the birefringence decays after 5 h of shear treatment. Figure 4 shows the length distributions of the samples of 2 and 10 h heating. The three samples of 2 h heating showed a similar length distribution between which only minor variations were visible. The peak of the length distribution of the fibrils was smaller after 10 h heating than after 2 h heating.

Effect of pulsed shear treatment

In the previous section, we found that at the start of the shear treatment, no significant birefringence was observed. After the start of the shear treatment, the birefringence increased immediately; the shear flow seemed to initiate the fibril formation. To elucidate the mechanism of this effect, we varied the shear treatment. Instead of continuous shear flow, samples were subjected to transient flows, using "pulses" of shear flow at variable intervals. Each pulse consisted of 30-s flow at a shear rate of 200 s^{-1}. Three variations of pulsed shear treatment were performed, as shown in Table 1 (samples G, H, and I).

Figure 5 shows the results of the pulsed shear treatments together with the average value of three experiments of continuous shear treatment (Figure 3). Sample G was given pulses each hour starting at t = 0 h. Sample H received one pulse at t = 0 h. During the 30-s shear pulses, the birefringence did not increase significantly,

meaning that the fibril length concentration did not increase during the pulse treatment. After 5 h of pulsed shear treatment, the birefringence signals of samples G and H were comparable to the average birefringence signal after continuous shear treatment (sample E). This shows that the total length concentrations of the three different treatments were similar. Sample G showed a linear increase of birefringence with time over 5 h, just like the continuously sheared samples.

From the decay of the birefringence after cessation of the flow, the length distributions of samples G and H were fitted (Figure 6). The length distributions of the two pulsed shear treatments did not differ significantly. The variances of the length distributions of pulsed shear treatments were larger than the variance of continuous shear treatment.

Another sample (sample I; Table 1) was given its first shear pulse after a lag time of 5 h. The birefringence of this sample was measured after 25 h (Figure 5). After 5 h, this sample showed negligible birefringence; few fibrils were present in the sample. However, after 25 h, the birefringence had increased to a value much higher than the sample of a comparable lag time (22.5 h) with no shear (Figures 2 and 5).

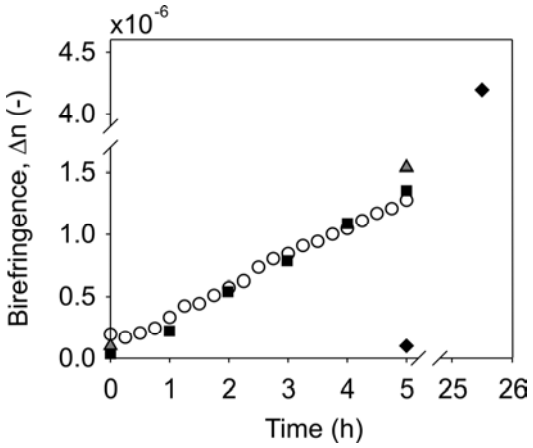

***Figure 5**. Increase of birefringence of four different shear treatments: (■) shear pulses every hour (sample G); (▲) a pulse at t = 0 h (sample H); (◆) a pulse after 5 h (sample I); (○) continuous shear treatment (average of three experiments).*

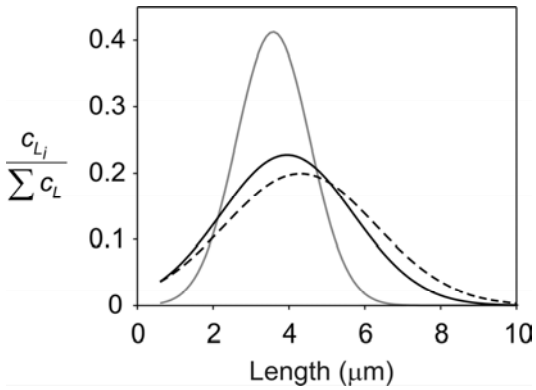

Figure 6*. Length distributions after 5 h of pulsed and continuous shear treatment (samples G, H, and D; Table 1): (solid black) shear pulses every hour; (dotted) a pulse at t = 0 h; (solid grey) continuous shear (average of three experiments).*

DISCUSSION

In the previous section, it was shown that shear flow significantly enhances the formation of β-lactoglobulin fibrils. Samples that were subjected to continuous shear flow showed a significant increase of birefringence almost immediately after the shear treatment started (Figure 3). This is in contrast with a sample that was kept at rest, for which it took 22.5 h before a birefringence signal was measurable (Figure 2). However, we also showed that there is no difference in fibril concentration between applying continuous shear flow, giving short shear pulses every hour, or giving only one short shear pulse (Figure 5). This shows that the onset of the shear flow is the key parameter for enhancing the fibril growth. The duration of subsequent shear treatment was found to be of no influence on the enhancement of the fibril formation.

Static light scattering showed that during the pre-treatment (comprising heating and cooling), aggregates were formed with a size in the range of nanometers. This size is smaller than the size of the fibrils, which are in the range of micrometers, and therefore, we will further refer to these small aggregates as pre-aggregates. Part of the pre-aggregates disintegrated during cooling, but the scattered intensity remained higher than the signal of native β-lactoglobulin molecules (Figure 1). A

reversible aggregation was previously shown for β-lactoglobulin by Arnaudov et al.[13] The enhancing effect of the onset of shear flow could be caused by breakup of the pre-aggregates, but during cooling, the pre-aggregates also disintegrated, and this did not result in enhanced fibril formation. As we will argue below, the onset of shear flow seems to induce nucleation of the fibril formation.

Previous studies found that other mechanical disturbances, such as sonication[18] and agitation,[17] enhanced the fibril formation of different proteins, but during these studies, the difference between pulsed and continuous treatment was not studied. Although sonication is a common method to break up macromolecules, it can also be used to induce nucleation (i.e., an often used method in the sugar industry to control the size of the sugar crystals or to nucleate protein crystallization[25]). A mechanical disturbance, such as agitation, is also a known method to enhance the nucleation of a crystallization process.[26-28] Before crystallization occurs, the system has to enter the metastable part of the phase diagram, and a nucleation event is necessary to start the crystallization process. There are many examples where nucleation is triggered by penetrating the metastable part of the phase diagram by cooling. Alternatively, a nucleation event can also be induced by adding mechanical energy to the (metastable) system by, for example, sonication or agitation. Following Oosawa and Asakura,[29] we propose that the fibril formation is a one-dimensional crystallization-like process, where the total number of proteins converted into fibrils is a function of concentration, and not a sharp transition as is the case in classical crystallization. This view is supported by experimental evidence that was found by measuring the total conversion as a function of β-lactoglobulin concentration (results of Rogers et al., unpublished). The theory of Oosawa and Asakura predicts a smooth transition, especially in the case of fibrils with a thickness of one or two proteins, as is the case for β-lactoglobulin fibrils. In this view, we expect that the formation of pre-aggregates, which initiate the fibril growth, is similar to the formation of nuclei in a classical (three-dimensional) crystallization process. As a consequence, the fibrillar growth can also be enhanced by a mechanical disturbance, such as the onset of shear flow. However, after one shear pulse had caused nucleation, we did not observe additional nucleation by giving more shear pulses at an interval of 1 h. Probably,

there were not enough proteins left to be nucleated into pre-aggregates after the first nucleation had taken place.

We found that the shear flow itself, apart from the onset of shear flow, has no additional influence on the amount of fibrils relative to pulsed shear. This is direct proof that orthokinetic coagulation, flow enhanced aggregation, does not play a role under the conditions as in our experiments. In order for orthokinetic coagulation to become important within the fibril formation, fibrils have to exceed a certain length depending on the shear rate. It can be estimated that at a shear rate of ~100 s^{-1}, we need to have fibrils present with a length in the order of 1 μm. In the initial stages of the fibril growth, this is certainly not the case, and the continuous shear flow itself will not enhance fibrillar growth. This situation can change when we use different experimental conditions, e.g. samples with a higher protein concentration or samples that are analyzed during later stages of the fibril formation process. We did observe differences in the length distribution after continuous or pulsed shear treatment. Continuous shear treatment resulted in a smaller variance of the Gaussian length distribution than pulsed shear treatment (Figure 6). This difference can be attributed to the homogenizing effect of continuous shear treatment.

Before applying shear flow, the solutions of β-lactoglobulin were heated. Without heating, no fibrils were formed within 5 h of continuous shear treatment. A longer heating time resulted in a faster fibril formation (Figure 3) and a slightly smaller average fibril length (Figure 4). A possible explanation is the presence of more pre-aggregates after a longer heating, which resulted in more competition between the pre-aggregates, which gave smaller but more fibrils.

CONCLUSIONS

We have shown that the onset of shear flow of sufficient magnitude is enough to initiate the formation of β-lactoglobulin fibrils. After initiation, extended shear treatment does not have any further effect on the fibril growth. Without the onset of shear flow, the initiation of the fibril formation is much slower. We propose that this process can be envisioned as a one-dimensional semi-crystallization process

as introduced by Oosawa and Asakura.[29] The formation of pre-aggregates is similar to that of the formation of nuclei and, as such, can be triggered by a mechanical disturbance, such as the onset of shear flow. We found no proof for the presence of orthokinetic coagulation in our experiments. However, this is expected to change when we change our experimental conditions toward higher protein concentrations, higher temperatures, or prolonged fibrillization times.

ACKNOWLEDGEMENTS

We thank H. Gruppen and J. Vereijken for the useful discussions about this work, and we also thank H. Schaink for his advice for the static light scattering experiments. We acknowledge the Dutch research school, VLAG, for their financial support of this research. We acknowledge funding from the BBSRC for SSR, and the European Commission for an IHP grant awarded to the Food Physics Group of Wageningen University for a Marie Curie Training Site Fellowship (contract HPMT-2000-00188).

REFERENCES

1. Kelly, J.W. The alternative conformations of amyloidogenic proteins and their multi-step assembly pathways. *Current Opinion in Structural Biology* **1998**, 8, 101.

2. Hardy, J.A.; Higgins, G.A. Alzheimer's disease: the amyloid cascade hypothesis. *Science* **1992**, 256, 184-185.

3. Bucciantini, M.; Giannoni, E.; Chiti, F.; Baroni, F.; Formigli, L.; Zurdo, J.; Taddei, N.; Ramponi, G.; Dobson, C.M.; Stefani, M. Inherent toxicity of aggregates implies a common mechanism for protein misfolding diseases. *Nature* **2002**, 416, 507.

4. Langton, M.; Hermansson, A.M. Fine-stranded and particulate gels of β-lactoglobulin and whey protein at varying pH. *Food Hydrocolloids* **1992**, 5, 523-539.

5. Gosal, W.S.; Clark, A.H.; Ross-Murphy, S.B. Fibrillar β-lactoglobulin gels: part 2. Dynamic mechanical characterization of heat-set systems. *Biomacromolecules* **2004**, 5, 2420-2429.

6. Veerman, C.; Ruis, H.; Sagis, L.M.C.; Van der Linden, E. Effect of electrostatic interactions on the percolation concentration of fibrillar β-lactoglobulin gels. *Biomacromolecules* **2002**, 3, 869-873.

7. Veerman, C.; Sagis, L.M.C.; Heck, J.; Van der Linden, E. Mesostructure of fibrillar bovine serum albumin gels. *International Journal of Biological Macromolecules* **2003**, 31, 139-146.

8. Veerman, C.; De Schiffart, G.; Sagis, L.M.C.; Van der Linden, E. Irreversible self-assembly of ovalbumin into fibrils and the resulting network rheology. *International Journal of Biological Macromolecules* **2003**, 33, 121-127.

9. Durand, D.; Gimel, J.C.; Nicolai, T. Aggregation, gelation and phase separation of heat denatured globular proteins. *Physica A* **2002**, 304, 253 - 265.

10. Arnaudov, L.N.; De Vries, R. Thermally induced fibrillar aggregation of hen egg white lysozyme. *Biophysical Journal* **2005**, 88, 515-526.

11. Rogers, S.S.; Venema, P.; Sagis, L.M.C.; Van der Linden, E.; Donald, A.M. Measuring the length distribution of amyloid fibrils: a flow birefringence technique. *Macromolecules* **2005**, 38, 2948-2958.

12. Gosal, W.S.; Clark, A.H.; Pudney, P.D.A.; Ross-Murphy, S.B. Novel amyloid fibrillar networks derived from a globular protein: β-lactoglobulin. *Langmuir* **2002**, 18, 7174-7181.

13. Arnaudov, L.N.; De Vries, R.; Ippel, H.; Van Mierlo, C.P.M. Multiple steps during the formation of β-lactoglobulin fibrils. *Biomacromolecules* **2003**, 4, 1614-1622.

14. Kavanagh, G.M.; Clark, A.H.; Ross-Murphy, S.B. Heat-induced gelation of globular proteins: part 3. Molecular studies on low pH β-lactoglobulin gels. *International Journal of Biological Macromolecules* **2000**, 28, 41-50.

15. Lefevre, T.; Subirade, M. Molecular differences in the formation and structure of fine-stranded and particulate β-lactoglobulin gels. *Biopolymers* **2000**, 54, 578-586.

16. Hamada, D.; Dobson, C.M. A kinetic study of β-lactoglobulin amyloid fibril formation promoted by urea. *Protein Science* **2002**, 11, 2417-2426.

17. Nielsen, L.; Khurana, R.; Coats, A.; Frokjear, S.; Brange, J.; Vyas, S.; Uversky, V.N.; Fink, A.L. Effect of environmental factors on the kinetics of insulin fibril formation: elucidation of the molecular mechanism. *Biochemistry* **2001**, 40, 6036-6046.

18. Stathopulos, P.B.; Scholz, G.A.; Hwang, Y.M.; Rumfeldt, J.A.O.; Lepock, J.R.; Meiering, E.M. Sonication of proteins causes formation of aggregates that resemble amyloid. *Protein Science* **2004**, 13, 3017-3027.

19. Klunk, W.E.; Jacob, R.F.; Mason, R.P. Quantifying amyloid β-peptide (Ab) aggregation using the congo red-Ab (CR-Ab) spectrophotometric assay. *Analytical Biochemistry* **1999**, 266, 66-76.

20. Klunk, W.E.; Jacob, R.F.; Mason, R.P. Quantifying amyloid by congo red spectral shift assay. In *Methods in Enzymology: Amyloids, Prions and other Protein Aggregates*, Wetzel, R., Ed. Academic Press: **1999**; Vol. 309, pp 285-305.

21. Klein, C.; Venema, P.; Sagis, L.M.C.; Van Dusschoten, D.; Wilhelm, M.; Spies, H.W.; Van der Linden, E.; Rogers, S.S.; Donald, A.M. Rheo-optical measurements by Fast Fourier Transform and Oversampling. *Applied Rheology* **2007**, 17, 45210-1-45210-7.

22. Doi, M.; Edwards, S.F. Dynamics of rod-like macromolecules in concentrated solution. Part 2. *Journal of the Chemical Society-Faraday Transactions 2* **1978**, 74, 918-932.

23. Marrucci, G.; Grizzuti, N. Predicted effect of polydispersity on rodlike polymer behaviour in concentrated solutions *Journal of Non-Newtonian Fluid Mechanics* **1984**, 14, 103-119.

24. Arnaudov, L.N.; De Vries, R. Theoretical modeling of the kinetics of fibrilar aggregation of bovine β-lactoglobulin at pH 2. *Journal of Chemical Physics* **2007**, 126, 145106.

25. Nanev, C.N.; Penkova, A. Nucleation of lysozyme crystals under external electric and ultrasonic fields. *Journal of Crystal Growth* **2001**, 232, 285-293.

26. Young, S.W. Mechanical stimulus to crystallization in supercooled liquids. *Journal of the American Chemical Society* **1911**, 33, 148.

27. Mullin, J.W.; Raven, K.D. Nucleation in agitated solutions. *Nature* **1961**, 190, 251.

28. Mullin, J.W.; Raven, K.D. Influence of mechanical agitation on the nucleation of some aqueous salt solutions. *Nature* **1962**, 195, 35-38.

29. Oosawa, F.; Asakura, S. Thermodynamics of the polymerization of protein. Academic Press London New York San Fransisco: **1975**.

Formation of fibrillar whey protein aggregates: Influence of heat and shear treatment, and resulting rheology

Chapter 3

This chapter has been accepted for publication as: C. Akkermans, A.J. Van der Goot, P. Venema, E. Van der Linden, R.M. Boom. Formation of fibrillar whey protein aggregates: Influence of heat and shear treatment, and resulting rheology. Food Hydrocolloids ***2007****, doi:10.1016/j.foodhyd.2007.07.001.*

ABSTRACT

We have studied the effect of a combined heat and shear treatment on the formation and rheological properties of fibrillar whey protein aggregates. The amount and length distribution of whey protein fibrils were characterized using flow-induced birefringence and transmission electron microscopy (TEM). Fibril solutions were characterized macroscopically using crossed polarizers and the flow behaviour was measured with steady-shear viscosity measurements. Fibril growth was dependent on protein concentration. The use of shear flow influenced the amount of fibrils formed when the protein concentration was sufficiently high (above 3 wt%). A shear rate was found for which the amount of fibrils was maximal. The increase in the amount of fibrils as a function of shear rate was explained by enhanced supply of protein monomers towards the fibril tips in the flow field, while the following decrease at higher shear rates could be caused by the breakage of non-matured bonds inside the fibril. Viscosity measurements of the fibril solutions showed that above a critical fibril concentration, the viscosity became independent of the fibril concentration.

INTRODUCTION

Fibrillar protein aggregates are promising building blocks for the preparation of anisotropic macrostructures in food products. It is desirable that the properties of the aggregates can be properly controlled. Many globular proteins have shown the ability to form long, thin fibrillar aggregates. Most research has focused on pure, well-defined protein systems, like β-lactoglobulin,[1] ovalbumin,[2] lysozyme,[3] and bovine serum albumin (BSA).[4] In this study, an industrial grade whey protein isolate (WPI) was used because of its relevance for practical applications.

The main proteins in WPI are β-lactoglobulin (70–80%), BSA and α-lactalbumin. In previous studies, β-lactoglobulin fibrils were obtained by heating at 80 °C, pH 2 and low ionic strength for 10–24 h.[5-8] The length of the fibrils obtained varied between 1 and 10 μm, while their diameter was around 4 nm, implying a fibril thickness of one or two monomers.[5] The persistence length of the fibrils is approximately 1.6 μm (determined from transmission electron microscopy (TEM)), which is in the same order as the length of the fibrils.[9] A β-lactoglobulin fibril is a polymeric assembly of protein molecules, based on the cross-β structural pattern, in which intermolecular β-sheets extend over the length of the fibril such that each β-strand within the β-sheets runs perpendicular to the fibril axis. The cross-β pattern, which was revealed by X-ray fibre diffraction,[10] is held together by hydrogen bonding between the atoms of the β-strands. The bonds between the proteins in the fibrils are initially weak, and become stronger in time (matures).[5] A possible explanation for the increase in bond strength is that in the early stages of aggregation, bonds are stabilized by hydrophobic and electrostatic interactions, while at a later stage, an extensive network of hydrogen bonds will be formed between the different β-strands in the β-sheets.[11]

β-Lactoglobulin was found to be the only protein that is incorporated into WPI fibrils, when they were formed by heating at pH 2 and low ionic strength.[12] An interesting macroscopic property of whey protein fibrils is the formation of birefringent, liquid-crystalline polydomains of fibrils when fibrils are prepared at

high protein concentration (above 7wt%) without applying flow. Below this concentration, isotropic fibril solutions were found.[12]

The fibril growth of proteins is generally characterized by a lag time, a nucleation event, followed by a period of growth.[13] The kinetics of the fibril formation of different proteins can be influenced by adding preformed fibrils (seeding),[14,15] continuous mixing,[15,16] short shear pulses,[17] or sonication.[18]

Mixing during heating has proven to be a suitable method for enhancing the fibril formation, but a systematic study on how the shear rate can influence the fibril formation during heating has not yet been performed. Therefore, we have studied the effect of simple shear flow during heating on the properties of whey protein fibrils. Part of this study was aimed at characterizing the amount and length distribution of whey protein fibrils as a function of shear rate and protein concentration, and comparing these results with our theoretical prediction for the effect of shear rate on fibril growth. Another part was aimed at the characterization of the flow behaviour of the fibril solutions by viscosity measurements.

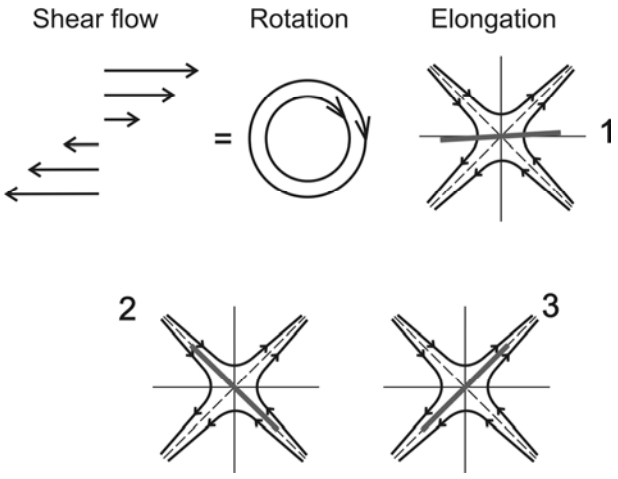

Figure 1. *Schematic representation of shear flow relative to a fibril in three different fibril positions: (1) aligned in the flow direction, (2) aligned along the compressional axis, (3) aligned along the extensional axis.*

THEORY: EFFECT OF SHEAR RATE ON FIBRIL GROWTH

Here, a simple scaling analysis is proposed that semi-quantitatively predicts the effect of shear rate on the growth of fibrils. We limit ourselves to a high Peclet number ($Pe = \dot{\gamma} / D_r >> 1$), and decompose shear flow in a rotational and elongational part of equal intensity (see Figure 1). As a result of the shear flow, the fibrils will be aligned close to the direction of the flow (position 1 of Figure 1), but when the end of a fibril crosses (by rotational diffusion) the local plane of zero shear, it will tumble over 180°. This process will repeat itself, leading to a periodic tumbling motion of a fibril around the direction of shear. The tumbling motion of a fibril was further simplified by assuming that a fibril can take only three different discrete positions, each for a certain time. In the first position, along the direction of shear (duration $t_{aligned}$), no protein monomers will be transported towards the tips of a fibril. In the second position, along the compressional axis of the shear flow (position 2 of Figure 1), protein monomers will be transported towards the fibril tips. Finally, in the third position, along the extensional axis of the shear flow, protein monomers are transported away from the fibril tips (position 3 of Figure 1). The time that a fibril is in aligned position ($t_{aligned}$) correlates with:[19]

$$t_{aligned} \sim Pe^{-2/3} \cdot D_r^{-1} \quad (1)$$

The tumbling time (t_{tumble}) correlates with:[19]

$$t_{tumble} \sim \pi / \dot{\gamma} \quad (2)$$

The total supply (S) of protein monomers towards a fibril tip during one tumbling motion is given by:

$$S \sim t_{tumble} \cdot c_m \cdot d^2 \cdot v \quad (3)$$

In this equation, d is the diameter of the fibril (being approximately equal to the diameter of a protein monomer), c_m is the concentration of protein monomers and v is the velocity at the tip of a fibril. In the elongational flow field, v will increase

Figure 2*. Shearing device with rotating inner cylinder (left) and static outer cylinder (right).*

linearly with fibril length (L) and shear rate ($\dot{\gamma}$). For high shear rates, the flux J towards the fibril tip is now approximated by:

$$J = \frac{S}{t_{tumble} + t_{aligned}} \sim c_m \cdot d^2 \cdot L \cdot \dot{\gamma}^{2/3} \cdot D_r^{1/3} \qquad (4)$$

Based on Equation 4, we expect an increase in supply of fibril material that scales as $\sim \dot{\gamma}^{2/3}$. Equation 4 describes the orthokinetic flux towards the fibril tips. In addition to the orthokinetic flux, there will also be diffusion of protein monomers towards the fibril tips even when no flow is applied (perikinetic flux). The orthokinetic flux is thus an additional contribution to the total flux of protein monomers towards the fibril tips.

MATERIAL AND METHODS

Stock solution of whey protein isolate (Bipro)

WPI, Bipro, was obtained from Davisco Foods International, Inc. (Le Sueur, MN, USA). A stock solution of Bipro was made by dissolving the protein in MilliQ water. After dissolving, the solution was set to pH 2 by adding a concentrated HCl solution (Merck, Darmstadt, Germany). To remove any undissolved protein, the solution was centrifuged at 19,000 g (rotor JA-14, J2-MC centrifuge, Beckman,

Fullerton, CA, USA) for 30 min at 4 °C, and filtered through a membrane (pore size 0.45 μm, diameter 100 mm, Schleicher & Schuell, Dassel, Germany). Traces of electrolytes were removed by dialysing the solution against a HCl solution of pH 2 until the ionic strength of the protein solution was equal to the solvent. For the dialysis, a membrane (Hemodialyzer, Cobe Nephross B.V., Boxtel, The Netherlands) was used with a pore size of 10 kDa. The nitrogen content of the protein solution was determined using Dumas analysis (NA 2100 Protein, CE instruments, Milan, Italy) according to the manufacturer's instructions, and was converted into protein concentration using a conversion factor of 6.38 for WPI.

Shearing device

To perform heating and shearing simultaneously while avoiding water evaporation, a shearing device with a Couette geometry was developed. Figure 2 shows a picture of this device. The device was made from titanium. The diameter of the inner cylinder was 40 mm and the length 145.5 mm. The diameter of the outer cylinder was 42 mm and the length was 148.5 mm. The top and bottom of the shearing device were designed as a cone-and-plate geometry with an angle of 2.8°. Due to this angle, the shear rate between the cone and plate is comparable to the shear rate between the two cylinders. The volume of the shearing device was 18 ml. The inner cylinder of the shearing device was rotated with a mechanical stirrer (type 2041, Heidolph Instruments, Schwabach, Germany) and the cell was heated by placing it in a water bath (Tamson 2500, Labovisco B.V., Zoetermeer, The Netherlands).

Experimental set-up

Table 1 gives an overview of the experiments that were performed during this study. All samples were heated for 2 h at 90 °C, and during this heat treatment, continuous shear treatment was applied. The shear rates ($\dot{\gamma}_p$) varied from 0 to 673 s^{-1}, and the whey protein concentration ranged from 0.5 to 5.2 wt%. Replicate experiments were performed for all samples with a protein concentration of 5.2 wt%. After heating, the samples were cooled and kept for 1 h at room temperature. All samples were placed between two crossed polarizers to observe whether the

fibril solutions obtained were optically isotropic or birefringent. The flow-induced birefringence was measured to analyse the amount and length distribution of fibrils. The samples with a whey protein concentration of 5.2 wt% were characterized in more detail using TEM and by measuring the steady shear viscosity.

Flow-induced birefringence

Optical measurements were performed with a strain-controlled ARES rheometer (Rheometric Scientific Inc., Piscataway, USA) with Couette geometry (rotating cup with a diameter of 33.8 mm and a static bob with a diameter of 30.0 mm). A laser beam of wavelength 670 nm passed vertically through the gap between the cup and the bob, and the birefringence was measured with a modified optical analysis module.[20] The analysis was performed in a temperature-controlled room at 20 °C.

To characterize the amount of fibrils, the flow-induced birefringence was measured at a shear rate, $\dot{\gamma}_{b1}$, of 73 s^{-1} for 30 s, which was sufficient to obtain a constant birefringence. At complete alignment of the fibrils, the flow-induced birefringence (Δn) is proportional to the total length concentration of the fibrils:[21]

$$\Delta n = M \int c_L dL \tag{5}$$

Here, c_L is the contribution to the total length per unit volume in the system as a result of the fibrils with a length between L and $L+dL$. The constant M is the contribution to the birefringence per unit length concentration and was determined for β-lactoglobulin fibrils by Rogers et al.[21] Since whey protein fibrils consist mainly of β-lactoglobulin,[12] the value of M for β-lactoglobulin was used for whey protein fibrils as well.

Most samples contained permanent birefringent domains and thus were not isotropic fibril solutions. The presence of birefringent domains had an effect on the flow-induced birefringence, because these samples showed residual birefringence if no flow was applied. Therefore, these fibril solutions were diluted to isotropic fibril solutions to measure the flow-induced birefringence only, and afterwards, the birefringence was multiplied by the dilution factor to obtain the birefringence

of the undiluted sample. Flow dichroism was found to be negligible for all samples.

Fibril length distribution

Rogers et al.[21] developed a method to derive the length distribution of β-lactoglobulin fibrils from the decay of flow-induced birefringence after cessation of the flow. With this method, only the length of fibrils in the semi-dilute concentration regime can be measured. To determine the length distribution of the fibrils, the samples were subjected to steady shear flow at a shear rate of 2.3 s^{-1} ($\dot{\gamma}_{b2}$) for 60 s, and after cessation of the flow, the decay of birefringence was measured. This shear rate is lower than the shear rate ($\dot{\gamma}_{b1}$) used to detect the amount of fibrils, because it is a compromise between maximal alignment of fibrils in the semi-dilute regime, and avoiding alignment of fibrils in the dilute regime or stretching of the semi-flexible fibrils.

Table 1. *Results of analysis with crossed polarizers for samples prepared at different protein concentrations and shear rates.*

Concentration (wt%)	Shear rate during heating $\dot{\gamma}_p$ (s^{-1})					
	0	84	168	337	505	673
0.5	I [a]	I	I	B1[b]		
1	I	B1	I	I		
2	I	B1	B1	B1		
3	B1			B2[c]		B3[d]
4	B2			B3		B3
5.2	B2	B3	B3	B3	B3	B3

The samples were observed against natural light without flow.

[a] I = isotropic solution: no birefringence in rest

[b] B1 = solution with few small birefringent domains (colour: white)

[c] B2 = solution with many small birefringent domains (colour: white, purple and blue)

[d] B3 = solution with few large birefringent domains (colour: white)

Viscosity

The steady shear viscosity was measured on a rheometer (MCR 301, Anton Paar, Graz, Austria) with a Couette geometry (static cup with a diameter of 28.92 mm and a rotating bob with a diameter of 26.7 mm). Rate sweeps were performed with a shear rate ($\dot{\gamma}_v$) varying between 0.01 and 100 s^{-1} (5 points per decade). Each shear rate was applied for 60 s, and during the last 6 s of this time period, the viscosity was measured. In this way, transient effects were excluded.

Transmission Electron Microscopy

TEM grids were prepared by negative staining immediately after the preparation of the samples. The samples were diluted 100 times. A droplet of the diluted sample was put onto a carbon support film on a copper grid. After 15 s, the droplet was removed with a filter paper. Then, a droplet of 2% uranyl acetate (SIGMA, Steinheim, Germany) was put onto the grid and removed after 15 s. The micrographs were made with a Philips CM 12 electron microscope operating at 80 kV (Eindhoven, The Netherlands).

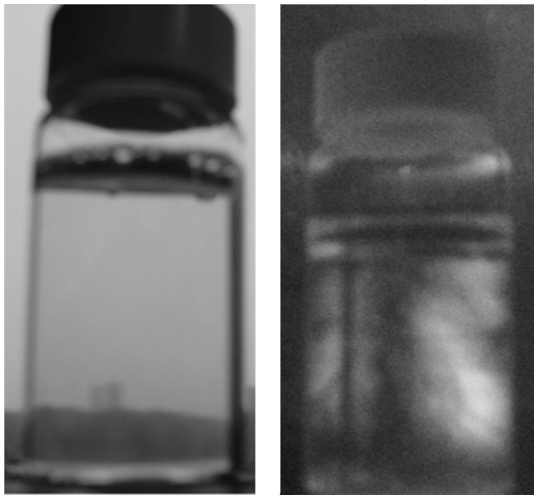

***Figure 3**. Pictures of a sample (4 wt% whey protein, shear rate of $\dot{\gamma}_p$ = 673 s^{-1}) without crossed polarizers (left) and between crossed polarizers (right).*

RESULTS

Isotropic and birefringent fibril solutions

After preparation, all samples were kept between two crossed polarizers and observed against natural light (Table 1). A few samples were isotropic (depicted in Table 1 as type I), but most samples contained birefringent domains. Although a full characterization of these domains was outside the scope of this study, clear differences could be observed between the samples with respect to the typical size and colour of the birefringent domains. The samples that were prepared with protein concentrations between 0.5 and 3wt% contained a few small white domains. Other samples contained many small white, purple and blue birefringent domains (depicted in Table 1 as type B2). The remaining samples contained a few large white domains (type B3) with a size in the same order of magnitude as the test tubes. This 'type B3' was observed for samples with the two highest protein concentrations (4 and 5.2 wt%) and for one sample with 3wt%, all prepared with shear flow. Figure 3 shows a picture of one of these samples (4 wt% protein concentration prepared at a shear rate of 673 s^{-1}). The picture on the left was taken without crossed polarizers and shows that the sample is transparent. The other picture was taken with the sample between crossed polarizers; large birefringent domains are visible.

Recent work of Bolder et al.[12] showed that solutions of whey protein fibrils contained birefringent polydomains when fibrils were prepared at high protein concentration without applying flow. These domains were only observed by the authors above a protein concentration of 7 wt%, and above this concentration, gelation also occurred. In our experiments, these domains were observed in samples with protein concentrations varying from 0.5 to 5.2 wt%, and the samples were still liquid-like solutions. This difference is probably due to the different preparation method.

Amount of fibrils

The effect of shear flow on the amount of fibrils was studied for whey protein concentrations in the range of 0.5-5.2 wt%. Figure 4 shows the birefringence

versus protein concentration for solutions prepared with and without shear flow. The use of shear flow resulted in a higher amount of fibrils, and this enhancing effect starts around a protein concentration of 3%. Below this protein concentration, the use of shear flow did not result in more fibrils. At higher concentrations (4 and 5.2 wt%), the effect of shear flow became more pronounced. Remarkably, preparation at the highest shear rate ($\dot{\gamma}_p$ = 673 s^{-1}) resulted in less fibrils than preparation at a lower shear rate ($\dot{\gamma}_p$ = 337 s^{-1}).

To study the effect of shear rate in more detail, Figure 5 shows the birefringence versus shear rate ($\dot{\gamma}_p$) for solutions of 5.2 wt% whey protein. The expected dependence of amount of fibrils as a function of shear rate is also plotted ($\sim \dot{\gamma}^{2/3}$). Initially, the amount of fibrils increased as a function of shear rate and the increase is comparable to the expected increase. However, above a shear rate of $\dot{\gamma}_p$ =337 s^{-1}, the birefringence decreased as a function of shear rate. The variation in replicate measurements was small for most shear rates, but for the two lower shear rates ($\dot{\gamma}_p$ = 84 and 168 s^{-1}), the variations were larger.

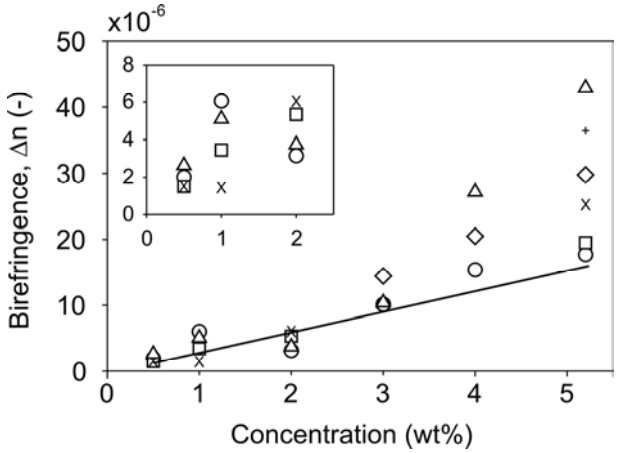

Figure 4*. Birefringence versus protein concentration after heat treatment for 2 h at different shear rates: (○) 0 s^{-1}, (□) 84 s^{-1}, (x)168 s^{-1}, (Δ) 337 s^{-1}, (+) 505 s^{-1} and (◇) 673 s^{-1}. Replicate experiments were performed at a protein concentration of 5.2 wt%, and the standard deviations of these data are given by the error bars in Figure 5. The line represents a linear trend fitted through the data of 0 s^{-1}.*

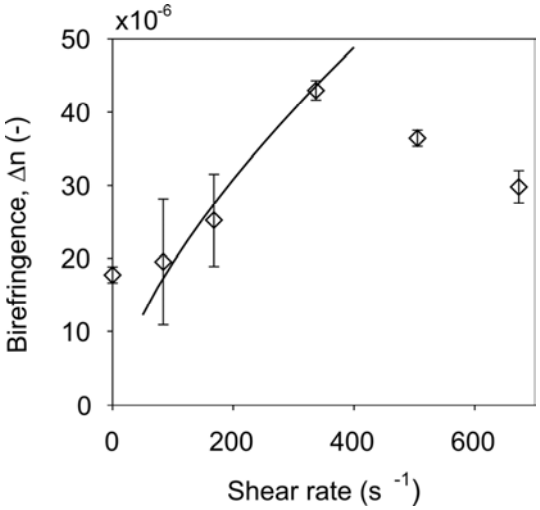

Figure 5*. Birefringence after a heat and shear treatment (2 h 90 °C) of solutions with a whey protein concentration of 5.2% at different shear rates. The error bars indicate the standard deviation of the measurements. The line represents scaling with* $\sim \dot{\gamma}^{2/3}$.

Length distributions of fibrils

From the decay of birefringence after cessation of the flow, length distributions were obtained. Figures 6a-e show the length distribution curves for protein concentrations ranging from 0.5 to 4 wt%. In each figure, the curves are shown for the samples prepared at different shear rates. No clear effect of shear flow or protein concentration on the fibril length distributions was observed for concentrations up to 3 wt%. The differences between the curves were mainly due to different fibril concentrations in the samples. Above a protein concentration of 4wt%, a higher shear rate resulted in a shift of the length distribution to smaller fibril lengths.

The curves were clearly different for a protein concentration of 1 wt%. The fibrils of $\dot{\gamma}_p$ = 0 and 337 s^{-1} were smaller than the fibrils of $\dot{\gamma}_p$ = 84 s^{-1}. In case of $\dot{\gamma}_p$ = 168 s^{-1}, the decay of birefringence was too fast and not suitable for obtaining a length distribution. This fast decay of birefringence was due to the low amount of fibrils present in this sample, which can be observed by the low birefringence signal for this sample in Figure 4. Figure 4 also showed that the amount of fibrils

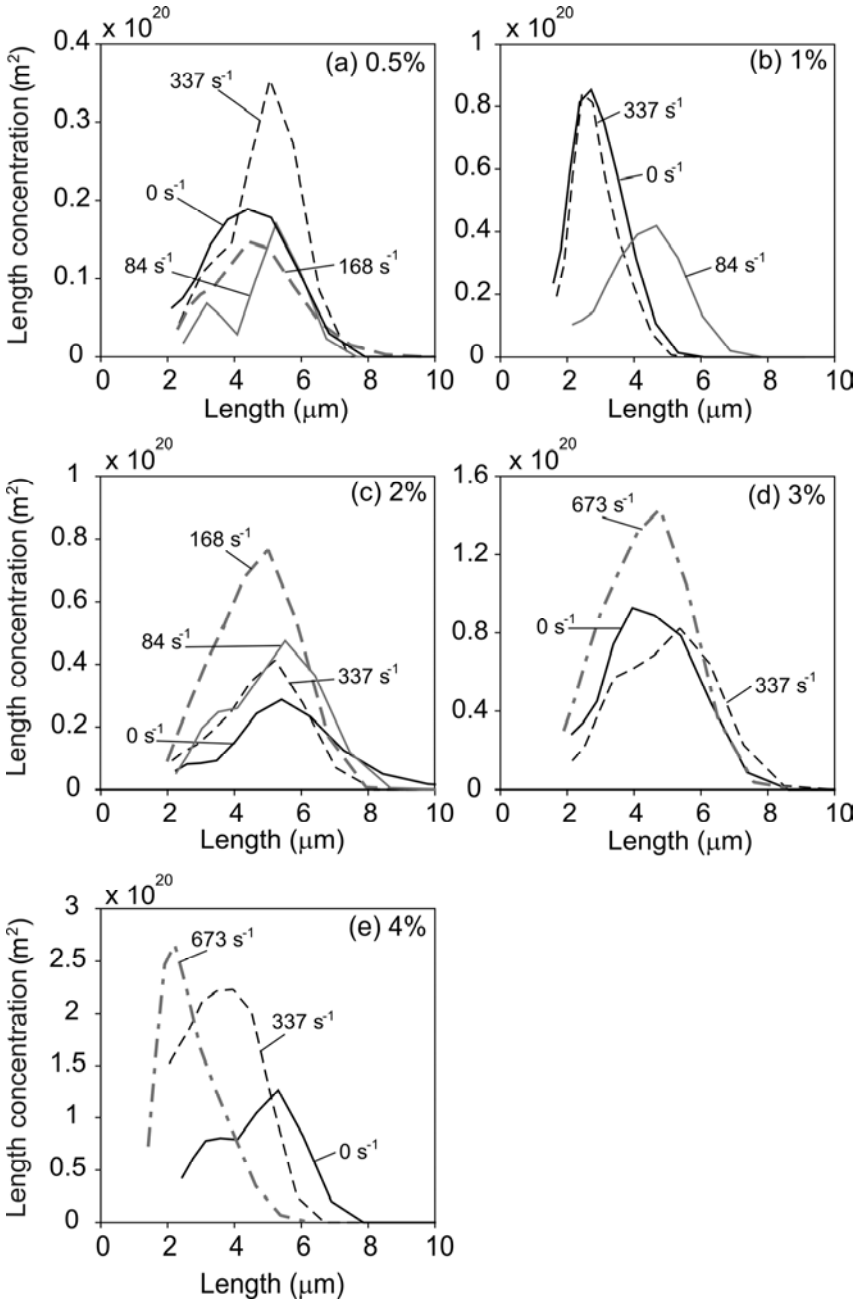

***Figure 6**. Length distribution curves of the samples prepared at different protein concentrations and different shear rates ($\dot{\gamma}_p$): (a) 0.5 wt%, (b) 1 wt%, (c) 2 wt%, (d) 3 wt% and (e) 4 wt%.*

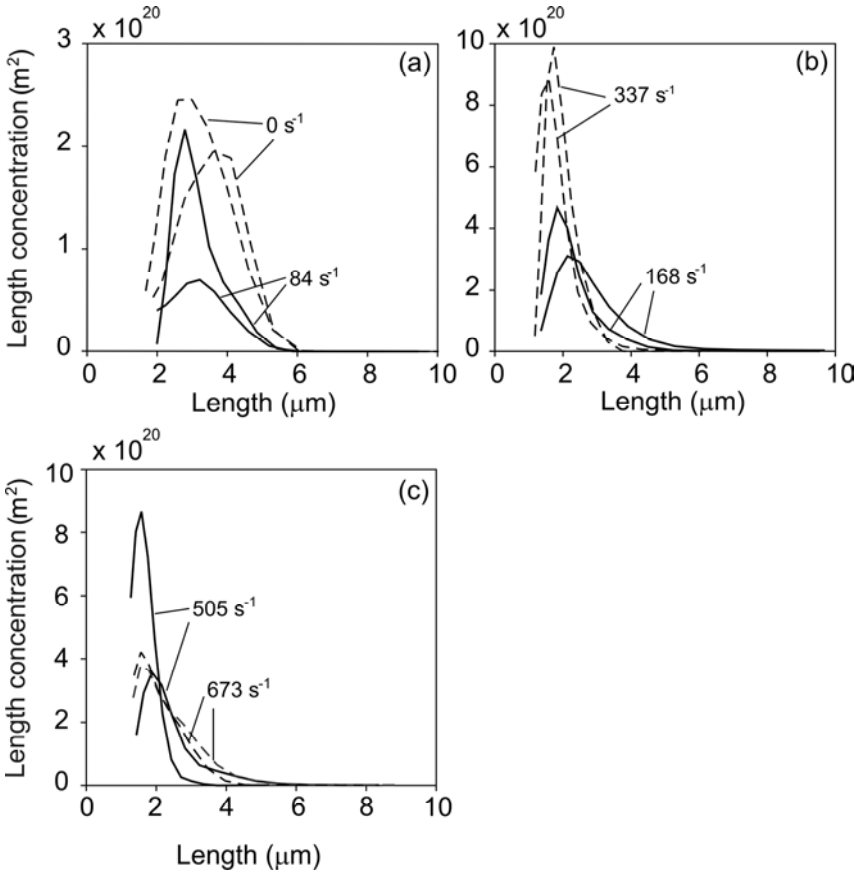

Figure 7*. Length distributions of fibrils of 5.2 wt% whey protein prepared at different shear rates: (a)* $\dot{\gamma}_p$ *= 0 and 84 s*$^{-1}$*, (b)* $\dot{\gamma}_p$ *= 168 and 337 s*$^{-1}$ *and (c)* $\dot{\gamma}_p$ *= 505 and 673 s*$^{-1}$*.*

was higher for $\dot{\gamma}_p$ = 0 and 337 s^{-1} than for the other two shear rates. We do not have an explanation at this time for this difference in amount and fibril length at these specific conditions.

Figures 7a-c show the length distributions of samples with a protein concentration of 5.2 wt% prepared at various shear rates. For most shear rates, the length distributions of duplicate experiments were comparable, except for the samples prepared at shear rates of 84 and 505 s^{-1}. Despite this variation (which seems to be inherent of the fibrillization process itself), clear trends can be observed between the samples. Up to a shear rate of $\dot{\gamma}_p$ = 337 s^{-1}, the peak of the length distribution

shifted to smaller fibril lengths while the polydispersity decreased with increasing shear rate. Above $\dot{\gamma}_p$ = 337 s^{-1}, the position of the peak did not change anymore, but the polydispersity started to increase. Figures 8a-d show TEM pictures of fibrils after treatment at different shear rates. These pictures show semi-flexible fibrils with length in the order of μm. Overlapping of the fibrils is due to the fixation method of the fibrils onto the TEM-grid and does not reflect the true state of the fibrils in the solution. These pictures confirm the results of the length distribution measurements, because smaller fibrils were present in the samples prepared at high shear rates ($\dot{\gamma}_p$ = 337 and 505 s^{-1}) compared with samples prepared without shear flow and at a low shear rate ($\dot{\gamma}_p$ = 168 s^{-1}).

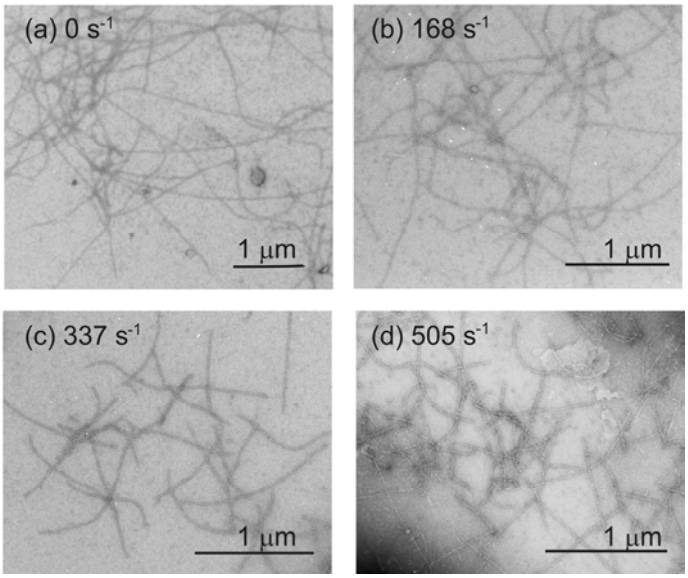

***Figure 8**. TEM pictures of fibrils of 5.2 wt% whey protein after heat treatment (2 h at 90 °C) at different shear rates: (a) $\dot{\gamma}_p$ = 0 s^{-1}, (b) $\dot{\gamma}_p$ = 168 s^{-1}, (c) $\dot{\gamma}_p$ = 337 s^{-1} and (d) $\dot{\gamma}_p$ = 505 s^{-1}.*

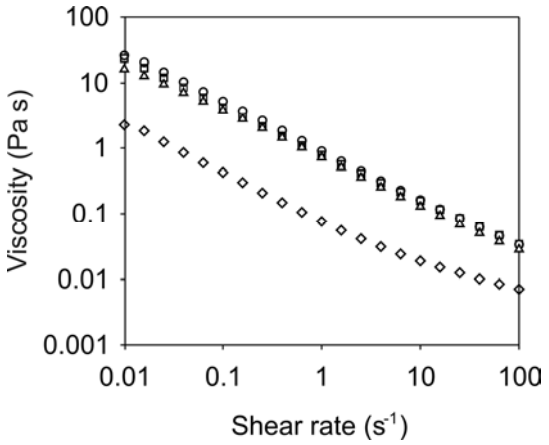

***Figure 9**. Flow curves for solutions of 5.2 wt% whey protein prepared at different shear rates ($\dot{\gamma}_p$): (◇) 0 s^{-1}, (□) 168 s^{-1}, (○) 337 s^{-1} and (Δ) 673 s^{-1}.*

Rheological properties of whey protein fibrils

Steady shear viscosity measurements were performed to study the flow behaviour of fibril solutions. Figure 9 shows the flow curves for solutions containing 5.2 wt% protein, which were prepared at different shear rates ($\dot{\gamma}_p$: 0, 168, 337 and 673 s^{-1}). Dilutions of two of these samples (5.2 wt% prepared at $\dot{\gamma}_p$ = 0 and 337 s^{-1}) were made. Figures 10 and 11 ($\dot{\gamma}_p$ = 0 s^{-1} and $\dot{\gamma}_p$ = 337 s^{-1}, respectively) show the flow curves for these dilutions. Shear thinning behaviour was observed for all fibril solutions. A Newtonian plateau at low shear rates was not observed, indicating that the fibrils already aligned at the lowest shear rate applied.

Dilution of the samples led to a reduced viscosity, which is typical for rod-like macromolecules.[22] The viscosities of the samples prepared at different (non-zero) shear rates, shown in Figure 9, were all higher than the viscosity of the sample prepared without shear flow. The flow curves of the samples prepared at different shear rates overlapped with each other. Also, the flow curves of samples prepared at $\dot{\gamma}_p$ = 84 and 505 s^{-1} overlapped with the flow curves of the other shear rates, but these curves are not depicted in Figure 9. As shown in Figures 5 and 7, the amount of fibrils and fibril length distributions varied between these samples, but this variation did not result in different flow behaviour. This suggests that these

samples contained domains of fibrils (reflecting the results of Table 1) that dominated the flow behaviour, instead of the individual fibrils. Thus, differences in fibril length or amount will not influence the flow curves.

A power law model ($\eta \sim \dot{\gamma}^{-n}$) was fitted to parts of the flow curves of Figures 9-11. The power law indices of the curves shown in Figure 9 were all between 0.71 and 0.74. These values are comparable to the reported power law indices of xanthan solutions around the transition from isotropic to biphasic regime.[23] This supports our suggestion that the concentrated solutions contained liquid-crystalline polydomains, at least to some degree. The solid lines in Figures 10 and 11 indicate which parts of the curves scaled according to this power law model. At high shear rates, the flow curves deviated from the power law model, because the viscosity approached the solvent viscosity. The values of the power law indices of the diluted samples ranged between 0.25 and 0.64, and are comparable to power law indices found for isotropic xanthan solutions by Lee and Brant.[23]

The fitted power law indices of the curves shown in Figures 10 and 11 are plotted against the birefringence of the different diluted samples in Figure 12. The power law indices decreased when the fibril solutions were diluted to lower fibril concentrations. When samples of comparable birefringence are compared, the power law indices of the samples prepared at a shear rate of 0 s^{-1} were higher than the power law indices of the samples prepared at a shear rate of 337 s^{-1}. An explanation for this observation is that the sample prepared at $\dot{\gamma}_p$ = 0 s^{-1} contained longer fibrils than the sample prepared at $\dot{\gamma}_p$ = 337 s^{-1} (see Figures 7a and b for the length distributions), resulting in a higher degree of shear thinning.

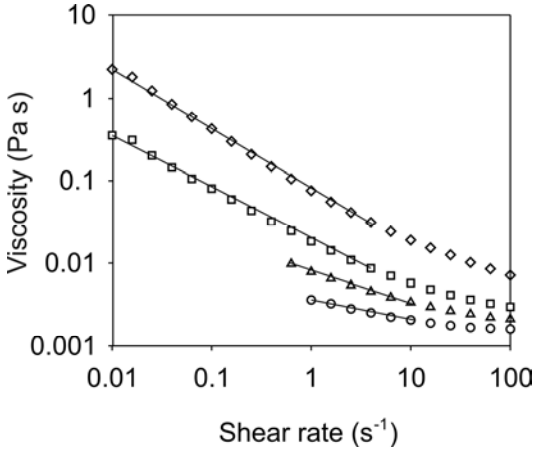

Figure 10. *Viscosity versus shear rate for different dilutions of a sample heated for 2 h at a protein concentration of 5.2 wt% and a shear rate of* $\dot{\gamma}_p = 0\ s^{-1}$*: (◇) c = 100%,* $\Delta n = 19 \cdot 10^{-6}$ *(undiluted), (□) c = 50%, (Δ) c = 25% and (○) c = 12.5%. The black lines indicate the parts of the curves that scale according to the power law model (*$\eta \sim \dot{\gamma}^{-n}$*).*

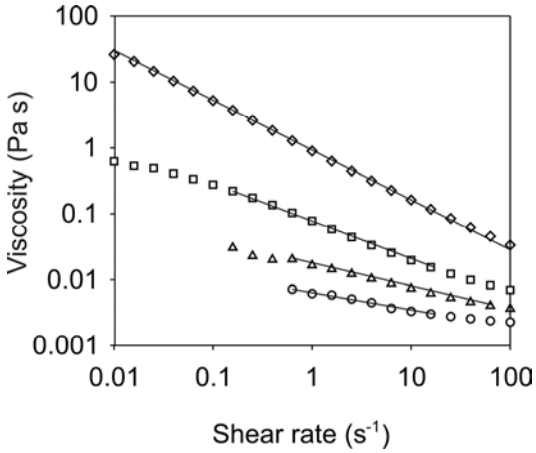

Figure 11. *Viscosity versus shear rate for different dilutions of a sample heated for 2 h at a protein concentration of 5.2 wt% and a shear rate of* $\dot{\gamma}_p = 337\ s^{-1}$*: (◇) c = 100%,* $\Delta n = 44 \cdot 10^{-6}$*, (undiluted), (□) c = 50%, (Δ) c = 25% and (○) c = 12.5%. The black lines indicate the parts of the curves that scale according to the power law model (*$\eta \sim \dot{\gamma}^{-n}$*).*

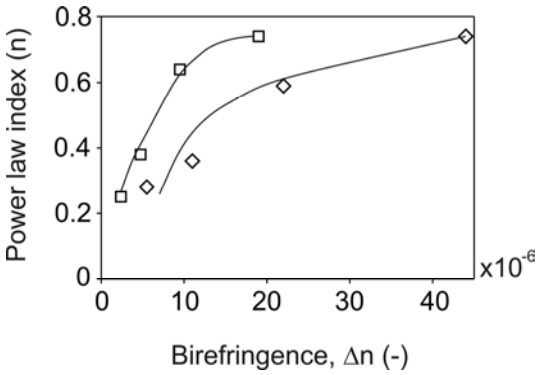

***Figure 12**. Power law indices versus birefringence, Δn, of the curves shown in Figure 10 ((□) $\dot{\gamma}_p$ = 0 s^{-1}) and 11 ((◇) $\dot{\gamma}_p$ = 337 s^{-1}). The lines indicate the general trends of the data.*

DISCUSSION

Effect of shear rate on fibril formation

The results in Figure 5 (protein concentration of 5.2 wt%) showed that the total fibril length concentration (as measured with birefringence) increased as a function of shear rate up to a shear rate of $\dot{\gamma}_p$ = 337 s^{-1}. The increase in birefringence as a function of the shear rate was comparable to the estimated increase in the theoretical section ($\sim \dot{\gamma}^{2/3}$). However, above a shear rate of $\dot{\gamma}_p$ = 337 s^{-1}, the birefringence decreased with increasing shear rate. This decrease was also observed at a protein concentration of 4 wt% (Figure 4). This result indicates that another process is also affecting the fibril formation in an opposing effect of shear. A possible explanation for this observation is that at a higher shear rate, part of the bonds between proteins in fibrils can break in the elongational part of the shear flow. Especially, the initial bonds between proteins in fibrils are rather weak,[5] and we believe that these initial weak bonds can be broken by the elongational component of shear flow. At a later stage, the fibrils have matured and the hydrogen bonds between the β-strands within the β-sheets are established.[10] We tested whether these matured fibrils can be broken by shear flow by subjecting a sample containing mature fibrils to a heat (2 h, 90 °C) and shear treatment ($\dot{\gamma}_p$ =

673 s^{-1}), but no changes in the amount and length distribution were observed. This shows that the mature fibrils cannot be broken by the shear flow.
An effect of shear flow was only observed at high protein concentrations, but at low protein concentrations (0.5-2 wt%), no effect of shear flow was observed. Apparently, the contribution of orthokinetic flux is not large at low protein concentrations. Also, a rather large variation in results seems to be inherent to the fibril formation process. Therefore, it is possible that the effect of shear flow was too small to be measured for these protein concentrations.

The effect of fibril concentration on viscosity

The flow curves of the undiluted samples (5.2 wt% protein) prepared with shear flow overlapped even though the amount of fibrils in the samples varied (Figure 9). This behaviour is different from the behaviour depicted in Figures 10 and 11, where a lower viscosity was observed for a lower concentration of fibrils. In Figure 13, the viscosity measured at three different shear rates ($\dot{\gamma}_v$) is plotted against the total fibril length concentration (birefringence) of the data of Figures 9-11. Two regions can be observed in this graph. One region (I) shows an exponential increase in viscosity with increasing total fibril length concentration, which seems to level off to a plateau at higher fibril concentrations. A second region (II) has a higher viscosity than the viscosity of region I, and the viscosity remained constant even if the total fibril length concentration increased. In this region, the undiluted samples are depicted of which the flow curves overlapped (Figure 9). A grey area in Figure 13 indicates the fibril concentration below which the samples were isotropic. This transition does not coincide with the transition from region I to region II. This suggests that the phase transition from isotropic fibril solutions to solutions containing birefringent polydomains did not result in a sudden change in viscosity. Plots similar to Figure 13 were reported for xanthan solutions,[23,24] and rigid rod cellulose suspensions.[25] For all these systems, the viscosities of isotropic solutions increased as a function of the fibril concentration in the same way as the viscosities of the fibril solutions of region I in Figure 13. This means that even though part of the samples of Figure 13 was not fully

isotropic, the birefringent polydomains present in the samples did not dominate the viscosity.

All samples of region II were subjected to shear flow (5.2 wt% protein) during preparation. The birefringent domains of the samples prepared with shear flow were larger (type B3 in Table 1) than the domains in the samples prepared without shear flow and/or at lower fibril concentrations (types B1 and B2 in Table 1). A possible explanation for the sudden and drastic increase in viscosity is that by applying shear flow, the fibrils were arranged into a different type of polydomains than without flow. We do not think that these solutions were already fully liquid-crystalline, because then one would expect a decrease in viscosity at higher fibril concentrations, which was for example observed for xanthan solutions,[23,24] and also predicted theoretically.[26] Future investigation should elucidate the exact nature of the ordering in region II.

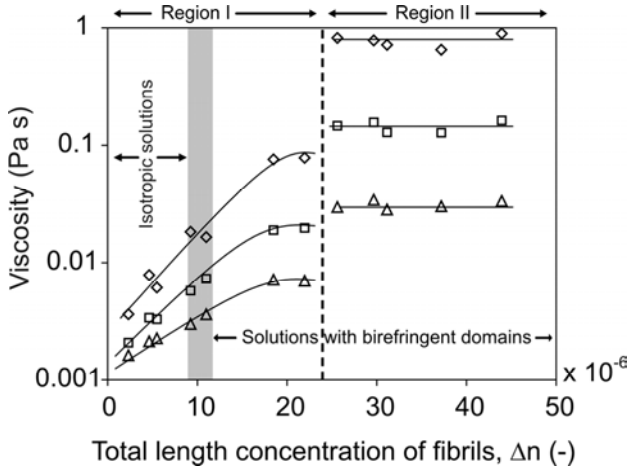

Figure 13. *Viscosities measured at different shear rates ($\dot{\gamma}_v$) plotted versus the total length concentration of fibrils (birefringence at $\dot{\gamma}_{b1}$ = 73 s^{-1}): (◇) $\dot{\gamma}_v$ = 1 s^{-1}, (□) $\dot{\gamma}_v$ = 10 s^{-1} and (Δ) $\dot{\gamma}_v$ = 100 s^{-1}.*

CONCLUSIONS

Simple shear flow can be an important parameter for influencing the properties of solutions of fibrillar whey protein aggregates. The amount of fibrils can be maximized by using the optimal shear rate and a sufficiently high protein concentration. The length of the fibrils can only be influenced to a minor extent; and if it occurs, shear flow leads to shorter fibrils. The viscosity of the resulting fibril solutions can be increased by the use of shear flow. Above a critical fibril concentration, the viscosity of fibril solutions was independent of the amount of fibrils. Possibly, the shear flow resulted here in a different packing of fibrils in polydomains of fibrils, leading to an increased viscosity.

ACKNOWLEDGEMENTS

The authors thank H. Baptist and the Virology department of Wageningen University (J. van Lent and H. Bloksma) for their assistance with the TEM analysis. We also thank H. Gruppen and J. Vereijken for the useful discussions about this research. We acknowledge the Dutch research school VLAG and the Dutch research programme MicroNed for the financial support of this research.

NOMENCLATURE

$\dot{\gamma}_{b1}$	shear rate (73 s^{-1}) during birefringence measurements: amount of fibrils
$\dot{\gamma}_{b2}$	shear rate (2.3 s^{-1}) during birefringence measurements: fibril length distribution
$\dot{\gamma}_{p}$	shear rate during sample preparation (s^{-1})
$\dot{\gamma}_{v}$	shear rate during viscosity measurements (s^{-1})
η	viscosity (Pa s)
c	fibril concentration: percentage of undiluted sample (%)
c_L	length concentration of fibrils (m^{-2})
c_m	concentration of protein monomers (m^{-3})
d	diameter of protein monomer (m)
D_r	rotational diffusion coefficient of fibril (s^{-1})
J	flux of monomers towards fibril tips due to shear flow (s^{-1})

L	fibril length (m)
Δn	birefringence (dimensionless)
n	power law index (dimensionless)
M	contribution to the birefringence per unit length concentration (m^2)
Pe	Peclet number (dimensionless)
S	supply of protein monomers towards fibril tip (dimensionless)
$t_{aligned}$	time fibrils spend in aligned position (s)
t_{tumble}	tumbling time of fibrils (s)
v	velocity at the tip of fibril (m s^{-1})

REFERENCES

1. Durand, D.; Gimel, J.C.; Nicolai, T. Aggregation, gelation and phase separation of heat denatured globular proteins. *Physica A* **2002**, 304, 253-265.
2. Veerman, C.; De Schiffart, G.; Sagis, L.M.C.; Van der Linden, E. Irreversible self-assembly of ovalbumin into fibrils and the resulting network rheology. *International Journal of Biological Macromolecules* **2003**, 33, 121-127.
3. Arnaudov, L.N.; De Vries, R. Thermally induced fibrillar aggregation of hen egg white lysozyme. *Biophysical Journal* **2005**, 88, 515-526.
4. Veerman, C.; Sagis, L.M.C.; Heck, J.; Van der Linden, E. Mesostructure of fibrillar bovine serum albumin gels. *International Journal of Biological Macromolecules* **2003**, 31, 139-146.
5. Arnaudov, L.N.; De Vries, R.; Ippel, H.; Van Mierlo, C.P.M. Multiple steps during the formation of β-lactoglobulin fibrils. *Biomacromolecules* **2003**, 4, 1614-1622.
6. Gosal, W.S.; Clark, A.H.; Pudney, P.D.A.; Ross-Murphy, S.B. Novel amyloid fibrillar networks derived from a globular protein: β-lactoglobulin. *Langmuir* **2002**, 18, 7174-7181.
7. Kavanagh, G.M.; Clark, A.H.; Ross-Murphy, S.B. Heat-induced gelation of globular proteins: part 3. Molecular studies on low pH β-lactoglobulin gels. *International Journal of Biological Macromolecules* **2000**, 28, 41-50.
8. Veerman, C.; Ruis, H.; Sagis, L.M.C.; Van der Linden, E. Effect of electrostatic interactions on the percolation concentration of fibrillar β-lactoglobulin gels. *Biomacromolecules* **2002**, 3, 869-873.
9. Sagis, L.M.C.; Veerman, C.; Van der Linden, E. Mesoscopic properties of semiflexible amyloid fibrils. *Langmuir* **2004**, 20, 924-927.

10. Bromley, E.H.C.; Krebs, M.R.H.; Donald, A.M. Aggregation across the length-scales in β-lactoglobulin. *Faraday Discussions* **2005**, 128, 13-27.

11. Dirix, C.; Meersman, F.; MacPhee, C.E.; Dobson, C.M.; Heremans, K. High hydrostatic pressure dissociates early aggregates of TTR105-115, but not the mature amyloid fibrils. *Journal of Molecular Biology* **2005**, 347, 903-909.

12. Bolder, S.G.; Hendrickx, H.; Sagis, L.M.C.; Van der Linden, E. Fibril assemblies in aqueous whey protein mixtures. *Journal of Agricultural and Food Chemistry* **2006**, 54, 4229-4234.

13. Rochet, J.C.; Lansbury Jr, P.T. Amyloid fibrillogenesis: theme and variations. *Current Opinion in Structural Biology* **2000**, 10, 60-68.

14. Hamada, D.; Dobson, C.M. A kinetic study of β-lactoglobulin amyloid fibril formation promoted by urea. *Protein Science* **2002**, 11, 2417-2426.

15. Nielsen, L.; Khurana, R.; Coats, A.; Frokjear, S.; Brange, J.; Vyas, S.; Uversky, V.N.; Fink, A.L. Effect of environmental factors on the kinetics of insulin fibril formation: elucidation of the molecular mechanism. *Biochemistry* **2001**, 40, 6036-6046.

16. Hill, S.E.; Krebs, B.; Goodall, D.G.; Howlett, G.J.; Dunstan, D.E. Shear flow induces amyloid fibril formation. *Biomacromolecules* **2006**, 7, 10-13.

17. Akkermans, C.; Venema, P.; Rogers, S. S.; Van der Goot, A. J.; Boom, R.M.; Van der Linden, E. Shear pulses nucleate fibril aggregation. *Food Biophysics* **2006**, 1, 144-150.

18. Stathopulos, P.B.; Scholz, G.A.; Hwang, Y.M.; Rumfeldt, J.A.O.; Lepock, J.R.; Meiering, E.M. Sonication of proteins causes formation of aggregates that resemble amyloid. *Protein Science* **2004**, 13, 3017-3027.

19. Bruinsma, R.; Gelbart, W.M.; Ben-Shaul, A. Flow-induced gelation of living (micellar) polymers. *Journal of Chemical Physics* **1992**, 96, 7710-7727.

20. Klein, C.; Venema, P.; Sagis, L.M.C.; Van Dusschoten, D.; Wilhelm, M.; Spies, H.W.; Van der Linden, E.; Rogers, S.S.; Donald, A.M. Rheo-optical measurements by Fast Fourier Transform and Oversampling. *Applied Rheology* **2007**, 17, 45210-1 - 45210-7.

21. Rogers, S.S.; Venema, P.; Sagis, L.M.C.; Van der Linden, E.; Donald, A.M. Measuring the length distribution of amyloid fibrils: a flow birefringence technique. *Macromolecules* **2005**, 38, 2948-2958.

22. Doi, M.; Edwards, S.F. Dynamics of rod-like macromolecules in concentrated solution. Part 2. *Journal of the Chemical Society - Faraday Transactions 2* **1978**, 74, 918-932.

23. Lee, H.C.; Brant, D.A. Rheology of concentrated isotropic and anisotropic xanthan solutions. 1. A rodlike low molecular weight sample. *Macromolecules* **2002**, 35, 2212-2222.

24. Lee, H.C.; Brant, D.A. Rheology of concentrated isotropic and anisotropic xanthan solutions. 2. A semiflexible wormlike intermediate molecular weight sample. *Macromolecules* **2002**, 35, 2223-2234.

25. Bercea, M.; Navard, P. Shear dynamics of aqueous suspensions of cellulose whiskers. *Macromolecules* **2000**, 33, 6011-6016.

26. Doi, M.; Edwards, S.F. The theory of polymer dynamics. Oxford University Press Inc.: New York, **1986**.

Micrometer-sized fibrillar protein aggregates from soy glycinin and soy protein isolate

Chapter 4

This chapter has been published as: C. Akkermans, A.J. Van der Goot, P. Venema, H. Gruppen, J.M. Vereijken, E. Van der Linden, R.M. Boom. Micrometer-sized fibrillar protein aggregates from soy glycinin and soy protein isolate. Journal of Agricultural and Food Chemistry ***2007****, 55, 9877-9882.*

ABSTRACT

Long, fibrillar semi-flexible aggregates were formed from soy glycinin and soy protein isolate (SPI) when heated at 85 °C and pH 2. Transmission electron microscopy analysis showed that the contour length of the fibrils was ~1 μm, the persistence length 2.3 μm, and the thickness a few nanometers. Fibrils formed from SPI were more branched than the fibrils of soy glycinin. Binding of the fluorescent dye Thioflavin T to the fibrils showed that β-sheets were present in the fibrils. The presence of the fibrils resulted in an increase in viscosity and shear thinning behaviour. Flow-induced birefringence measurements showed that the behaviour of the fibrils under flow can be described by scaling relations derived for rod-like macromolecules. The fibril formation could be influenced by the protein concentration and heating time. Most properties of soy glycinin fibrils are comparable to β-lactoglobulin fibrils.

INTRODUCTION

Many proteins of animal origin give rise to aggregation into long, semi-flexible aggregates. These types of aggregates are interesting as ingredients in food products because they are able to modify various physical properties, such as viscosity, flow behaviour, and gelation on a weight efficient basis. Examples of proteins that can form these fibrils are β-lactoglobulin,[1-5] ovalbumin,[6] BSA,[7] and lysozyme.[8] Since plants are a more sustainable protein source than animals, it becomes interesting to study the capability of plant proteins to form these fibrils.

The most abundant food protein studied with respect to fibril formation is β-lactoglobulin, which aggregates into long, semi-flexible fibrils upon heating above the denaturation temperature, at low pH and low ionic strength.[1-5] The length of the fibrils obtained ranges from 1 to 10 μm, and the thickness is in the order of a few nanometers.[2] Factors that influence the fibril formation are protein concentration, heating time, and shearing or stirring during heating.[9-11] Fibrils with a similar morphology could also be formed from whey protein isolate (WPI),[12] which is a more relevant starting material from an industrial point of view.

Soybeans contain two major storage proteins: glycinin and β-conglycinin. Glycinin consists of five different subunits (MW~20,000-36,000 Da),[13,14] and is completely denatured when heated at 85 °C at pH 3.8 and low ionic strength.[15] β-Conglycinin has three subunits (MW~45,000-72,000 Da).[16] Although long (>1 μm) fibrillar soy protein aggregates have not yet been observed, there have been some studies on the heat-induced gelation of soy protein above and below the isoelectric point. Puppo et al.[17] showed that transparent soy protein isolate gels were formed at pH 2.75 and pH 8 (which hints in the direction of strand-like aggregates). Hermansson[18] observed gels containing shorts strands (~100 nm) after heating at pH 7, for both glycinin gels and β-conglycinin-rich gels.

In this paper, we show that micrometer-sized fibrillar aggregates can be formed from soy glycinin and soy protein isolate. Since most information is available on β-lactoglobulin/ WPI fibrils, we compare the properties of soy protein fibrils with the properties of β-lactoglobulin fibrils. The results described in this paper include a physical characterization of soy glycinin fibrils with the use of transmission

electron microscopy (TEM), flow-induced birefringence, viscosity measurements, and Thioflavin T (ThT) fluorescence. The effect of different parameters (heating time, concentration, and applying shear flow) on the fibril concentration of soy glycinin is explored. Furthermore, the effect of using SPI instead of soy glycinin to obtain these fibrils is studied.

MATERIAL AND METHODS

Soy protein isolation: glycinin and soy protein isolate

This protein isolation method was adapted from Kuipers et al.[19,20] Soybean meal was prepared by milling soybeans (Hyland soybeans, Fa. L.I. Frank, Twello, The Netherlands) in a Fritsch Pulverisette 14702. First, a 4 mm sieve was used and then a 0.5 mm sieve (Fritsch Gmb, Albisheim, Germany). Milling was performed in the presence of liquid N_2 to prevent excessive heating. The soybean meal was defatted five times with hexane at room temperature (w/v ratio SBM/hexane 1:5), followed by drying in air. Hexane was removed from the suspension by filtration.

To isolate the soy protein, a protein extract was prepared by suspending the soybean meal (145 g of meal in 1.5 l of buffer) in a 30 mM Tris-HCl buffer (pH 8), containing 10 mM 2-mercaptoethanol. The suspension was stirred at room temperature for 1.5 h, followed by centrifugation (30 min, 20 °C, 19,000 g, Beckman) and filtration (Whatman, Schleicher & Schuell, type 595½) to remove the insoluble parts.

To obtain soy glycinin, the supernatant was set to pH 6.4 to induce precipitation of glycinin. After stirring for 1 h, the suspension was centrifuged (30 min, 20 °C, 19,000g, Beckman). The precipitate was re-suspended and adjusted to pH 8. After stirring overnight, the protein solution was centrifuged (30 min, 20 °C, 19,000 g, Beckman), and the supernatant was dialyzed (MWCO 12,000-14,000; Visking, Medicell International Ltd.) against demineralised water to remove electrolytes. The pH of the dialyzed solution was set to 8 and the solution was freeze-dried.

To obtain soy protein isolate (SPI), the supernatant of the pH 8 protein extract described above was set to pH 4.8 to induce precipitation of soy proteins. After stirring for 1 h, the suspension was centrifuged (30 min, 20 °C, 19,000 g,

Beckman). The precipitate was washed twice with Millipore water, and after each washing step, the suspension was centrifuged. The precipitate was re-suspended and set to pH 8. After stirring overnight and resetting the pH to 8, the solution was freeze-dried.

The protein content of the isolates was measured using Dumas analysis, using a nitrogen factor of 5.56 for soy glycinin and 5.71 for SPI. The protein content varied between 82 and 88%. The protein composition of soy glycinin and SPI was determined using High-Pressure Size-Exclusion-Chromatography according to the method described by Kuipers et al.[20] Different batches of isolated glycinin were used during this study, and the glycinin content of the batches was between 90 and 94%; the remaining part consisted primarily of β-conglycinin. SPI consisted of 80% glycinin and ~20% β-conglycinin.

Protein stock solutions

Protein stock solutions of glycinin and SPI were made by dissolving the protein in Millipore water. The pH of the solutions was set to 2 by adding a concentrated HCl solution, followed by centrifugation (30 min, 4 °C, 15,000 g, Beckman) and filtration (Minisart, Sartorius, 0.45 μm for soy glycinin, and 1.2 μm for SPI) to remove undissolved protein. The protein concentration of the solutions was measured using Dumas analysis, using a nitrogen factor of 5.56 for soy glycinin and 5.71 for SPI.

Sample preparations

All samples were heated at 85 °C at pH 2 in a titanium shearing device with Couette geometry. Details of this shearing device have been described in a previous paper.[9] The following conditions were used to prepare the samples: heating time of 2 or 20 h, protein concentration of 10, 20, or 40 g/l, and quiescent conditions or shear flow (shear rate of 323 s^{-1}). One sample was prepared from SPI; the rest were prepared from soy glycinin. Table 1 gives an overview of all experiments, and some were performed multiple times to study the experimental variation.

Table 1. *Overview of heating conditions used during this study (all samples were heated at 85 ºC and pH 2).*

Protein	Conc. (g/l)	Time (h)	Shear flow [a]	
Glycinin	10	2	+	–
	10	20	+ *(3)* [b]	– *(2)*
	20	2	+	–
	20	20	+ *(6)*	–
	40	2	+	–
	40	20	+ *(5)*	–
SPI	40	20	+	

[a]Shear flow was applied during heating at a shear rate of 323 s^{-1} (+) or samples were heated without the use of shear flow (–).

[b]The amount of replicate experiments is indicated between brackets.

Flow-induced birefringence

Flow-induced birefringence was measured on a strain-controlled ARES rheometer (Rheometric Scientific) with Couette geometry (rotating cup with a diameter of 33.8 mm and a static bob with a diameter of 30.0 mm). A laser beam of wavelength 670 nm passed vertically through the gap between the cup and the bob. The birefringence was measured with a modified optical analysis module.[21]

The flow-induced birefringence of all samples was measured at a shear rate of 73 s^{-1} for 30 s to characterize the fibril length concentration. For one sample (heating conditions: 20 g/l protein, 20 h, with shear flow), steady shear rate sweeps from 0.01 to 100 s^{-1} were performed on three dilutions of this sample (undiluted, 1.2x diluted, and 1.6x diluted). Each shear rate was applied for 30 s, which was sufficient to obtain a steady birefringence signal.

Fibril concentration from flow-induced birefringence

In order to measure the fibril concentration (amount of proteins aggregated into fibrils), the birefringence signal, Δn, was measured at a shear rate of 73 s^{-1} (see previous section for a description of the birefringence measurement). Assuming full alignment of the fibrils, the birefringence signal could be converted into the fibril concentration using Equation 1.[22]

$$\Delta n = M \cdot \int c_L \cdot dL \quad (1)$$

The constant M (m^2), which depends on the anisotropy in polarizability per unit fibril length, is necessary to convert the birefringence, Δn, into the total fibril length concentration, $c_{L,\mathrm{tot}}$ (m^{-2}) ($c_{L,tot} = \int c_L \, dL$). Equation 2 describes the relation between the total fibril length concentration and the fibril concentration, c_{fib} (in g/m^3).

$$c_{L,tot} = c_{fib} \cdot N_a / (l_{fib} \cdot M_w) \quad (2)$$

In Equation 2, N_a is Avogadro's number and M_w is the molecular mass for which we used 24,700 Da (assuming equal proportions of the five major subunits to be present in the fibrils). For the fibril line density (l_{fib}), the same value that was determined for β-lactoglobulin fibrils was used (0.28×10^9 m^{-1}),[23] because the thickness of the glycinin fibrils seems comparable to β-lactoglobulin fibrils (see Figure 1a).

To be able to use the birefringence signal to calculate the fibril concentration, the value of M is needed for soy glycinin fibrils. Therefore, fibrils and proteins were separated, and the amount of protein that was not present in the fibrils was measured. Since this analysis is time-consuming, it was only done for four samples (heating conditions: protein concentration of 20 g/l, 20 h, with shear flow). The samples were diluted to a protein concentration of 1 g/l, and 2 ml of these diluted samples was filtered using centrifugal filter units (MWCO 100,000; Centricon YM-100, Millipore) (1000 g for 30 min at 20 °C). The retentate was washed twice with pH 2 solution after each centrifugation run to remove non-aggregated protein left in the retentate. The amount of non-aggregated protein was determined from the amount of protein present in the filtrates using Dumas analysis. In the third filtrate, no protein was detected anymore. The difference between the total amount of protein and non-aggregated protein was used as the amount of protein aggregated into fibrils. The amount of protein aggregated into fibrils of these four samples was between 2.5 and 4.3 g/l, and the constant M was calculated to be 2.8×10^{-20} m^2 (using the average fibril concentration and average birefringence of

these samples). For whey protein isolate fibrils, a comparable value for *M* was determined ($3.3x10^{-20}$ m^2) using the same method to separate fibrils and proteins.[24]

Transmission electron microscopy

TEM grids were prepared by negative staining immediately after the preparation of the samples. The samples were diluted, and a droplet of the diluted sample was put onto a carbon support film on a copper grid. After 15 s, the droplet was removed with a filter paper. Then, a droplet of 2% uranyl acetate was put onto the grid and removed after 15 s. The micrographs were made using a Philips CM 12 electron microscope operating at 80 kV.

Determination of persistence length

The persistence length of seven fibrils was determined from the TEM pictures. The contour of the fibrils in the TEM picture was digitized using a polynomial function (8th or 10th order). The average correlation, $<u(s)\cdot u(s')>$, was determined for different segment lengths $(s - s')$ along the fibrils. The persistence length, L_p, was determined by fitting Equation 3 to the segment lengths. This equation describes the correlation of wormlike chains in two dimensions:[25]

$$< u(s) \cdot u(s') >= exp(-\frac{(s - s')}{2 \cdot Lp}) \qquad (3)$$

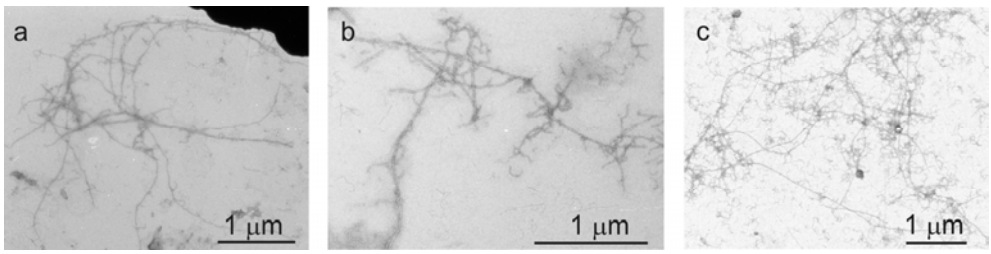

Figure 1. *TEM pictures of soy protein fibrils (heating conditions: 20 h, 85 °C, with shear flow, pH 2): (a) fibrils prepared from soy glycinin (20 g/l protein), (b) fibrils prepared from soy glycinin (40 g/l protein), (c) fibrils prepared from SPI (40 g/l protein).*

Viscosity

Flow curves were measured on a stress-controlled rheometer (Anton Paar, Physica, MCR 301) with a Couette geometry. Steady shear viscosities were measured for shear rates from 0.01 to 100 s^{-1}. Each shear rate was applied for 120 s up to a shear rate of 1 s^{-1}; above this shear rate, each rate was applied for 30 s. Only data points were used for which a steady state viscosity was obtained after 30 or 120 s.

Thioflavin T fluorescence

A Thioflavin T solution (18 mg/l) was prepared by dissolving Thioflavin T (Merck-Schuchardt) in a phosphate buffer (10 mM phosphate, 150 mM NaCl at pH 7.0), and the solution was filtered (Minisart, Sartorius, 0.2 μm) to remove undissolved ThT. Samples of 24 μl were added to 4 ml of the ThT solution. The fluorescence of the samples was measured using a luminescence spectrophotometer (LS50B, Perkin-Elmer). ThT was excited at a wavelength of 460 nm, and the emission of the sample (I_{ThT}) was measured at 486 nm.

RESULTS

Characterization of soy glycinin fibrils

In this section, we show that micrometer-sized, semi-flexible fibrils can be formed from soy glycinin. Fibrils were formed after heating a soy glycinin solution for 20 h with shear flow, at 85 °C and pH 2. In Figure 1, TEM pictures are shown of the fibrils after heating soy glycinin solutions of 20 g/l protein (Figure 1a) and 40 g/l protein (Figure 1b). Long fibrils were formed with a diameter of a few nanometers, which were slightly branched and curved. No clear differences were observed in fibril morphology when the fibrils were prepared at different protein concentrations. When Thioflavin T was added to the fibril solution, an increase in fluorescent emission (measured at a wavelength of 486 nm) was observed. Table 2 shows the measured intensity for the soy glycinin fibrils. This increase in emission shows that β-sheets were present in the fibrils to which Thioflavin T was bound.

Figure 2 shows the fibril length distribution that was obtained from the TEM pictures by measuring the contour lengths of the soy glycinin fibrils (n = 101). The

***Table 2**. Birefringence signals and ThT fluorescence emission of soy glycinin and SPI solutions (heating conditions: 40 g/l protein, 20 h, 85 °C, with shear flow, pH 2).*

Protein	Δn	I_{ThT}
Soy glycinin	$29\pm0.2\times10^{-6}$	508±19
SPI	$13\pm0.1\times10^{-6}$	972±19[a]

[a]This value was extrapolated from a 2× diluted sample (I_{ThT}=486), because the undiluted sample was outside the linear range of the spectrophotometric analysis.

average fibril length was 1.1 μm, while the measured fibril lengths ranged from 0.1 to 4 μm, which shows that the fibril length was polydisperse. The persistence length of the fibrils was measured by determining the average correlation, $\langle u(s)\cdot u(s')\rangle$, of different segment lengths, $(s - s')$, along the fibrils (N = 7). Figure 3 shows the correlations for different segment lengths of all fibrils. A persistence length was determined for each fibril. The average persistence length was 2.3 ±1.4 μm, and the correlation for this average fibril length using Equation 3 is depicted in Figure 3. The measured correlations of the different fibrils are scattered around this average correlation. This analysis shows that the persistence length of the fibrils is comparable to the contour length, which is generally observed in the case of semi-flexible fibrils.

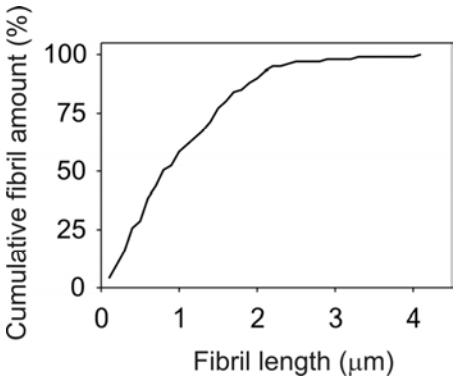

***Figure 2**. Cumulative fibril length distribution of soy glycinin fibrils obtained by measuring fibril lengths (N = 101) from TEM pictures (heating conditions of sample: 20 g/l protein, 20 h, 85 °C, with shear flow, pH 2).*

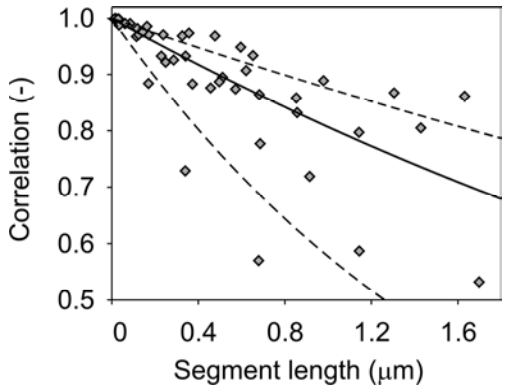

Figure 3*. Correlation <u(s)·u(s')> versus segment length (s-s') for all fibrils for which the persistence length was determined (N=7). The lines represents the correlation according to Equation 3 for which the average persistence length (2.3 μm) was used (solid line) and average length plus or minus the standard deviation (1.4 μm) (dotted lines).*

The behaviour of the fibrils in solution was measured using flow-induced birefringence and viscosity measurements. In the case of the birefringence measurements, concentration scaling for rods in the dilute and semi-dilute regime was applied (Doi–Edwards theory). In the dilute regime, rods diffuse unhindered of each other, resulting in a rotational diffusion coefficient, D_r, for rods that is independent of the concentration, c. In the semi-dilute regime, rods start to overlap with each other, resulting in a rotational diffusion coefficient that is dependent on the concentration ($D_r \sim c^{-2}$).[26] Flow-induced birefringence can be used to test this concentration scaling because the degree of alignment of the rods depends on the rotational diffusion and the applied shear rate. Flow-induced birefringence of a soy glycinin fibril solution was measured at different shear rates and three different dilutions of this sample (undiluted, 1.2x dilution, and 1.6x dilution). In the case of the dilute concentration regime, plotting the birefringence multiplied by the dilution factor, v, should put the curves of the three diluted samples onto one master curve because in this concentration regime, the rotational diffusion is independent of the concentration.[22] In the case of the semi-dilute concentration regime, plotting the data according to Equation 4 should put the curves onto one master curve because in this concentration regime, the rotational diffusion depends on the protein concentration.[22]

$$v \cdot \Delta n = \dot{\gamma} \cdot v^{-2} \quad (4)$$

Figure 4a shows the birefringence signals of the three diluted fibril solutions as a function of shear rate. The birefringence increased as a function of shear rate, which shows that an increasing shear rate resulted in more alignment of the fibrils. For high shear rates, the curves of the three diluted fibril solutions overlapped, which means that for high shear rates the fibrils scale like rods in the dilute concentration regime. Figure 4b shows the same data, but scaled according to rods in the semi-dilute concentration regime. At low shear rates, the curves of the three diluted fibril solutions overlapped, and this means that the fibrils scale like rods in the semi-dilute concentration regime at low shear rates. This analysis shows that the soy glycinin fibrils scale like rods in the dilute (high shear rates) and semi-dilute (low shear rates) concentration regime. This behaviour was also observed for β-lactoglobulin fibrils by Rogers et al.,[22] and they explained that the multiple scaling could be caused by the polydisperse fibril length. At low shear rates, only long fibrils (which are in the semi-dilute regime) were aligned, while upon further increasing the shear rate, smaller fibrils (which are in the dilute regime) became aligned.

Figure 5 shows viscosity measurements of the samples of Figure 4, together with the viscosity of an unheated soy glycinin solution at pH 2. The presence of the fibrils resulted in a clear increase in viscosity compared to the unheated sample. All dilutions showed shear thinning behaviour, and the viscosity decreased when less fibrils were present. At high shear rates, the viscosity started to approach the viscosity of the solvent (0.001 Pa s).

Factors influencing the formation of soy glycinin fibrils

Three different parameters (protein concentration, heating time, and shear flow) were varied to study the influence of heating conditions on the formation of soy glycinin fibrils. The fibril concentration in the samples was determined from flow-induced birefringence measurements at a shear rate of 73 s^{-1}. Figure 6a,b shows

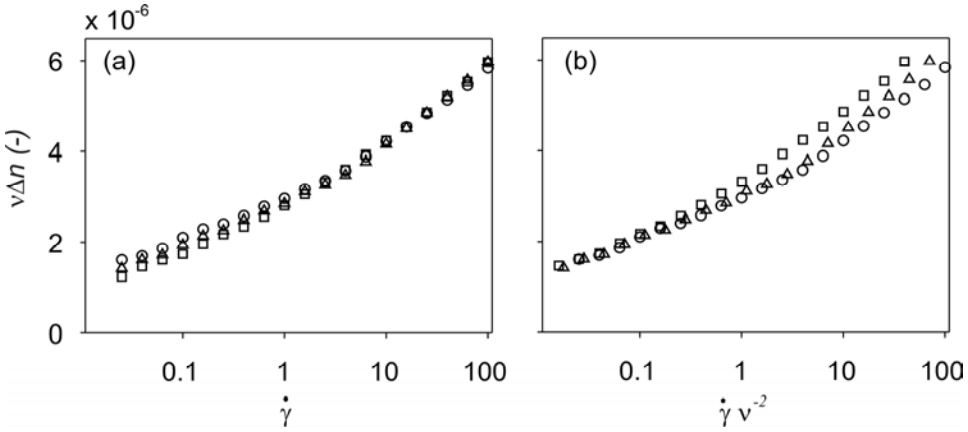

***Figure 4**. Dilute (a) and semi-dilute scaling (b) of three dilutions ((○) undiluted, (Δ) 1.2x dilution, (□) 1.6x dilution) of one soy glycinin fibril solution (heating conditions: 20 g/l protein, 20 h, 85 °C, with shear flow, pH 2). Birefringence signals were multiplied by the dilution factor, ν, and for semi-dilute scaling, the shear rate was divided by ν^2.*

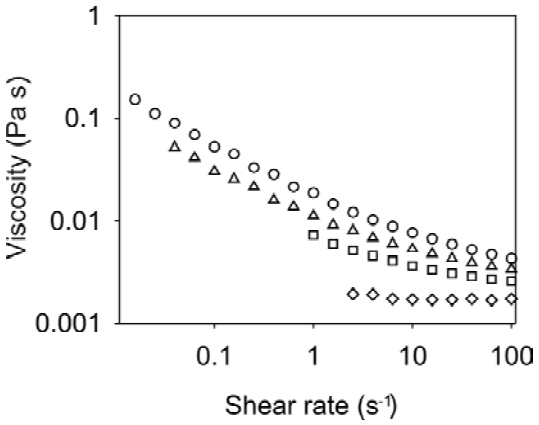

***Figure 5**. Viscosity plotted versus shear rate for the three dilutions ((○) undiluted, (Δ) 1.2x dilution, (□) 1.6x dilution) of one sample (heating conditions: see Figure 4) and (◇ an unheated glycinin solution (20 g/l, pH 2).*

the fibril concentrations as a function of the protein concentration of the samples heated for 2 h (a) and 20 h (b). Some of the samples were prepared using shear flow, while the others were prepared without shear flow. Heating for 20 h was performed multiple times, and the standard deviations of these measurements are indicated by the error bars. The variation in the results is rather large, but despite this variation, some trends can be observed. A higher protein concentration or a longer heating time resulted in a higher fibril concentration. The use of shear flow did not have a significant effect when a heating time of 20 h was used. When a heating time of 2 h was used, shear flow seems to enhance the fibril formation.

Fibrils of soy protein isolate (SPI)

Figure 1c shows a TEM picture of fibrils obtained by heating an SPI solution (containing 80% soy glycinin and 20% β-conglycinin) of 40 g/l protein for 20 h, with shear flow, at 85 °C and pH 2. The length of the SPI fibrils was in the order of 1 μm, which is similar to the soy glycinin fibrils. SPI fibrils were more branched than the soy glycinin fibrils (see Figure 1a,b).

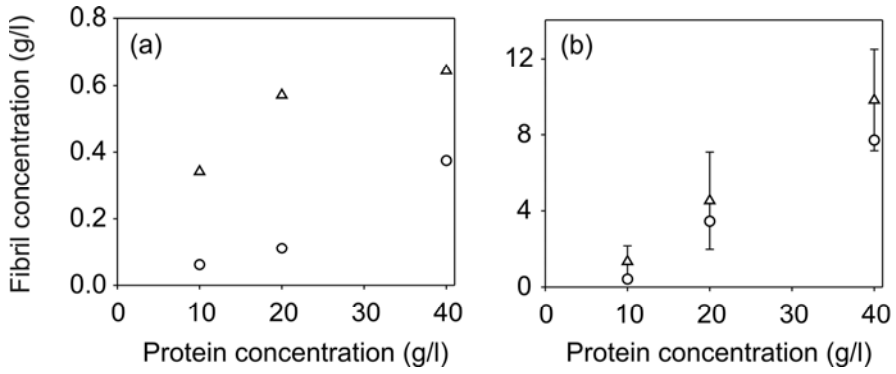

***Figure 6**. Fibril concentration versus protein concentration for samples of soy glycinin heated for (a) 2 h and (b) 20 h, prepared (Δ) with and (○) without shear flow. Please note the difference in scaling of (a) and (b).*

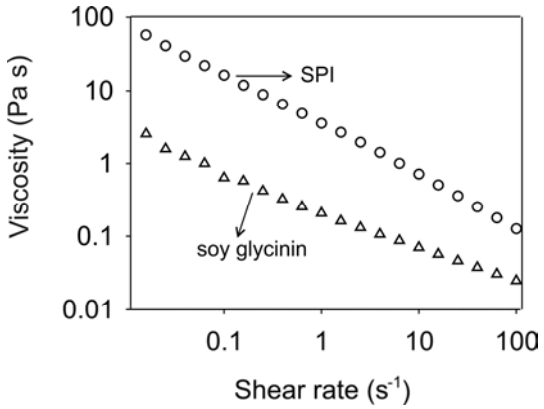

Figure 7*. Flow curves of soy glycinin and SPI fibril solutions (heating conditions: 40 g/l protein, 20 h, 85 °C, with shear flow, pH 2).*

Differences in fibril concentration between soy glycinin and SPI were measured using flow-induced birefringence and Thioflavin T fluorescence. Table 2 shows the values for samples containing SPI and soy glycinin fibrils (both heated for 20 h at 85 °C, with shear flow, and a protein concentration of 40 g/l). As previously observed for soy glycinin fibrils, the presence of SPI fibrils also resulted in an increase in Thioflavin T fluorescent emission (measured at 486 nm). This confirms that β-sheets were present in the SPI fibrils to which Thioflavin T was bound. The ThT fluorescence intensity of the sample containing SPI fibrils was higher than the intensity of the sample containing soy glycinin fibrils, while the birefringence of the sample containing SPI fibrils was lower than the birefringence of the sample containing soy glycinin fibrils. Since both the birefringence and the ThT fluorescence intensity are a measure of the fibril concentration, it seems that the responses of the two methods are different for SPI than for soy glycinin. On the basis of the TEM pictures, we conclude that the SPI fibrils are less prone to alignment than the soy glycinin fibrils due to their branches, which resulted in a lower birefringence signal for SPI fibrils. The higher ThT fluorescence intensity for SPI fibrils indicates that for these two specific samples more protein was incorporated into the SPI fibrils than into the soy glycinin fibrils.

Figure 7 shows the flow curves of soy glycinin and SPI fibrils. Both samples were shear thinning, and the viscosity of the SPI fibril solution was higher than the

viscosity of the soy glycinin solution. This higher viscosity for SPI fibrils was probably caused by the higher amount of protein present in the fibrils.

DISCUSSION

In this discussion, we will compare soy protein fibrils with fibrils of β-lactoglobulin and WPI fibrils because much information is available about these fibrils, and WPI is an industrially relevant mixture of proteins.

Compared to β-lactoglobulin and WPI, the morphology of soy glycinin and SPI fibrils is partly similar because β-lactoglobulin and WPI can also form micrometer-sized, semi-flexible fibrils with a diameter of a few nanometers.[1,2,4,5,9,12] Furthermore, Thioflavin T can also bind to the β-sheets present in β-lactoglobulin and WPI fibrils.[24,27] The persistence length of soy glycinin is similar to the persistence length of β-lactoglobulin fibrils.[28] Birefringence measurements showed that the behaviour of soy glycinin fibrils under flow can be described by scaling relations derived for rod-like macromolecules, and viscosity measurements showed that the presence of soy glycinin fibrils resulted in an increase in viscosity and shear thinning behaviour. Previous research showed similar behaviour under flow for β-lactoglobulin and WPI fibrils.[9,11,22] The fibril concentration of soy glycinin could be influenced by the protein concentration, heating time, and use of shear flow during heating. Previous studies on WPI fibrils showed that the WPI fibril concentration could also be influenced by the same factors.[9,11]

So far, we have addressed the similarities between fibrils formed from SPI and soy glycinin and fibrils formed from WPI and β-lactoglobulin. However, there are also some differences. A large experimental variation in fibril concentration was observed for soy glycinin fibrils (Figure 6), and partly, this has also been observed for fibrils formed from WPI.[9] However, the variation seems larger for soy glycinin fibrils, which could be caused by the heterogeneous nature of soy glycinin.[13,14]

Fibrils of soy glycinin and SPI fibrils are more branched than fibrils of β-lactoglobulin and WPI fibrils when they are prepared at similar conditions (heating at pH 2 at a protein concentration of 50 g/l or lower).[4,9] Furthermore, SPI fibrils

were more branched than soy glycinin fibrils. The difference between soy glycinin and SPI is a higher concentration of β-conglycinin, which means that this protein influences the morphology of SPI fibrils. Further research should clarify the role of β-conglycinin on the morphology of soy protein fibrils. In the case of WPI, no differences have been observed in morphology compared to β-lactoglobulin, and β-lactoglobulin seems to be the only whey protein that is incorporated into WPI fibrils.[12]

To summarize, many properties of soy protein fibrils are similar to β-lactoglobulin and WPI fibrils, which makes them possible candidates as sustainable structural ingredients in food products. In particular, the high viscosity and shear thinning behaviour of soy protein fibrils show that they have a promising ability to modify physical properties.

ACKNOWLEDGMENTS

The authors thank M. Gao and M. Jansen for their contribution to a part of the experimental work and J. Van Lent, H. Bloksma (Virology Department, Wageningen University), and H. Baptist (Food Physics Group, Wageningen University) for their assistance with the TEM analysis. This research was financially supported by the Dutch graduate school VLAG, and the Dutch research programme MicroNed.

REFERENCES

1. Kavanagh, G.M.; Clark, A.H.; Ross-Murphy, S.B. Heat-induced gelation of globular proteins: part 3. Molecular studies on low pH β-lactoglobulin gels. *International Journal of Biological Macromolecules* **2000**, 28, 41-50.

2. Arnaudov, L.N.; De Vries, R.; Ippel, H.; Van Mierlo, C.P.M. Multiple steps during the formation of β-lactoglobulin fibrils. *Biomacromolecules* **2003**, 4, 1614-1622.

3. Durand, D.; Gimel, J.C.; Nicolai, T. Aggregation, gelation and phase separation of heat denatured globular proteins. *Physica A* **2002**, 304, 253-265.

4. Veerman, C.; Ruis, H.; Sagis, L.M.C.; Van der Linden, E. Effect of electrostatic interactions on the percolation concentration of fibrillar β-lactoglobulin gels. *Biomacromolecules* **2002**, 3, 869-873.

5. Gosal, W.S.; Clark, A.H.; Pudney, P.D.A.; Ross-Murphy, S.B. Novel amyloid fibrillar networks derived from a globular protein: β-lactoglobulin. *Langmuir* **2002**, 18, 7174-7181.

6. Veerman, C.; De Schiffart, G.; Sagis, L.M.C.; Van der Linden, E. Irreversible self-assembly of ovalbumin into fibrils and the resulting network rheology. *International Journal of Biological Macromolecules* **2003**, 33, 121-127.

7. Veerman, C.; Sagis, L.M.C.; Heck, J.; Van der Linden, E. Mesostructure of fibrillar bovine serum albumin gels. *International Journal of Biological Macromolecules* **2003**, 31, 139-146.

8. Arnaudov, L.N.; De Vries, R. Thermally induced fibrillar aggregation of hen egg white lysozyme. *Biophysics Journal* **2005**, 88, 515-526.

9. Akkermans, C.; Van der Goot, A.J.; Venema, P.; Van der Linden, E.; Boom, R.M. Formation of fibrillar whey protein aggregates: influence of heat- and shear treatment and resulting rheology. *Food Hydrocolloids* **2007**, doi:10.1016/j.foodhyd.2007.07.001.

10. Akkermans, C.; Venema, P.; Rogers, S.S.; Van der Goot, A.J.; Boom, R.M.; Van der Linden, E. Shear pulses nucleate fibril aggregation. *Food Biophysics* **2006**, 1, 144-150.

11. Bolder, S.G.; Sagis, L.M.C.; Venema, P.; Van der Linden, E. Effect of stirring and seeding on whey protein fibril formation. *Journal of Agricultural and Food Chemistry* **2007**, 55, 5661-5669.

12. Bolder, S.G.; Hendrickx, H.; Sagis, L.M.C.; Van der Linden, E. Fibril assemblies in aqueous whey protein mixtures. *Journal of Agricultural and Food Chemistry* **2006**, 54, 4229-4234.

13. Scallon, B.; Thanh, V.H.; Floener, L.A.; Nielsen, N.C. Identification and characterization of DNA clones encoding group-II glycinin subunits. *Theoretical and Applied Genetics* **1985**, 70, 510-519.

14. Fischer, R.L.; Goldberg, R.B. Structure and flanking regions of soybean seed protein genes. *Cell* **1982**, 29, 651-660.

15. Lakemond, C.M.M.; de Jongh, H.H.J.; Hessing, M.; Gruppen, H.; Voragen, A.G.J. Heat denaturation of soy glycinin: influence of pH and ionic strength on molecular structure. *Journal of Agricultural and Food Chemistry* **2000**, 48, 1991-1995.

16. Utsumi, S.; Matsumura, Y.; Mori, T. Structure-function relationships of soy proteins. In: *Food Proteins and Their Applications*; Damodaran, S., Praf, A., Eds.; Marcel Dekker: New York, **1997**; p 257.

17. Puppo, M.C.; Lupano, C.E.; Anon, M.C. Gelation of soybean protein isolates in acidic conditions - effect of pH and protein concentration. *Journal of Agricultural and Food Chemistry* **1995**, 43, 2356-2361.

18. Hermansson, A.M. Structure of soya glycinin and conglycinin gels. *Journal of Food Science and Agriculture* **1985**, 36, 822-832.

19. Kuipers, B.J.; Van Koningsveld, G.A.; Alting, A.C.; Driehuis, F.; Gruppen, H.; Voragen, A.G.J. Enzymatic hydrolysis as a means of expanding the cold gelation conditions of soy proteins. *Journal of Agricultural and Food Chemistry* **2005**, 53, 1031-1038.

20. Kuipers, B.J.H.; Van Koningsveld, G.A.; Alting, A.C.; Driehuis, F.; Voragen, A.G.J.; Gruppen, H. Opposite contributions of glycinin- and β-conglycinin-derived peptides to the aggregation behavior of soy protein isolates. *Food Biophysics* **2006**, 1, 178-188.

21. Klein, C.; Venema, P.; Sagis, L.M.C.; Van Dusschoten, D.; Wilhelm, M.; Spies, H.W.; Van der Linden, E.; Rogers, S.S.; Donald, A.M. Rheo-optical measurements by fast Fourier transform and oversampling. *Applied Rheology* **2007**, 17, 45210-1 - 45210-7.

22. Rogers, S.S.; Venema, P.; Sagis, L.M.C.; Van der Linden, E.; Donald, A.M. Measuring the length distribution of amyloid fibrils: a flow birefringence technique. *Macromolecules* **2005**, 38, 2948-2958.

23. Aymard, P.; Nicolai, T.; Durrand, D. Static and dynamic scattering of β-lactoglobulin aggregates formed after heat-induced denaturation at pH 2. *Macromolecules* **1999**, 32, 2542-2552.

24. Bolder, S.G.; Sagis, L.M.C.; Venema, P.; Van der Linden, E. Thioflavin T and birefringence assays to determine the conversion of proteins into fibrils. *Langmuir* **2007**, 23, 4144-4147.

25. Gittes, F.; Mickey, B.; Nettleton, J.; Howard, J. Flexural rigidity of microtubules and actin filaments measured from thermal fluctuations in shape. *The Journal of Cell Biology* **1993**, 120, 923-934.

26. Doi, M.; Edwards, S.F. Dynamics of rod-like macromolecules in concentrated solution. Part 2. *Journal of the Chemical Society - Faraday Transactions 2* **1978**, 74, 918-932.

27. Krebs, M.R.H.; Bromley, E.H.C.; Donald, A.M. The binding of Thioflavin-T to amyloid fibrils: localisation and implications. *Journal of Structural Biology* **2005**, 149, 30-37.

28. Sagis, L.M.C.; Veerman, C.; Van der Linden, E. Mesoscopic properties of semiflexible amyloid fibrils. *Langmuir* **2004**, 20, 924-927.

Peptides are building blocks of heat induced fibrillar protein aggregates of β-lactoglobulin formed at pH 2

Chapter 5

*This chapter has been accepted for publication as: C. Akkermans, P. Venema, A.J. Van der Goot, H. Gruppen, E.J. Bakx, R.M. Boom, E. Van der Linden. Peptides are building blocks of heat induced fibrillar protein aggregates of β-lactoglobulin formed at pH 2. Biomacromolecules **2008**, doi:10.1021/bm7014224.*

ABSTRACT

The proteinaceous material present in β-lactoglobulin fibrils formed after heating (20 h at 85 °C) at pH 2 was identified during this study. Fibrils were separated from the non-aggregated material, and the fibrils were dissociated using 8 M guanidine chloride and 0.1 M 1,4-dithiothreitol (pH 8). Characterization of the different fractions was performed using Thioflavin T fluorescence, High-Performance Size-Exclusion Chromatography, Reversed Phase HPLC and Mass-Spectrometry (MALDI-TOF). β-Lactoglobulin was found to be hydrolyzed into peptides with molecular masses between 2,000 and 8,000 Da, and the fibrils were composed of a part of these peptides and not intact β-lactoglobulin. The majority of the peptides (both aggregated and non-aggregated) were a result from cleavage of the peptide bonds before or after aspartic acid residues. Explanations for the presence of certain peptides in the fibrils are the hydrophobicity, low charge, charge distribution and capacity to form β-sheets.

INTRODUCTION

The whey protein β-lactoglobulin aggregates into fibrillar, amyloid-like aggregates when heated above the denaturation temperature at pH 2 and low ionic strength. The fibrils obtained by this heat treatment have a thickness of ~ 4 nm and a length between 1 and 10 μm.[1-6] The proteinaceous material present in these fibrils is held together by intermolecular β-sheets, which extend over the fibril length. The β-strands run perpendicular to the fibril axis.[7] Their extreme dimensions make these fibrils interesting for several applications, amongst others as weight-effective thickeners for food products.[8]

A drawback is the limited proportion of β-lactoglobulin that is incorporated into the fibrils.[5,9] Bolder et al.[9] suggested that this limitation is caused by protein hydrolysis, which takes place during the heat treatment at pH 2. They assumed that intact β-lactoglobulin molecules were incorporated into the fibrils, and the hydrolysis reaction reduces the amount of β-lactoglobulin available for the formation of the fibrils.[10] This reasoning is in line with a study of Hamada and Dobson,[11] who reported the incorporation of intact β-lactoglobulin in the fibrils when high molarities of urea were used to induce fibril formation. Heating an aqueous solution of β-lactoglobulin has only been reported to lead to fibril formation at acidic pH, which suggests a more active role of the acid hydrolysis reaction in the process of fibril formation. Possibly, the peptides derived from the protein hydrolysis are also incorporated in the fibrils. In the case of lysozyme fibrils, both intact lysozyme as well as peptides were observed to be present in the fibrils after heating (65 °C) at acidic pH (pH 1.6 or 2).[12-14] These peptides corresponded to fragments resulting from hydrolysis of the peptide bonds between aspartic acid residues (D) and any other amino acid residue (X).[12] Aspartic acid was reported to be preferably hydrolyzed under acid conditions when the β-carboxyl group is protonated.[15,16]

Studying the proteinaceous material present in fibrils derived from β-lactoglobulin after heating at pH 2 will give more information about the fibril formation itself, and the reasons for the limited conversion of β-lactoglobulin into fibrils. Therefore, the objective of this study was to observe whether intact β-

lactoglobulin and/ or peptides were present in the fibrils, and to characterize the fibril building blocks.
To characterize the fibril building blocks, fibrils and non-aggregated material were separated, and the fibrils were dissociated. Characterization of the material present in the different fractions was done using Thioflavin T fluorescence, High-Performance Size-Exclusion Chromatography (HP-SEC), Reversed-Phase (RP) HPLC and mass-spectrometry (MALDI-TOF MS).

MATERIAL AND METHODS

Unless mentioned otherwise, all chemicals were of analytical grade and purchased from Merck (Darmstadt, Germany), Sigma (Steinheim, Germany) or Invitrogen (Carlsbad, CA, USA).

Sample preparation

A protein solution of bovine β-lactoglobulin (variant A and B, product no. 61329, Sigma-Aldrich) was made by dissolving the protein in Millipore water. The pH of the solution was set to 2 by adding a concentrated HCl solution, followed by centrifugation (30 min, 15,000 g, 4 °C) and filtration (0.45 µm, Minisart®, Sartorius, Hannover, Germany) to remove undissolved protein. The protein concentration of the solution was measured using Dumas analysis (NA 2100 Protein, CE instruments, Milan, Italy), using a nitrogen factor of 6.38 for β-lactoglobulin. Fibrils were formed by heating a protein solution (30 g/l) for 20 h at 85 °C at pH 2 in a shearing device at a constant shear rate of 323 s^{-1}. Shear flow was applied to enhance the fibril formation. The results regarding the effect of shear flow, and details about the shearing device used are reported in a previous paper.[17]

Separation of fibrils and non-aggregated protein material

The heated sample (TH) was diluted to a protein concentration of 0.8 g/l. Fibrils and non-aggregated proteinaceous material of the diluted sample were separated using centrifugal filters (MWCO 100,000, Centricon YM-100, Millipore, Billerica,

USA) (30 min, 1000 g, 20 ºC). The retentate (R), containing the fibril fraction, was washed twice with a pH 2 HCl solution after each centrifugation run to remove non-aggregated protein material left in the retentate. The filtrate was recovered after each washing step, and after the last washing step, the retentate was recovered. The protein concentration in the 3 filtrates was measured using Dumas analysis, and the third filtrate did not contain any protein. Further analysis was done on the first filtrate (F) and the retentate (R). The proportion of proteinaceous material present in the three filtrates was 72%, and based on the difference, the proportion of proteinaceous material in the retentate was 28%. After the preparation of the filtrate and retentate, different analysis methods were used to characterize the composition of the total heated sample (TH), filtrate (F), retentate (R) and unheated β-lactoglobulin (β-lg).

HP-SEC: non-dissociating conditions

HP-SEC measurements were conducted using an ÄKTA purifier system (GE Healthcare, Uppsala, Sweden) operated by Unicorn software. The samples (TH, F, R and β-lg) were kept at pH 2. After centrifugation (18,000 g, 10 min, 20 ºC), 100 µl sample was applied onto the column (Shodex Protein KW-803, 300 x 8 mm, Showa Denko K. K., Tokyo, Japan). The column was equilibrated and run with a HCl solution of pH 2 using a flow rate of 0.3 ml/min. Diluting the fibrils in a HCl solution of pH 2 is not expected to result in dissociation of the fibrils.[3] The absorbance was monitored at 214 nm. The column was calibrated using various proteins with molecular masses between 300 and 42,000 Da.

To have an indication of the proportion of fibrils that passed the HP-SEC column, the area below the SEC elution profiles of the total heated sample and β-lactoglobulin was compared with the amount of protein that was injected onto the SEC column. There was a linear correlation between the area below the HP-SEC elution profile and the amount of protein injected onto the column. β-Lactoglobulin and the total heated sample could be described by the same linear relation and the variance was small (slope of 0.43 and variance of 0.06 AU·ml/mg protein). Since unheated β-lactoglobulin did not contain any fibrils, we concluded

that almost all material passed the SEC-column for this sample, implying that almost all material of the total heated sample also passed the column.

HP-SEC: fibril dissociating conditions

This method was previously used for soy protein aggregates.[18] SEC experiments were conducted using an ÄKTA purifier system (GE Healthcare) operated by Unicorn software. The samples (TH, F and R) were freeze-dried (β-lactoglobulin was purchased in dried form), and ~ 2 mg of the freeze-dried sample was dissolved in 0.5 ml of 0.15 M Tris-HCl buffer (pH 8) containing 8 M guanidine chloride and 0.1 M 1,4-dithiothreitol (DTT). After mixing for 45-60 min, 0.215 ml of acetonitrile, containing 2% (v/v) trifluoroacetic acid (TFA) was added, followed by mixing for 45-60 min. After mixing, the samples were centrifuged (18,000 g, 10 min, 20 ºC). Samples of 20 µl were applied onto the column (Shodex Protein KW-803, 300 x 8 mm, Showa Denko K. K., Tokyo, Japan). The column was equilibrated and run with 6 M urea, containing 30% (v/v) acetonitrile and 0.1% (v/v) TFA. The flow rate was 0.2 ml/min, and the absorbance was monitored at 214 nm. The column was calibrated using various proteins with molecular masses between 300 and 67,000 Da.

Transmission electron microscopy (TEM)

A TEM picture was made from the material present in the peak of the total heated sample (TH) that eluted first from the HP-SEC column (non-dissociating conditions) (peak 1 of Figure 1b). The TEM grid was prepared by negative staining. A droplet of the sample (10x diluted) was put onto a carbon support film on a copper grid. After 15 s, the droplet was removed with a filter paper. Then, a droplet of 2% uranyl acetate was put onto the grid and removed after 15 s. The micrograph was taken with a JEOL electron microscope (JEM1011, Tokyo, Japan) operating at 80 kV.

Thioflavin T fluorescence

A Thioflavin T (ThT) solution (18 mg/l) was prepared by dissolving ThT in a 10 mM sodium phosphate buffer (pH 7) containing 150 mM NaCl, and the solution

was filtered (0.2 µm, Minisart®, Sartorius) to remove undissolved ThT. Samples of 48 µl were added to 4 ml ThT solution. The fluorescence of the samples was measured using a luminescence spectrophotometer (LS50B, Perkin Elmer, Waltham, Massachusetts, USA). ThT was excited at a wavelength of 460 nm and the emission of the sample (I_{ThT}) was measured at 486 nm. The emission of the ThT solution itself was subtracted from the measured intensity.

Reversed phase HPLC (RP-HPLC)

The RP-HPLC measurements were based on a method previously used by Creusot and Gruppen.[19] Samples were freeze-dried, and ~ 2 mg of the freeze-dried sample was dissolved in 0.45 ml of 0.15 M Tris-HCl buffer (pH 8), containing 8 M guanidine chloride and 0.1 M DTT. After mixing for 45-60 min, 0.05 ml acetonitrile, containing 2% (v/v) formic acid (FA), was added, followed by mixing for 45-60 min. After mixing, the samples were centrifuged (18,000 g, 10 min, 20 ºC). Samples of 40 µl were separated using a Vydac C18 column (218MS52, 250 x 21. mm, 5 µm, Grace Vydac, Hesperia, CA, US) by HPLC (Spectra system HPLC, Thermo Separation Products, Fremont, CA, US) operated by Chromeleon software. The flow rate was 0.2 ml/ min, and the absorbance was monitored at 214 nm. Eluent A was water containing 0.1% FA, and eluent B was acetonitrile containing 0.085% FA. After 10 min of isocratic elution with 5% of eluent B, further elution was done using a linear gradient from 5 to 50% of eluent B in 70 min, and 50% to 95% of eluent B in 10 min. This gradient was followed by isocratic elution with 95% of eluent B for 5 min, a linear gradient from 95 to 5% of eluent B in 1 min, and isocratic elution of 5% eluent B for 14 min.

Mass spectrometry (MALDI-TOF MS)

The matrix solution was dimethoxy-4-hydroxycinnamic acid (SA), which was dissolved in 50% (v/v) acetonitrile and 0.3% (v/v) TFA (10 mg SA/ ml). Freeze-dried samples (~4 mg/ml) were dissolved in a 0.15 M Tris-HCl buffer (pH 8), containing 8 M guanidine chloride and 0.1 M DTT, and mixed for 45-60 min. To eliminate disturbances of the high guanidine concentration, 20 µl of this solution was diluted in 1 ml of 50% (v/v) acetonitrile and 0.3% (v/v) TFA. Due to this

dilution step, no re-aggregation took place. A volume of 2 µl diluted sample was mixed with 18 µl matrix solution, and 1 µl of this solution was loaded onto a ground steel plate (MTP 384, Bruker Daltonics, Bremen, Germany). After drying, MALDI-TOF spectra were obtained using an Ultraflex TOF (Bruker Daltonics), which was operated by FlexControl software (Bruker Datonics). The samples were analyzed with two different methods both in positive mode. The first method was optimized for the range of 700-3200 Da using the reflector, the delayed extraction time was 120 ns and an acceleration voltage 25 kV was used. This method was calibrated towards the mono-isotopic masses of Angiotensin I, Angiotensin II, Substance P, Somatostatin, ACTH1-37 and ACTH 18-39 (Bruker calibration mix 1, Bruker Daltonics). The second method was optimized for the mass range between 3000 and 30000 Da in linear mode, the acceleration voltage was 25 kV after a delayed extraction of 340 ns. The method was calibrated with the average masses of insulin, ubiquitin, cytochrome c and myoglobin (Bruker ProtMix 1, Bruker Daltonics). The molecular masses were determined using FlexAnalysis (Bruker Daltonics) without smoothing or baseline correction.

Identification of peptides

The molecular masses of the peptides determined with MALDI-TOF MS were compared with all possible peptides that could result from β-lactoglobulin (variant A and B) when the X-D or D-X bond is cleaved or aspartic acid (D) is completely removed. Since the protein was heated at acidic pH, deamidation of asparagine (N) and glutamine (Q) and oxidation of methionine (M) were also considered. Oxidation of methionine will result in an increase of the measured peptide mass with 16 Da, while deamidation will result in an increase of the peptide mass with 1 Da. Furthermore, it has been reported that a cyclic anhydride or imide intermediate can be formed before another cleavage event of a peptide bond of aspartic acid, which results in a peptide mass of 18 Da lower than the original peptide mass.[20]

The following assumptions were made with respect to positive identifications of peptide masses:

- Peptide masses were allowed to deviate 1 Da from the original peptide if the molecular mass was below 4000 Da, because mono-isotopic masses were detected for most peptides below this molecular mass.
- Peptides with molecular masses above 4000 Da were allowed to deviate 2 Da, because above this mass, average masses were detected.
- Since deamidation results in a small increase of the peptide mass, the original peptide and the deamidated peptide will not result in a single peak in the MALDI-TOF spectrum. Therefore, the number of possible deamidations (n) was added to the maximum mass (1+n below 4000 Da, and 2+n above 4000 Da) that a peptide mass could be above the original peptide mass.
- Oxidation and the formation of the intermediate product will result in a larger difference of peptide mass (+16 and -18 Da, respectively). These two reactions were only allowed to occur if the original peptide was also detected.

RESULTS AND DISCUSSION

Formation, separation and dissociation of β-lactoglobulin fibrils

Fibrils were prepared by heating (85 °C) and shearing (shear rate of 323 s^{-1}) a β-lactoglobulin solution (30 g/l) at pH 2 for 20 h. After the preparation of the fibrils, fibrils and non-aggregated proteinaceous material were separated into two different fractions: the retentate, containing the fibrils, and filtrate, containing the non-aggregated material. The non-separated sample will be referred to as the total heated sample.

The quality of the separation was studied using ThT fluorescence and HP-SEC (non-dissociating conditions). ThT binds to β-sheets that are present in the fibrils,[21] and is thus a measurement for the amount of fibrils present in the samples. Table 1 shows the ThT fluorescence intensities of unheated β-lactoglobulin, the total sample, the retentate and the filtrate before the fibrils were dissociated. The total heated sample and the retentate both have a high fluorescent intensity, indicating that fibrils were present in these samples. The fluorescent intensity of the filtrate was zero; no fibrils were present in the filtrate. Unheated β-

lactoglobulin had a small fluorescent intensity, which is probably caused by the β-sheets originally present in the protein.

The expected fibril concentration of the total heated sample (shown in Table 1) is based on the amount of material present in the retentate (28 wt% of 0.8 g/l gives 0.2 g/l). When the fluorescent intensities of the retentate and the total heated sample are compared, it can be concluded that the measured intensities are in accordance with the expected fibril concentration. The expected fibril concentration in the heated sample is five times lower than the concentration in the retentate, and the fluorescent intensity is also five times lower.

Figure 1 shows the HP-SEC elution profiles of unheated β-lactoglobulin, the total heated sample, the retentate and the filtrate. As expected, unheated β-lactoglobulin gave one large peak, eluting around 10 ml. The heated sample gave two peaks; one peak eluted in the void volume of the column (6 ml), corresponding to a molecular mass of at least 80 kDa, and the other peak eluted between 9 and 14 ml. The first peak was collected and a TEM picture was made from the material of peak 1. Fibrillar aggregates with a fibril length in the order of 1 μm were present in this peak (see insert of Figure 1b). The material not present in fibrils eluted in the second peak between 9 and 14 ml.

Table 1. *Protein concentration (C_p in g/l), expected fibril concentration (C_f in g/l) and fluorescent emission intensities, I_{ThT}, (486 nm) of the different samples before dissociation (dissolved at pH 2) and after dissociation (dissolved in 8 M Guanidine Chloride and 0.1 M DTT at pH 8) of the fibrils.*

	Before dissociation			After dissociation	
Sample[a]	C_p	C_f	I_{ThT}	C_p	I_{ThT}
β-lg	10	*0*	6	3	6
TH	0.8	*0.2*	45	3	0
R	1	*1*	227	0.1	0
F	0.6	*0*	0	4	0

[a]β-lg = β-lactoglobulin, TH = total heated sample, R = retentate (fibrils) and F = filtrate (non-aggregated material

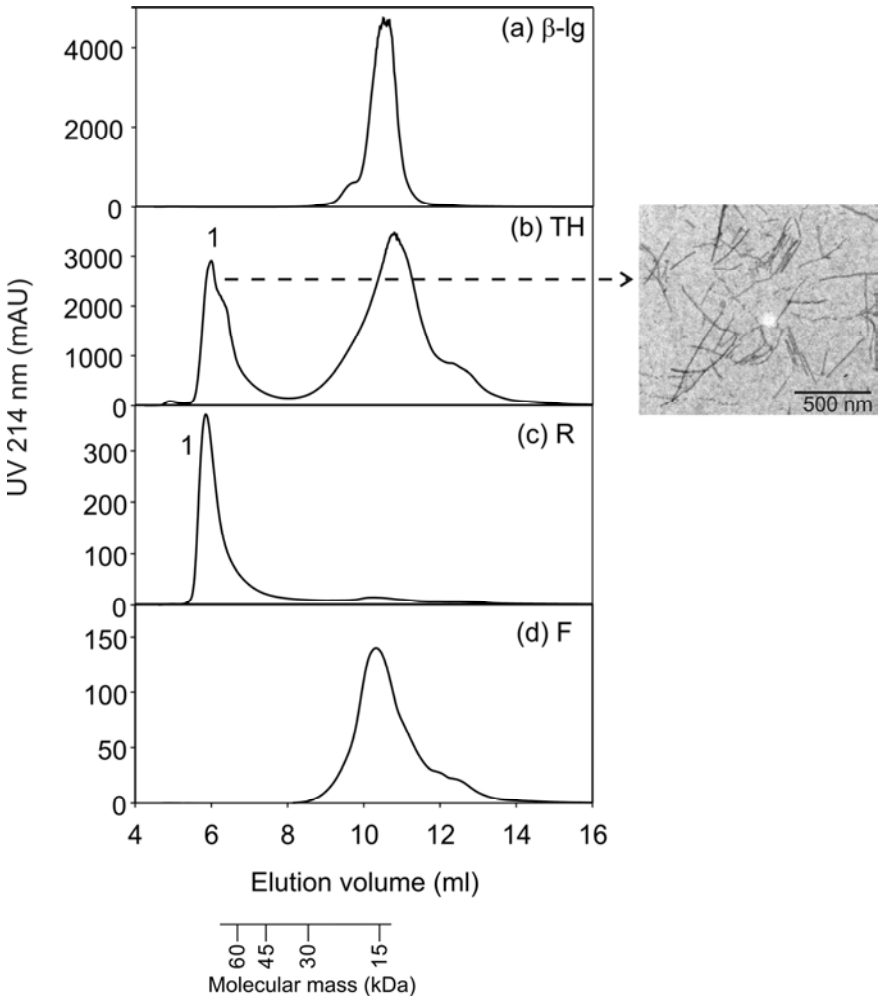

Figure 1. *HP-SEC (non-dissociating conditions) elution profiles of (a) β-lg = β-lactoglobulin, (b) TH = total heated sample (TH), (c) R = retentate (fibrils), and (d) F = filtrate (non-aggregated protein material). The intensities of the UV signals of c and d are lower, because the total heated sample was diluted before the separation. The insert of 1b is a TEM picture made from the material of peak 1. The secondary x-axis indicates the corresponding molecular mass at the elution volume.*

The elution profile of the retentate shows one peak eluting in the void volume, and a small portion of material eluting at a similar position as the second peak of the heated sample. This means that the retentate primarily consisted of fibrils (eluting in the void volume) and a small amount of non-aggregated material. In the elution profile of the filtrate, only protein material eluted at the same position as the second peak of the heated sample, which confirms that the filtrate did not contain fibrils as was also shown above using the ThT fluorescent intensity.
The proportion of protein present in peak 1 of Figure 1b was 27 wt%, which is based on the relative area below the elution profile (assuming that the molar extinction coefficient is not modified due to the heat treatment and aggregation). This is very close to 28 wt% (the proportion of material present in the retentate), and confirms that most fibrils passed the SEC column.
After establishing a successful separation of the fibrils from the non-aggregated material, the next step was to dissociate the fibrils. This was done by dissolving the fibrils in 8 M Guanidine Chloride containing 0.1 M DTT (pH 8). Thioflavin T fluorescence was used to observe whether the fibrils were completely dissociated. Table 1 shows the measured fluorescent intensities of the samples (unheated β-lactoglobulin, heated sample, filtrate and retentate) before and after dissociation of the fibrils. Unheated β-lactoglobulin and the filtrate did not contain fibrils, and therefore the intensity was low (unheated β-lactoglobulin) or zero (filtrate) after dissociation. The heated sample and the retentate gave high fluorescent intensities before dissociation of the fibrils, but after dissociation, the fluorescent intensities were zero for both samples. This shows that the fibrils were completely dissociated by dissolving them in 8 M Guanidine Chloride and 0.1 M DTT (pH 8).

Characterization of proteinaceous material in fibrils and non-aggregated fraction

Figure 2 shows the HP-SEC elution profiles of the various samples, and the HP-SEC column was run under fibril dissociating conditions. Unheated β-lactoglobulin gave one large peak (8.8 ml) and a smaller one, which correspond to the monomeric and dimeric form of β-lactoglobulin, respectively. In the elution profile of the total heated sample, retentate and filtrate, no peak was visible at the

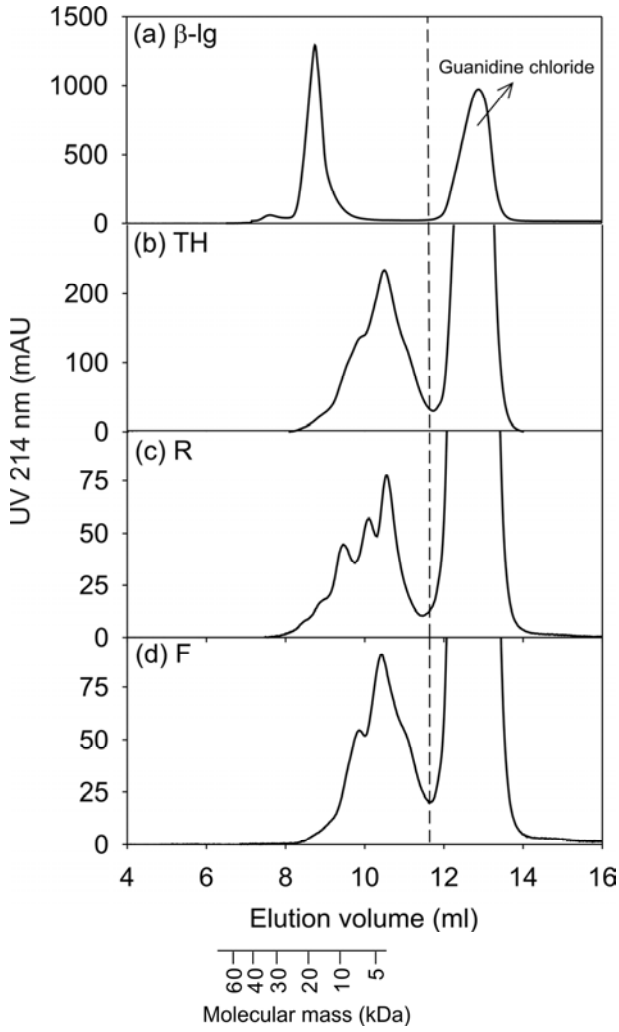

***Figure 2**. HP-SEC (fibril dissociating conditions) elution profiles of (a) β-lg=β-lactoglobulin, (b) TH = total heated sample, (c) R = retentate (fibrils), and (d) F = filtrate (non-aggregated protein material). Fibrils were dissociated using 8 M guanidine chloride and 0.1 M DTT (pH 8). The increase in UV signal of the elution profile after 11.5 ml (indicated by the dotted line) is due to the elution of guanidine chloride. The secondary x-axis indicates the corresponding molecular mass at the elution volume.*

position of unheated β-lactoglobulin, and most material (> 95%) eluted later (between 9 and 11.5 ml) than unheated β-lactoglobulin. This shows that after heating at pH 2, most β-lactoglobulin was converted into peptides. This means that the fibrils are not composed of intact β-lactoglobulin molecules, but of peptides derived from the acid hydrolysis that takes place during heating at pH 2.

Molecular masses of the peptides present in the heated sample, retentate and filtrate were characterized using MALDI-TOF. Figure 3 shows the spectra of the total heated sample, the retentate and the filtrate. Peptides were detected with molecular masses between 2000 and 8000 Da. No peak was observed at the position at which β-lactoglobulin (18,300 Da) would appear, while the spectrum of unheated β-lactoglobulin itself did have a peak at this position (result not shown).

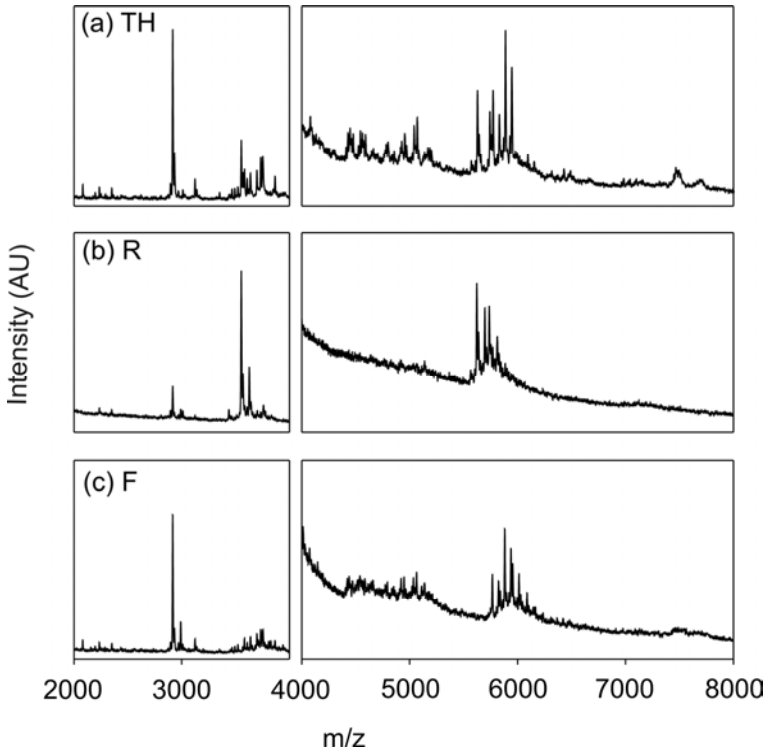

Figure 3. *MALDI-TOF spectra (fibril dissociating conditions) of (a) TH = total heated sample, (b) R = retentate (fibrils), and (c) F = filtrate (non-aggregated material).*

This confirmed that most β-lactoglobulin was hydrolyzed into peptides during the heat treatment at pH 2, and that the fibrils were not composed of intact β-lactoglobulin.

The most sensitive amino acid bonds for hydrolysis due to heating at pH 2 are the bonds between aspartic acid residues (D) and any other amino acid residue (X).[15,16] Therefore, we compared the molecular masses that were measured with the possible theoretical masses after cleavage of X-D and D-X, or complete removal of aspartic acid. The MALDI-TOF spectra contained 130 peaks, and a high percentage of these peaks (80%) could be correlated to masses of peptides after cleavage of X-D, D-X or complete removal of D. For many peptides, peaks of chemically modified peptides were observed (oxidation of methionine and the formation of a cyclic anhydride or imide intermediate before another cleavage event), which means that for these peptides, two or more peaks were observed in the MALDI-TOF spectra.

In total, 55 peptides could be identified in all samples, and 12 of these peptides were present in the retentate (fraction containing fibrils). The whole sequence of β-lactoglobulin (variant A as well as variant B) could be covered with the peptides that were detected. This shows that when β-lactoglobulin is heated at pH 2, peptide bonds involving aspartic acid residues are preferably hydrolyzed.

Table 2. *Overview of possible peptides derived from β-lactoglobulin present in fibrils, which were detected in the retentate (R) and heated sample (TH).*

		Molecular mass (Da)	
Amino-acid sequence peptides	Location	Theoretical	Measured
LIVTQTMKGLDIQKVAGTWYSLAMAASDISLL	1-32	3437.7	3437.8
LIVTQTMKGLDIQKVAGTWYSLAMAASDISLLD	1-33	3552.9	3552.9[a]
LIVTQTMKGLDIQKVAGTWYSLAMAASDISLLDA QSAPLRVYVEELKPTPEG	1-52	5622	5623[a,b]
LIVTQTMKGLDIQKVAGTWYSLAMAASDISLLDA QSAPLRVYVEELKPTPEGD	1-53	5737	5738[a,b]

[a]One or two peaks were also detected with a molecular mass of 16 or 32 Da higher, which could correspond to the same peptide of which methionine was oxidized one or two times.

[b]A peak was also detected with a molecular mass of 18 Da lower, which could correspond to the cyclic anhydride or imide intermediate of this peptide before another cleavage event.

Table 3. *Overview of possible peptides derived from β-lactoglobulin present in fibrils, which were detected in the retentate (R), filtrate (F) and heated sample (TH).*

		Molecular mass (Da)	
Amino-acid sequence peptides	Location	Theoretical	Measured
IQKVAGTWYSLAMAASDISLL	12-32	2238.2	2238.3
(D)IQKVAGTWYSLAMAASDISLL(D)	12-33 (11-32)	2353.2	2353.3
LIVTQTMKGLDIQKVAGTWYSLAMAAS	1-27	2896.5	2897.5 [b]
KALKALPMHIRLSFNPTQLEEQCHI	138-162	2916.6	2917.7[a]
LIVTQTMKGLDIQKVAGTWYSLAMAASD	1-28	3011.6	3011.5[a]
(D)YKKYLLFCMENSAEPEQSLACQCLVRTPEV(D)	99-129 (98-128) (B)	3607.2	3607.5[a,c]
TDYKKYLLFCMENSAEPEQSLVCQCLVRTPEV	97-128 (A)	3733.8	3733.0
(D)IQKVAGTWYSLAMAASDISLLDAQSAPLRVYV EELKPTPEGDLEILLQKWEN(D)	12-64 (11-63) (A)	5919	5921[b]

[a,b]See Table 2

[c]No monoisotopic separation was detected for this peptide, and this is the average molecular mass.

In Tables 2-5 (Table 4 and 5 can be found in the supporting information), all possible peptides are shown with the theoretical and measured molecular masses. Table 2 shows four peptides that were present in the retentate and the total heated sample, and not present in the filtrate. Therefore, these peptides were only present in the fibrils. In Table 3, the possible peptides are shown that were present in the retentate, filtrate and total heated sample. These peptides were thus present in the fibrils and in the non-aggregated fraction. In Table 4 (supporting information), the peptides are depicted that were not present in the retentate, and thus not present in the fibrils. Additionally, there were also three peptides (all not present in the retentate) for which there were multiple possibilities, because the theoretical masses of the peptides were close to each other (Table 5).

Figure 4 shows a schematic overview of the different peptides that were detected. The aggregating peptides are divided into regions that were only present in the retentate and total heated sample (black), and those that were also present in the filtrate (grey). The region 1-11 is present in the fibrils only, the region from 12-33 is frequently present in the peptides of the fibrils, and the region from 64-96 is never present in the peptides of the fibrils. The absence of this region in the fibrils explains the limited conversion of protein into fibrils that is often observed for this

system,[5,9] because this shows that not all peptides derived from β-lactoglobulin are incorporated into the fibrils.

The hydrophobicity of the different peptides was determined using RP-HPLC. Figure 5 shows the elution profiles for β-lactoglobulin, the total heated sample (TH), retentate (R), and filtrate (F). The heated sample and the filtrate contained a large variety of peptides, and the elution profiles were similar except for the peptides eluting around 65 min, which were present in a much lower amount in the filtrate. These specific peptides were dominantly present in the retentate, while hardly any other peptides were present in the retentate. This means that the peptides present in the fibrils eluted around 65 min, and that these peptides are the more hydrophobic peptides of the heated sample. β-Lactoglobulin also eluted at

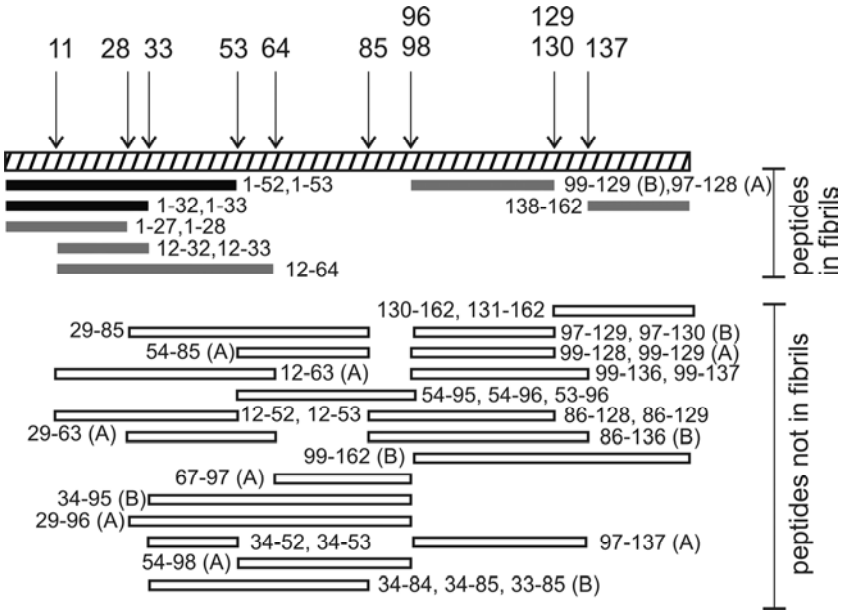

Figure 4*. Schematic overview of peptides derived from β-lactoglobulin (depicted by the striped line) detected after the heat treatment at pH 2. The peptides are divided into peptides present in: R and TH (black); R, TH and F (grey); and TH and F (white). The cleavage positions (D) are indicated with arrows (position 64 is only present in genetic variant A). Unless mentioned otherwise, these peptides can be derived from both the A and B variant. Peptides that differ 1 amino-acid (for instance peptides 1-52 and 1-53 are shown as one fragment).*

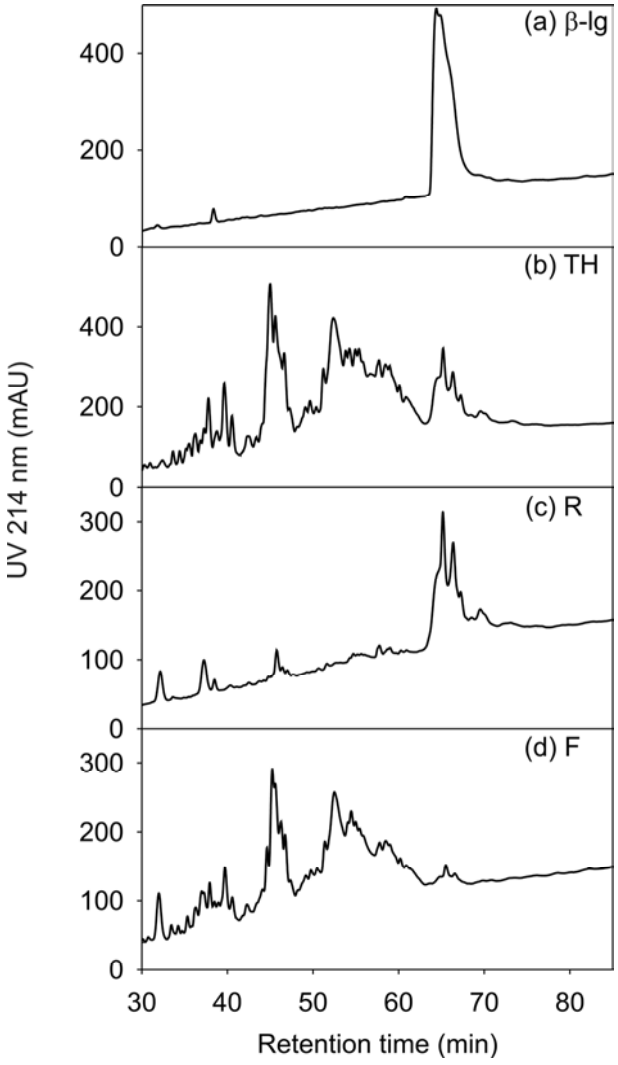

Figure 5. *RP-HPLC elution profiles (fibril dissociating conditions): (a) β-lg=β-lactoglobulin, (b) TH = total heated sample, (c) R = retentate (fibrils), (d) F = filtrate (non-aggregated material).*

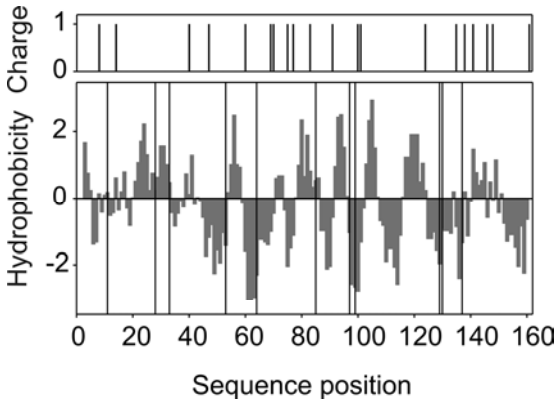

***Figure 6**. Schematic overview of the hydrophobicity (calculated according to Kyte & Doolittle[22] using a window of 5 residues) and charge at pH 2 of the 162 amino acids present in β-lactoglobulin. The vertical lines in the hydrophobicity plot indicate the positions of aspartic acid (position 64 is only present in variant A).*

this position, which means that the absolute hydrophobicity of the peptides in the fibrils is similar to the hydrophobicity of β-lactoglobulin itself.

A schematic overview of the hydrophobicity and charge of β-lactoglobulin was composed to observe how the different hydrophobic and hydrophilic regions are distributed along the protein chain (Figure 6). The positions of aspartic acid residues are indicated in this figure by vertical lines. The region that is frequently present in the fibrils (12-33) is hydrophobic, which is in accordance with the RP-HPLC results (more hydrophobic peptides are present in the fibrils). With respect to the charge, the region that is frequently present in the peptides of the fibrils (12-33) has a low charge, and also most of the other regions that were present in the peptides of the fibrils (1-11, 33-64 and 97-129) have a low charge. The region that is absent in the fibrils (64-96) has many positively charged amino-acid residues at pH 2.

Explanations for the presence of certain regions in the peptides of the fibrils could be the hydrophobicity and the low charge. For other proteins, it has been shown that these factors are indeed of influence for the capacity of certain regions in proteins to form amyloid fibrils, but also the capacity to form β-sheets is an important factor. In the case of α/ β protein acylphosphatase, it was for instance

shown that regions with a high hydrophobicity and high capacity to form β-sheets determine the rate of fibril formation.[23] Especially, the amino-acid proline is known to be energetically unfavorable for the formation of β-sheets.[24] For amylin fibrils (linked to diabetes type II), it has been shown that the presence of proline can disturb the formation of β-sheets.[25,26] The region 1-33 of β-lactoglobulin does not contain proline and has a high capacity to form β-sheets, while the region that is absent in the fibrils (64-96) has a low capacity to form β-sheets (the capacity to form β-sheets of the different regions of β-lactoglobulin was shown in a paper of Euston et al.[27]).

With respect to the effect of charge, it has been shown for a novo-designed amyloid peptide (STVIIE) that the total charge of the peptides, and that the position of the charges on the peptide influence the capacity to form fibrils. For this small peptide, a net charge of 1 was the optimal charge, and the charge should be positioned at the edge of the peptide.[28,29] The peptides that were found in β-lactoglobulin fibrils were larger than this peptide and thus have a charge higher than 1. For the regions 1-33, 1-53, and 97-128, it can be observed in Figure 6 that the few charges present are more situated near the edges than in the middle part of the sequence.

Based on the information described above, it can be concluded that the low charge, charge distribution along the sequence, hydrophobicity, and capacity to form β-sheets explain why these specific peptides were present in the fibrils. The part of the sequence that is completely absent in the peptides of the fibrils has a high charge and low capacity to form β-sheets.

CONCLUSIONS

Fibrils formed from β-lactoglobulin after heating at pH 2 are composed of peptides and intact β-lactoglobulin is not present in the fibrils. The peptides were mainly a result of cleavage of the bonds between aspartic acid residues and any other amino acid residue or complete removal of aspartic acid residues. The hydrophobicity, net charge, charge distribution and capacity to form β-sheets mainly explain the presence and absence of specific regions of the β-lactoglobulin sequence in the

fibrils. The absence of a specific region in the fibrils also explains the limited conversion of proteinaceous material into the fibrils.

ACKNOWLEDGEMENT

The authors thank H. Baptist (Wageningen University) and the Virology department of Wageningen University (J. van Lent and H. Bloksma) for their assistance with the TEM analysis. This research was financially supported by the Dutch graduate school VLAG, and the Dutch research program MicroNed.

REFERENCES

1. Durand, D.; Gimel, J.C.; Nicolai, T. Aggregation, gelation and phase separation of heat denatured globular proteins. *Physica A* **2002**, 304, 253-265.
2. Gosal, W.S.; Clark, A.H.; Pudney, P.D.A.; Ross-Murphy, S.B. Novel amyloid fibrillar networks derived from a globular protein: β-lactoglobulin. *Langmuir* **2002**, 18, 7174-7181.
3. Rogers, S.S.; Venema, P.; Sagis, L.M.C.; Van der Linden, E.; Donald, A.M. Measuring the length distribution of amyloid fibrils: a flow birefringence technique. *Macromolecules* **2005**, 38, 2948-2958.
4. Veerman, C.; Ruis, H.; Sagis, L.M.C.; Van der Linden, E. Effect of electrostatic interactions on the percolation concentration of fibrillar β-lactoglobulin gels. *Biomacromolecules* **2002**, 3, 869-873.
5. Arnaudov, L.N.; De Vries, R.; Ippel, H.; Van Mierlo, C.P.M. Multiple steps during the formation of β-lactoglobulin fibrils. *Biomacromolecules* **2003**, 4, 1614-1622.
6. Kavanagh, G.M.; Clark, A.H.; Ross-Murphy, S.B. Heat-induced gelation of globular proteins: part 3. Molecular studies on low pH β-lactoglobulin gels. *International Journal of Biological Macromolecules* **2000**, 28, 41-50.
7. Bromley, E.H.C.; Krebs, M.R.H.; Donald, A.M., Aggregation across the length-scales in β-lactoglobulin. *Faraday Discussions* **2005**, 128, 13-27.
8. Veerman, C.; Baptist, H.; Sagis, L.M.C.; Van der Linden, E. A new multistep Ca^{2+}-induced cold gelation process for β-lactoglobulin. *Journal of Agricultural and Food Chemistry* **2003**, 51, 3880-3885.

9. Bolder, S.G.; Sagis, L.M.C.; Venema, P.; Van der Linden, E. Effect of stirring and seeding on whey protein fibril formation. *Journal of Agricultural and Food Chemistry* **2007**, 55, 5661-5669.

10. Bolder, S.G.; Vasbinder, A.J.; Sagis, L.M.C.; Van der Linden, E. Heat-induced whey protein isolate fibrils: conversion, hydrolysis and disulphide bond formation. *International Dairy Journal* **2006**, 17, 846-853.

11. Hamada, D.; Dobson, C.M. A kinetic study of β-lactoglobulin amyloid fibril formation promoted by urea. *Protein Science* **2002**, 11, 2417-2426.

12. Frare, E.; Polverino de Laureto, P.; Zurdo, J.; Dobson, C.M.; Fontana, A. A highly amyloidogenic region of hen lysozyme. *Journal of Molecular Biology* **2004**, 340, 1153-1165.

13. Krebs, M.R.H.; Wilkins, D.K.; Chung, E.W.; Pitkeathly, M.C.; Chamberlain, A.K.; Zurdo, J.; Robinson, C.V.; Dobson, C.M. Formation and seeding of amyloid fibrils from wild-type hen lysozyme and a peptide fragment from the β-domain. *Journal of Molecular Biology* **2000**, 300, 541-549.

14. Mishra, R.; Sorgjerd, K.; Nystrom, S.; Nordigarden, A.; Yu, Y.C.; Hammarstrom, P. Lysozyme amyloidogenesis is accelerated by specific nicking and fragmentation but decelerated by intact protein binding and conversion. *Journal of Molecular Biology* **2007**, 366, 1029-1044.

15. Schultz, J. Cleavage at aspartic acid. *Methods in Enzymology* **1967**, 11, 255-263.

16. Inglis, A.S. Cleavage at aspartic acid. *Methods in Enzymology* **1983**, 91, 324-332.

17. Akkermans, C.; Van der Goot, A.J.; Venema, P.; Van der Linden, E.; Boom, R.M. Formation of fibrillar whey protein aggregates: influence of heat- and shear treatment and resulting rheology. *Food Hydrocolloids* **2007**, doi:10.1016/j.foodhyd.2007.07.001.

18. Kuipers, B.J.H.; Van Koningsveld, G.A.; Alting, A.C.; Driehuis, F.; Voragen, A.G.J.; Gruppen, H. Opposite contributions of glycinin- and β-conglycinin-derived peptides to the aggregation behavior of soy protein isolates. *Food Biophysics* **2006**, 1, 178-188.

19. Creusot, N.; Gruppen, H. Hydrolysis of whey protein isolate with *Bacillus licheniformis* protease: Fractionation and identification of aggregating peptides. *Journal of Agricultural and Food Chemistry* **2007**, 55, 9241-9250.

20. Li, A.; Sowder, R.C.; Henderson, L.E.; Moore, S.P.; Garfinkel, D.J.; Fisher, R.J. Chemical cleavage at aspartyl residues for protein identification. *Analytical Chemistry* **2001**, 73, 5395-5402.

21. Krebs, M.R.H.; Bromley, E.H.C.; Donald, A.M. The binding of thioflavin-T to amyloid fibrils: localisation and implications. *Journal of Structural Biology* **2005**, 149, 30-37.

22. Kyte, J.; Doolittle, R.F. A simple method for displaying the hydropathic character of a protein. *Journal of Molecular Biology* **1982**, 157, 105-132.

23. Chiti, F.; Taddei, N.; Baroni, F.; Capanni, C.; Stefani, M.; Ramponi, G.; Dobson, C.M. Kinetic partitioning of protein folding and aggregation. *Nature Structural Biology* **2002**, 9, 137-143.

24. Euston, S.R.; Ur-Rehman, S.; Costello, G. Denaturation and aggregation of beta-lactoglobulin - a preliminary molecular dynamics study. *Food Hydrocolloids* **2007**, 21, 1081-1091.

25. Minor, D.L.; Kim, P.S. Measurement of the β-sheet-forming propensities of amino acids. *Nature* **1994**, 367, 660-663.

26. Moriarty, D.F.; Raleigh, D.P. Effects of sequential proline substitutions on amyloid formation by human amylin(20-29). *Biochemistry* **1999**, 38, 1811-1818.

27. Westermark, P.; Engstrom, U.; Johnson, K.H.; Westermark, G.T.; Betsholtz, C. Islet amyloid polypeptide: pinpointing amino acid residues linked to amyloid fibril formation. *Proceedings of the National Academy of Science of the United States of America* **1990**, 87, 5036-5040.

28. Lopez de la Paz, M.; Serrano, L. Sequence determinants of amyloid fibril formation. *Proceedings of the National Academy of Science of the United States of America* **2004**, 101, 87-92.

29. Lopez de la Paz, M.; Goldie, K.; Zurdo, J.; Lacroix, E.; Dobson, C.M.; Hoenger, A.; Serrano, L. De novo designed peptide-based amyloid fibrils. *Proceedings of the National Academy of Science of the United States of America* **2002**, 99, 16052-16057.

SUPPORTING INFORMATION

Table 4*. Overview of possible peptides derived from β-lactoglobulin that were not present in fibrils, which were detected in the filtrate (F) and/ or the heated sample (H).*

		Molecular mass (Da)	
Amino-acid sequence peptides	Location	Theoretical	Measured
AQSAPLRVYVEELKPTPEG	34- 52	2084.1	2084.2
(D)AQSAPLRVYVEELKPTPEG(D)	34- 53 (33- 52)	2199.1	2199.2
YKKYLLFCMENSAEPEQSLACQCLVRTPEV	99-128 (B)[a]	3492.1	3493.7[b]
YKKYLLFCMENSAEPEQSLVCQCLVRTPEV	99-128 (A)[a]	3520.1	3521.9[b]
(D)YKKYLLFCMENSAEPEQSLVCQCLVRTPEV(D)	99-129 (98-128) (A)	3632.7	3636.6
ECAQKKIIAEKTKIPAVFKIDALNENKVLVLDT	65- 97 (A)	3684.4	3683.5[b]
(D)TDYKKYLLFCMENSAEPEQSLACQCLVRTP EV(D)	97-129 (96-128) (B)	3823.4	3825.7[c]
EALEKFDKALKALPMHIRLSFNPTQLEEQCHI	131-162	3748.9	3750.6
(D)LEILLQKWENDECAQKKIIAEKTKIPAVFKI(D)	54- 85 (53- 84) (A)	3754.1	3755.8[d]
(D)TDYKKYLLFCMENSAEPEQSLVCQCLVRTP EV(D)	97-129 (96-128) (A)	3851.4	3851.6[b]
DEALEKFDKALKALPMHIRLSFNPTQLEEQCHI	130-162	3864.0	3865.7[b,d]
(D)TDYKKYLLFCMENSAEPEQSLACQCLVRTPE VD(D)	97-130 (96-129) (B)	3938.5	3940.2[b]
ISLLDAQSAPLRVYVEELKPTPEGDLEILLQKWEN	29- 63 (A)	4010	4013
IQKVAGTWYSLAMAASDISLLDAQSAPLRVYVEE LKPTPEG	12-52	4421	4423[c]
YKKYLLFCMENSAEPEQSLACQCLVRTPEVDDEA L EKF	99-136 (B)	4440	4443[d]
YKKYLLFCMENSAEPEQSLVCQCLVRTPEVDDEA L EKF	99-136 (A)	4468	4472
(D)IQKVAGTWYSLAMAASDISLLDAQSAPLRVYV EELKPTPEG(D)	12-53 (11-52)	4536	4538[c]
(D)YKKYLLFCMENSAEPEQSLACQCLVRTPEVDD EALEKF(D)	99-137 (98-136) (B)	4555	4559[d]
(D)YKKYLLFCMENSAEPEQSLVCQCLVRTPEVDD EALEKF(D)	99-137 (98-136) (A)	4583	4586
LEILLQKWENGECAQKKIIAEKTKIPAVFKIDALNE NKVLVL	54-95 (B)	4793	4795[c]

(D)TDYKKYLLFCMENSAEPEQSLVCQCLVRTPEV DDEALEKF(D)	97-137 (96-136) (A)	4799	4801
LEILLQKWENDECAQKKIIAEKTKIPAVFKIDALNE NKVLVL	54-95 (A)	4851	4853[c]
(D)LEILLQKWENGECAQKKIIAEKTKIPAVFKIDAL NENKVLVL(D)	54- 96 (53-95) (B)	4908	4910[c]
ALNENKVLVLDTDYKKYLLFCMENSAEPEQSLAC QCLVRTPEV	86-128 (B)	4918	4920
ALNENKVLVLDTDYKKYLLFCMENSAEPEQSLVC QCLVRTPEV	86-128 (A)	4946	4949
(D)LEILLQKWENDECAQKKIIAEKTKIPAVFKIDAL NENKVLVL(D)	54- 96 (A)	4966	4968
DLEILLQKWENGECAQKKIIAEKTKIPAVFKIDALN ENKVLVLD	53- 96 (B)	5023	5022
(D)ALNENKVLVLDTDYKKYLLFCMENSAEPEQSL ACQCLVRTPEV(D)	86-129 (85-128) (B)	5033	5037[d]
(D)ALNENKVLVLDTDYKKYLLFCMENSAEPEQSL VCQCLVRTPEV(D)	86-129 (85-128) (A)	5061	5064
DLEILLQKWENDECAQKKIIAEKTKIPAVFKIDALN ENKVLVLD	53- 96 (A)	5081	5080
(D)LEILLQKWENDECAQKKIIAEKTKIPAVFKIDAL NENKVLVLDT(D)	54- 98 (53-97) (A)	5182	5180[c,d]
AQSAPLRVYVEELKPTPEGDLEILLQKWENGECAQ KKIIAEKTKIPAVFKI	34- 84 (B)	5765	5767
IQKVAGTWYSLAMAASDISLLDAQSAPLRVYVEE LKPTPEGDLEILLQKWEN	12-63 (A)	5803	5807
AQSAPLRVYVEELKPTPEGDLEILLQKWENDECAQ KKIIAEKTKIPAVFKI	34- 84 (A)	5823	5825[c,d]
ALNENKVLVLDTDYKKYLLFCMENSAEPEQSLAC QCLVRTPEVDDEALEKF	86-136 (B)	5866	5867[c]
(D)AQSAPLRVYVEELKPTPEGDLEILLQKWENGEC AQKKIIAEKTKIPAVFKI(D)	34- 85 (33- 84) (B)	5879.9	5881.5
(D)AQSAPLRVYVEELKPTPEGDLEILLQKWENDEC AQKKIIAEKTKIPAVFKI(D)	34- 85 (33- 84) (A)	5938	5940[d]
DAQSAPLRVYVEELKPTPEGDLEILLQKWENGECA QKKIIAEKTKIPAVFKID	33- 85 (B)	5995	5996[d]
(D)ISLLDAQSAPLRVYVEELKPTPEGDLEILLQKW ENGECAQKKIIAEKTKIPAVFKI(D)	29- 85 (28-84) (B)	6422	6425
(D)ISLLDAQSAPLRVYVEELKPTPEGDLEILLQKW	29- 85	6480	6486

ENDECAQKKIIAEKTKIPAVFKI(D)	(28-84) (A)		
AQSAPLRVYVEELKPTPEGDLEILLQKWENGECAQ KKIIAEKTKIPAVFKIDALNENKVLVL	34- 95 (B)	6974	6979
YKKYLLFCMENSAEPEQSLACQCLVRTPEVDDEA LEKFDKALKALPMHIRLSFNPTQLEEQCHI	99-162 (B)	7455	7462
(D)ISLLDAQSAPLRVYVEELKPTPEGDLEILLQKW ENDECAQKKIIAEKTKIPAVFKIDALNENKVL VL(D)	29-96 (28-95) (A)	7689	7693

[a]This peptide originates from one of the genetic variants (indicated further on in the Table by (A) or (B)).

[b]No monoisotopic separation was detected for this peptide, and this is the average molecular mass.

[c]A peak was also detected with a molecular mass of 18 Da lower, which could correspond to the clyclic anhydride or imide intermediate of this peptide before another cleavage event.

[d]One or two peaks were also detected with a molecular mass of 16 or 32 Da higher, which could correspond to the same peptide of which methionine was oxidized one or two times.

***Table 5**. Overview of peptides that were detected in the filtrate (F) and/ or the heated sample (H). For these peptides, multiple peptides derived from β-lactoglobulin are possible.*

		Molecular mass (Da)	
Amino-acid sequence peptides	Location	Theoretical	Measured
AQSAPLRVYVEELKPTPEGDLEILLQKWEN	34- 63 (A)	3465.8	3467.5[c]
ECAQKKIIAEKTKIPAVFKIDALNENKVLVL	65- 95 (A)	3466.0	
(D)AQSAPLRVYVEELKPTPEGDLEILLQKWEN(D)	34- 64 (33-63) (A)[a]	3580.9	3582.3
LEILLQKWENGECAQKKIIAEKTKIPAVFKI	54- 84 (B)[a]	3581.0	
(D)ECAQKKIIAEKTKIPAVFKIDALNENKVLVL(D)	65- 96 (64-95) (A)	3581.0	
DAQSAPLRVYVEELKPTPEGDLEILLQKWEND	33- 64 (A)	3695.9	3697.8[d]
(D)LEILLQKWENGECAQKKIIAEKTKIPAVFKI(D)	54- 85 (B)	3696.1	
DECAQKKIIAEKTKIPAVFKIDALNENKVLVLD	64- 96 (A)	3696.1	

[a,c,d] See Table 4.

Enzyme induced formation of β-lactoglobulin fibrils by AspN endoproteinase

Chapter 6

This chapter has been submitted for publication.

ABSTRACT

This paper describes a low temperature, enzymatic route to induce fibrillar structures in a protein solution. The route comprises two steps. First, β-lactoglobulin was hydrolyzed into peptides at pH 8 and 37 °C with the enzyme AspN endoproteinase, which resulted in the formation of random aggregates. After hydrolysis, the pH was lowered to 2. As a result, long fibrillar aggregates were formed which was observed using transmission electron microscopy and Thioflavin T fluorescence measurements.

INTRODUCTION

Long fibrillar protein aggregates can be obtained by heating (80-90 °C) an aqueous solution of β-lactoglobulin for several hours (2-24 h) at pH 2. The fibrils obtained have a length between 1 to 10 μm, and a thickness of a few nanometers.[1-4] We showed previously that the fibrils formed under these conditions consist of peptides originating from intact β-lactoglobulin molecules.[5] These peptides were formed due to acid hydrolysis of the bonds between aspartic acid residues and any other amino acid residue. The molecules inside these fibrils are held together by intermolecular β-sheets. The presence of these β-sheets can be monitored using the fluorescent dye Thioflavin T (ThT), which binds to the β-sheets.[6,7] Therefore, the ThT fluorescent intensity is often used as an indicator for the presence and concentration of fibrils derived from β-lactoglobulin.[8]

Since protein hydrolysis turned out to be necessary to obtain the peptides of the fibrils, it can be hypothesized that enzymatic hydrolysis may also lead to the formation of peptides that can form fibrils. Previous studies have shown that enzymatic hydrolysis of β-lactoglobulin can lead to the formation of aggregates, and as a result gelation occured.[9,10] However, long fibrillar aggregates were not observed in these studies.

During the current study, we investigated whether enzymatic hydrolysis of β-lactoglobulin can be applied as a method for the formation of peptides that can act as building blocks for fibrillar aggregates. The enzyme AspN endoproteinase was chosen, because this enzyme cleaves the peptide bonds N-terminal to aspartic acid residues,[11] which would lead to similar peptides as during the heat induced acid hydrolysis. β-Lactoglobulin was incubated with the enzyme at pH 8 and 37 °C. We studied the formation of β-lactoglobulin aggregates using this method, and investigated the necessity of incubation at pH 2 after the hydrolysis step to induce fibril formation.

MATERIAL AND METHODS

Unless mentioned otherwise, all chemicals were of analytical grade and purchased from Merck (Darmstadt, Germany), Sigma Aldrich (Steinheim, Germany) or Invitrogen (Carlsbad, CA, USA).

Enzymatic hydrolysis of β-lactoglobulin

A 2 wt% β-lactoglobulin (product no. 61329, Sigma Aldrich) solution was dissolved in a buffer (pH 8) containing 50 mM Tris-HCl and 2 mM zinc acetate. The enzyme AspN endoproteinase (P8104S, New England Biolabs, Ipswich, M.A., U.S.A.) was dissolved in Millipore water (0.17 mg/ml), and was added to the β-lactoglobulin solution (10^{-3} mg enzyme/ ml). The solution was incubated at 37 °C and mixed during the incubation. Samples were taken after various hydrolysis times ($t_{hydrolysis}$ = 0.25 - 24 h). Subsequently, the samples were quenched to pH 2 by adding an HCl solution (18% v/v). At pH 2 and room temperature, the samples were mixed, and the incubation time at pH 2 was 48 h minus the hydrolysis time.

High-Performance Size-Exclusion-Chromatography (HP-SEC)

HP-SEC experiments were conducted using an ÄKTA purifier system (GE Healthcare, Uppsala, Sweden) operated by Unicorn software. Three samples ($t_{hydrolysis}$ = 2, 11 and 24 h) were freeze-dried, and ~ 2 mg of the freeze-dried sample was dissolved in 0.5 ml of a 0.15 M Tris-HCl buffer (pH 8) containing 8 M guanidine chloride and 0.1 M 1,4-dithiothreitol (DTT). After mixing for 45-60 min, 0.215 ml of acetonitrile, containing 2% (v/v) tri-fluoroacetic acid (TFA) was added, followed by further mixing for 45-60 min. After mixing, the samples were centrifuged (18,000 g, 10 min, 20 ºC). Samples of 20 µl were applied onto the column (Shodex Protein KW-803, 300 x 8 mm, Showa Denko K. K., Tokyo, Japan). The column was equilibrated and run with 6 M urea, containing 30% (v/v) acetonitrile and 0.1% (v/v) TFA. The flow rate was 0.2 ml/min, and the absorbance was monitored at 214 nm. The column was calibrated using various proteins with molecular masses between 300 and 67,000 Da.

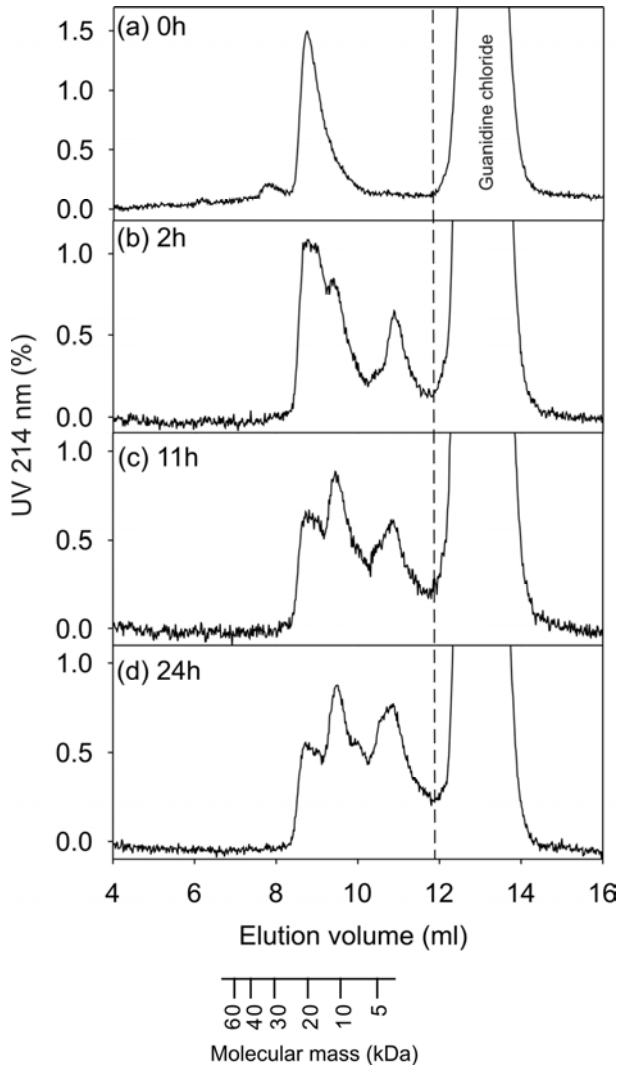

Figure 1. *HP-SEC elution profiles of β-lactoglobulin solutions after different hydrolysis times ($t_{hydrolysis}$ = 0, 2, 11 and 24 h) and incubation at pH 2 (incubation time = 48 h – $t_{hydrolysis}$). The secondary x-axis indicates the corresponding molecular mass at the elution volume. The increase in absorbance after 12 ml is due to the elution of guanidine chloride.*

Transmission Electron Microscopy (TEM)

TEM pictures were made from the sample with an hydrolysis time of 24 h at pH 8, and of the same sample in which the pH was lowered to 2. TEM grids were prepared by negative staining. A droplet of the sample (50x diluted) was put onto a carbon support film on a copper grid. After 15 s, the droplet was removed with a filter paper. Then, a droplet of 2% uranyl acetate was put onto the grid and removed after 15 s using a filter paper. The micrographs were taken with a JEOL electron microscope (JEM2100, Tokyo, Japan) operating at 100 kV.

Thioflavin T fluorescence

A Thioflavin T (ThT) solution (18 mg/l) was prepared by dissolving ThT in a 10 mM sodium phosphate buffer (pH 7) containing 150 mM NaCl. The solution was filtered (0.2 µm, Minisart®, Sartorius) to remove undissolved ThT. Samples of 48 µl were added to 4 ml ThT solution. The fluorescence of the samples was measured using a luminescence spectrophotometer (LS50B, Perkin Elmer, Waltham, Massachusetts, USA). ThT was excited at a wavelength of 460 nm and the emission of the sample (I_{ThT}) was measured at 486 nm.

***Table 1**. ThT fluorescent intensities (I_{ThT}) of different samples immediately after the enzymatic hydrolysis (pH 8), and after incubation at pH 2.*

$t_{hydrolysis}$ (h) (pH 8)	I_{ThT} after $t_{hydrolysis}$	$t_{incubation}$ (h) (pH 2)	I_{ThT} after $t_{incubation}$
0	32[1]	*48*	62[1]
0.25	25	*47.75*	235
0.5	27	*47.5*	364
1	32	*47*	123
2	40	*46*	108
4	50	*44*	565
6	58	*42*	114
11	67	*37*	234
24	107	*24*	520

[1] No enzyme was added to this solution to ensure the prevention of hydrolysis.

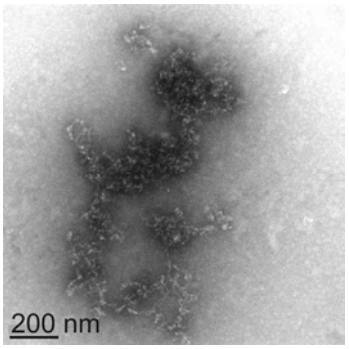

***Figure 2**. TEM picture of β-lactoglobulin after enzymatic hydrolysis at pH 8 for 24 h.*

RESULTS

β-Lactoglobulin was hydrolyzed by the enzyme AspN endoproteinase, and samples were taken after different hydrolysis times ($t_{hydrolysis}$ = 0.25 - 24 h). During the enzymatic hydrolysis, the solution became turbid, suggesting the formation of large random aggregates with a typical dimension larger than the wavelength of light. The samples were then quenched to pH 2, and kept at this pH for 48 h minus the hydrolysis time. When the pH was lowered to 2, the samples became less turbid.

Figure 1 shows the HP-SEC elution profiles of three samples ($t_{hydrolysis}$= 2, 11 and 24 h) and the elution profile of untreated β-lactoglobulin ($t_{hydrolysis}$ = 0h). The untreated β-lactoglobulin eluted around 8.8 ml. The hydrolysis products eluted later than β-lactoglobulin, indicating that they have a smaller molecular mass. As expected, the relative amount of β-lactoglobulin decreased as a function of hydrolysis time. After 24 h of hydrolysis, approximately 80% of β-lactoglobulin was converted into smaller molecules.

Table 1 shows the fluorescent intensity (I_{ThT}) as a function of hydrolysis time. For each hydrolysis time, the intensity is shown before (immediately after the specific hydrolysis time), and after incubation at pH 2 ($t_{incubation}$). The fluorescent intensity after hydrolysis increased as a function of hydrolysis time, which indicated that during the enzymatic hydrolysis step at pH 8, aggregates were formed containing a certain amount of intermolecular β-sheets. The fluorescent intensity after

incubation at pH 2 was higher for each hydrolysis time than the intensity before incubation at pH 2. This shows that incubation at pH 2 resulted in the formation of more intermolecular β-sheets. The experiments showed no clear correlation between fluorescent intensity and processing time. The complex kinetics of fibril formation, as discussed by Arnaudov et al.,[4] in combination with the low fibril concentrations (which leads to difficulties in taking representative samples) probably accounts for the lack of correlation in time.

Figure 2 shows an example of an aggregate that was formed after enzymatic hydrolysis at pH 8. It is a random shaped aggregates with a diameter of ~1 μm. At pH 8, we only observed this type of random aggregates. The presence of these large, random aggregates also explains why the solution became turbid during the enzymatic hydrolysis.

Figure 3 a, b shows TEM pictures of the samples after 24 h hydrolysis at pH 8 and 24 h incubation at pH 2. Long fibrillar aggregates are now visible that have a length in the order of 1 μm. Obviously, incubation at acidic pH was necessary to obtain fibrils for these conditions. Apart from the long fibrillar aggregates, random shaped aggregates (~50 nm) were also present in the samples, but the large random aggregates as present at pH 8 seem to have disappeared. To confirm the necessity of protein hydrolysis as a first step for protein fibrillization, TEM pictures were made of a β-lactoglobulin solution (2 wt%) that was kept at pH 8 for 24 h without enzyme added, and subsequently incubated at pH 2 for 48 h at room temperature. This sample did not contain aggregates.

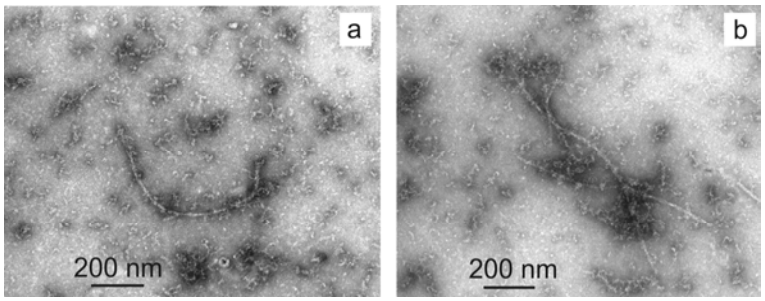

***Figure 3 (a, b)**. TEM pictures of β-lactoglobulin after enzymatic hydrolysis at pH 8 for 24 h and incubation at pH 2 for 24 h.*

DISCUSSION

This study shows that long fibrillar aggregates from β-lactoglobulin can be obtained by hydrolyzing β-lactoglobulin into peptides by the enzyme AspN endoproteinase. This confirms the results of previous research, which showed that peptides, and not intact proteins, are the building blocks of fibrillar aggregates of β-lactoglobulin when they were formed by heating at pH 2.[5] Fibril formation only took place after incubation at pH 2, and not at pH 8. In our previous study, we explained the presence of specific peptides in the fibrils by their capacity to form β-sheets, the net charge and the hydrophobicity of those peptides originating from β-lactoglobulin. The fact that lowering the pH to an acidic pH was necessary to obtain fibrils suggests that the positive charge of the peptides is an important factor to obtain fibrils instead of random aggregates. Since a heat treatment above the denaturation temperature was not used during this study, it can also be concluded that this heat treatment is not a prerequisite for transforming peptides into fibrils. Previous work showed already that fibrils of β-lactoglobulin could be formed at room temperature after a short heat treatment of 2 h, during which no fibril formation took place yet.[12]

At pH 8, the fluorescent intensity increased in time, while random aggregates were formed. At pH 2, random aggregates (smaller in size than at pH 8) and fibrils were observed, which led to a higher fluorescent intensity than at pH 8. In other words, the random aggregates contained β-sheets that resulted in an increase in fluorescent intensity, but the amount of β-sheets was less than the amount obtained at pH 2. Bromley et al.[13] also observed that non-fibrillar aggregates of β-lactoglobulin contained β-sheets. ThT fluorescence is thus not a prove for the presence of fibrils, and other methods, such as microscopy (TEM and AFM), X-ray diffraction or flow-induced birefringence,[4,8,13] need to be used to confirm the presence of fibrils. Furthermore, the random aggregates might contain a certain amount of peptides that have the capacity to aggregate into fibrils. As a result, the formation of random aggregates leads to a lower availability of peptides to form fibrils.

For the enzymatic hydrolysis, zinc acetate was added to the solution. It has been shown that zinc can have either a positive[14] or a negative[15] effect on the rate of fibril formation of the non-beta amyloid component (NAC) and β-amyloid of Alzheimer's disease fibrils. However, the fibril morphology was not influenced by zinc, and the fibril formation itself was not induced by zinc.[14]

ACKNOWLEDGEMENTS

The authors thank H. Baptist and J. van Lent for their assistance with the TEM analysis. We also thank H. Gruppen and J. Vereijken for the useful discussions about this research. We acknowledge the Dutch research school VLAG and the Dutch research program MicroNed for the financial support of this research.

REFERENCES

1. Durand, D.; Gimel, J.C.; Nicolai, T. Aggregation, gelation and phase separation of heat denatured globular proteins. *Physica A* **2002**, 304, 253 - 265.

2. Gosal, W.S.; Clark, A.H.; Pudney, P.D.A.; Ross-Murphy, S.B. Novel amyloid fibrillar networks derived from a globular protein: β-lactoglobulin. *Langmuir* **2002**, 18, 7174-7181.

3. Rogers, S.S.; Venema, P.; Sagis, L.M.C.; Van der Linden, E.; Donald, A.M. Measuring the length distribution of amyloid fibrils: a flow birefringence technique. *Macromolecules* **2005**, 38, 2948-2958.

4. Arnaudov, L.N.; De Vries, R.; Ippel, H.; Van Mierlo, C.P.M. Multiple steps during the formation of β-lactoglobulin fibrils. *Biomacromolecules* **2003**, 4, 1614-1622.

5. Akkermans, C.; Venema, P.; Van der Goot, A.J.; Gruppen, H.; Bakx, E.J.; Boom, R.M.; Van der Linden, E. Peptides are building blocks of heat induced fibrillar protein aggregates of β-lactoglobulin formed at pH 2. *Biomacromolecules* **2008**, doi: 10.1021/bm7014224.

6. Krebs, M.R.H.; Bromley, E.H.C.; Donald, A.M. The binding of Thioflavin-T to amyloid fibrils: localisation and implications. *Journal of Structural Biology* **2005**, 149, 30-37.

7. Naiki, H.; Higuchi, K.; Hosokawa, M.; Takeda, T. Fluorometric determination of amyloid fibrils in Vitro using the fluorescent dye, Thioflavine T. *Analytical Biochemistry* **1989**, 177, 244-249.

8. Bolder, S.G.; Sagis, L.M.C.; Venema, P.; Van der Linden, E. Thioflavin T and birefringence assays to determine the conversion of proteins into fibrils. *Langmuir* **2007**, 23, 4144-4147.

9. Otte, J.; Lomholt, S.B.; Ipsen, R.; Stapelfeldt, H.; Bukrinsky, J.T.; Qvist, K.B. Aggregate formation during hydrolysis of β-lactoglobulin with a Glu and Asp specific protease from *Bacillus licheniformis*. *Journal of Agricultural and Food Chemistry* **1997**, 45, 4889-4896.

10. Doucet, D.; Foegeding, E.A. Gel formation of peptides produced by extensive enzymatic hydrolysis of β-lactoglobulin. *Biomacromolecules* **2005**, 6, 1140-1148.

11. Grimwood, B.G.; Plummer Jr., T.H.; Tarentino, A. L. Purification and characterization of a neutral zinc endoproteinase secreted by *flavobacterium meningosepticum*. *Archives of Biochemistry and Biophysics* **1994**, *311*, 127-132.

12. Akkermans, C.; Venema, P.; Rogers, S.S.; Van der Goot, A.J.; Boom, R.M.; Van der Linden, E. Shear pulses nucleate fibril aggregation. *Food Biophysics* **2006**, 1, 144-150.

13. Bromley, E.H.C.; Krebs, M.R.H.; Donald, A.M. Aggregation across the length-scales in β-lactoglobulin. *Faraday Discussions*. **2005**, 128, 13-27.

14. Khan, A.; Ashcroft, A.E.; Higenell, V.; Korchazhkina, O.V.; Exley, C. Metal accelerate the formation and direct the structure of amyloid fibrils of NAC. *Journal of Inorganic Biochemistry* **2005**, 99, 1920-1927.

15. Ha, C.; Ryu, J.; Beum Park, C. Metal ions differentially influence the aggregation and deposition of Alzheimer's β-amyloid on a solid template. *Biochemistry* **2007**, 46, 6118-6125.

Properties of protein fibrils in whey protein isolate solutions: microstructure, flow behaviour and gelation

Chapter 7

This chapter has been submitted for publication.

ABSTRACT

We studied how protein fibrils (~1 μm in length, prepared by heating at pH 2) can be used to modify structural properties of concentrated WPI solutions. Using TEM, flow-induced birefringence and ThT fluorescence, we observed that the fibrils become shorter upon increasing the pH, and clusters were present at pH 5-7. For pH 3.5 and 7, the effect of adding fibrils to WPI solutions was studied. Different behaviour was observed, which makes this system rather complex. Rheological measurements showed that the presence of fibrils induced shear thickening (only at pH 3.5) and shear thinning behaviour, and resulted in an increase in viscosity and gel strength. Unstable flow regimes were observed for both pH values, which hints in the direction of phase separation. For pH 7, a phase separated dispersion was observed in the macrostructure after gelation using SEM.

INTRODUCTION

There is a need for the development of new functional food ingredients that can be used to modify the textural properties of food products. In view of the current trends towards foods with a high concentration of protein (high protein foods), and new meat-replacement products, it is desirable to make these ingredients protein based. The development of high protein foods is based on the observation that proteins increase the satiety level after consumption, and thus can help to achieve body-weight reduction.[1,2] New meat-replacement products are desired, because there are many environmental and economical problems attached to the production of meat.[3-5]

Ingredients that are often used to modify the structural properties of protein systems are polysaccharides, such as xanthan gum, or proteins, such as gelatin. Bryant and McClements[6] (pH 7) showed that xanthan gum can be used to induce phase separation in heat-denatured WPI (whey protein isolate) solutions. Walkenström and Hermansson[7] studied gelation of WPI with gelatin. At pH 7.5, the gel formation of WPI was independent of gelatin, and a bi-continuous network was observed. At pH 3, WPI and gelatin formed a strongly aggregated network in which the two polymers are mixed. Vardhanabhuti et al.[8] added whey protein polymers (prepared by heating at pH 7) to WPI gels (10% protein, pH 7), and were able to modify the gel properties. They also found that adding these polymers gave stronger gels, and changed the type of gel structure from particulate to fine-stranded.

Protein fibrils are highly anisotropic protein aggregates, which have a length of 1-10 μm and a diameter of 1-10 nm. Fibrils of WPI can be obtained by heating the protein for several hours at pH 2.[9-11] Applying flow (simple shear flow or stirring) results in enhanced fibril formation.[12,13] For β-lactoglobulin (the major whey protein), it has been shown that during the heat treatment at pH 2, the protein is hydrolyzed into peptides, and part of these peptides are present in the fibrils.[14] Due to their extremely anisotropic dimensions, protein fibrils might be used as ingredients to modify the textural properties of food products. Previous research showed that WPI fibril solutions have a high viscosity, and show shear thinning

behaviour.[13] Furthermore, cold-set gels (at pH 7 or 8) with a low amount of protein can be made by adding calcium-chloride to the WPI fibrils.[15]
However, the behaviour of these fibrils in a concentrated protein system in order to modify the textural properties of this system has not been studied yet. Therefore, the objective of this study was to observe how protein fibrils modify the structural properties of concentrated protein solutions and gels. In this way, it can be observed how fibrils can be used to create products with a higher viscosity, to modify the flow behaviour, or to create anisotropic structures.
The first part of this study describes the properties of a fibril solution at different pH values by measuring the fibril concentration using birefringence and Thioflavin T fluorescence measurements, and observing changes in fibril morphology using TEM (Transmission Electron Microscopy). In the second part, the properties of WPI/ fibril solutions at pH 3.5 and 7 were studied by their visual appearance and flow behaviour. The third part comprises the properties of fibrils in WPI gels at pH 3.5 and 7, which was done by observing changes in micro- and macrostructure using SEM (Scanning Electron Microscopy) and measuring the rheological properties.

MATERIAL AND METHODS

Preparation of protein fibrils

Protein fibrils were prepared from whey protein isolate (bipro, Davisco Foods International, Inc., Le Sueur, MN, USA). WPI was dissolved in Millipore water, and the pH was set at 2 by adding a concentrated HCl solutions (18 wt%). To remove undissolved protein, the solution was centrifuged (19,000 g, 30 min, 4 °C). The protein concentration of the solution was 2.8 wt%, which was determined using DUMAS analysis (NA 2100 Protein, CE instruments, Milan, Italy), using a protein factor of 6.38 for WPI. To induce fibril formation, the protein solution was heated and stirred for 20 h at 90°C. After fibrillization, fibrils and non-aggregating peptides were present in this solution. Nevertheless, we address this solution as ‘fibril solution’ in the remaining part of the paper. To analyze the effect of pH on

the properties of the fibril solution, the pH was set to different pH values (pH 3, 4, 5, 7 or 8) by adding 1 M NaOH.

Preparation of WPI solutions and WPI/ fibril solutions

To prepare solutions of WPI and WPI/ fibrils, WPI was added to either Millipore water or the fibril solution (see previous section for preparation of the fibril solution), and WPI was dispersed by stirring. The pH was set to 3.5 or 7 by adding 1 M NaOH or 18 wt% HCl. The protein concentrations (0, 2.5, 7.5, 12.5, 17.5 and 22.5 wt%) mentioned in the remaining part of the paper refer to the amount of WPI added to Millipore water or the fibril solution.

Preparation of WPI gels

Gels were prepared from WPI solutions and WPI/ fibril solutions in a shearing device (Wageningen University, The Netherlands). The details of the shearing device were described by Manski et al.[16] and Peighambardoust et al.[17] The gels were subjected to a heating profile, and Table 1 shows the processing conditions of the gels. Gels were prepared from solutions of pH 3.5 (gels A) and pH 7 (gels B). Some gels were subjected to shear flow during the entire heating profile (A2-, A2+, B2-, and B2+), one gel was subjected to shear flow only during the temperature increase (A3+), and the rest was kept under quiescent conditions (A1-, A1+, B1-, and B1+). The WPI concentration of the gels was 12.5 wt%, and gels were prepared without and with fibrils added, which is indicated by '-' (without) or '+' (with) in Table 1. After the gel preparation, the gels were analyzed using rheological measurements and SEM. The gels without fibrils were also prepared at a protein concentration of 17.5 wt%, because the gels of 12.5 wt% were too weak for SEM analysis.

Transmission electron microscopy

The microstructure of the fibrils was observed using TEM. TEM grids of the fibril solution at different pH values were prepared by negative staining. The samples were diluted 100 times, and a droplet of the diluted sample was put onto a carbon support film on a copper grid. After 15 s, the droplet was removed with a filter

paper. Then, a droplet of 2 wt% uranyl acetate (Sigma, Steinheim, Germany) was put onto the grid and removed after 15 s. The micrographs were made using a Philips CM 12 electron microscope (Eindhoven, The Netherlands) operating at 80 kV.

Flow-induced birefringence

The flow-induced birefringence of the fibril solution at different pH values was measured on a strain-controlled ARES rheometer (Rheometric Scientific Inc., Piscataway, USA) with Couette geometry (rotating cup with a diameter of 33.8 mm and a static bob with a diameter of 30 mm). A laser beam with a wavelength of 670 nm passed along the axis of vorticity through the gap between the cup and the bob. The birefringence was measured with a modified optical analysis module.[18] The birefringence was measured at a shear rate of 73 s^{-1} for 30 s. When the fibrils are aligned, the birefringence signal is proportional to the total fibril length concentration.[19]

Thioflavin T fluorescence

A Thioflavin T (ThT) solution (18 mg/l) was prepared by dissolving ThT (Merck, Darmstadt, Germany) in a 10 mM sodium phosphate buffer (pH 7) containing 150 mM NaCl, and the solution was filtered (0.2 µm, Minisart®, Sartorius) to remove undissolved ThT. Samples of 24 µl were added to 4 ml ThT solution. The fluorescence of the samples was measured using a luminescence spectrophotometer (LS50B, Perkin Elmer, Waltham, Massachusetts, USA). ThT was excitated at a wavelength of 460 nm and the emission of the sample (I_{ThT}) was measured at 486 nm. The emission of the ThT solution itself was subtracted from the measured intensity.

***Table 1**. Overview of processing conditions during gel preparation.*

				Temperature increase				Temperature decrease			
Gel	WPI conc. (%)	-/ + fibrils[1]	pH	$T_{initial}$ (°C)	Rate (°C/min)	T_{final} (°C)	Shear rate (s^{-1})	$T_{initial}$ (°C)	Rate (°C/min)	T_{final} (°C)	Shear rate (s^{-1})
A1-	12.5/ 17.5[2]	-	3.5	30	0.8	85	0	85	1.2	30	0
A2-	12.5/ 17.5	-	3.5	30	0.8	85	120	85	1.2	30	120
A1+	12.5	+	3.5	30	0.8	85	0	85	1.2	30	0
A2+	12.5	+	3.5	30	0.8	85	120	85	1.2	30	120
A3+	12.5	+	3.5	30	0.8	85	120	85	1.2	30	0
B1-	12.5/ 17.5	-	7	30	1.1	80	0	80	1.1	30	0
B2-	12.5/ 17.5	-	7	30	1.1	80	120	80	1.1	30	120
B1+	12.5	+	7	30	1.1	80	0	80	1.1	30	0
B2+	12.5	+	7	30	1.1	80	120	80	1.1	30	120

[1] Fibril solution: see ‘Preparation of protein fibrils’.

[2]Gels with a concentration of 17.5 wt% were used for SEM micrographs.

Viscosity

Flow curves of the unheated WPI (22.5 wt% only) and WPI/fibril solutions were measured on a rheometer (MCR 301, Anton Paar, Graz, Austria) with a cone/plate geometry. Rate sweeps were performed with a shear rate varying between 0.01 and 100 s^{-1} (5 points per decade). Each shear rate was applied for 120 s (0.01- 1 s^{-1}) or 30 s (1-100 s^{-1}), and during the last 6 s of this time period, the viscosity was measured. In this way, transient effects were excluded.

Gel strength

The elastic moduli (G') and tan(δ) of the gels (see Table 1 for gel preparations) were measured on a rheometer (MCR 301, Anton Paar) using a plate/plate geometry (diameter 25 mm, gap 3 mm) with serrated plates. Strain sweeps were performed using strains from 0.01 to 100% (15 points/ decade, frequency 1 Hz).

Scanning electron microscopy

The microstructure of the gels (see Table 1 for gel preparations) was observed using SEM at ambient temperature. Dry samples were prepared according to the method described by Muller et al.[20] The samples were cut into squares (~1 cm x 1 cm), and subsequently, put into different DMSO solutions (15%, 30%, and 50% v/v in Millipore water) for 60 min each. The samples were frozen slowly in cold nitrogen gas above liquid nitrogen, subsequently, brought into liquid nitrogen, and freeze fractured on a brass table using a razorblade and a hammer. After fracturing, the samples were put into 50% (v/v) DMSO for > 60 min, and subsequently re-hydrated to water through the reversed DMSO concentration range (60 min each). The samples were dehydrated in a series of ethanol solutions (10%, 30%, 50%, 70%, 90% v/v) for 20 min each, and three times 100% ethanol for 10 min each. Samples in the 100% ethanol were critical point dried with carbon dioxide (CPD 020, Balzers, Liechtenstein). The samples were glued on a sample holder using conductive carbon cement (Leit- C, Neubauer Chemicalien, Germany) with their fracture side upwards. The samples in the holder were sputter coated with 20 nm Platinum (JFC 1200, JEOL, Japan), and analyzed with a FESEM (JEOL 6300 F, Tokyo, Japan) at room temperature at a working distance

of 8 mm, with SE detection at 2-3.5 kV. All images were recorded digitally (Orion, 6 E.L.I. sprl., Belgium) at a scan rate of 100 seconds (full frame) at a size of 2528 x 2030 dpi, 8 bit (grayscale).

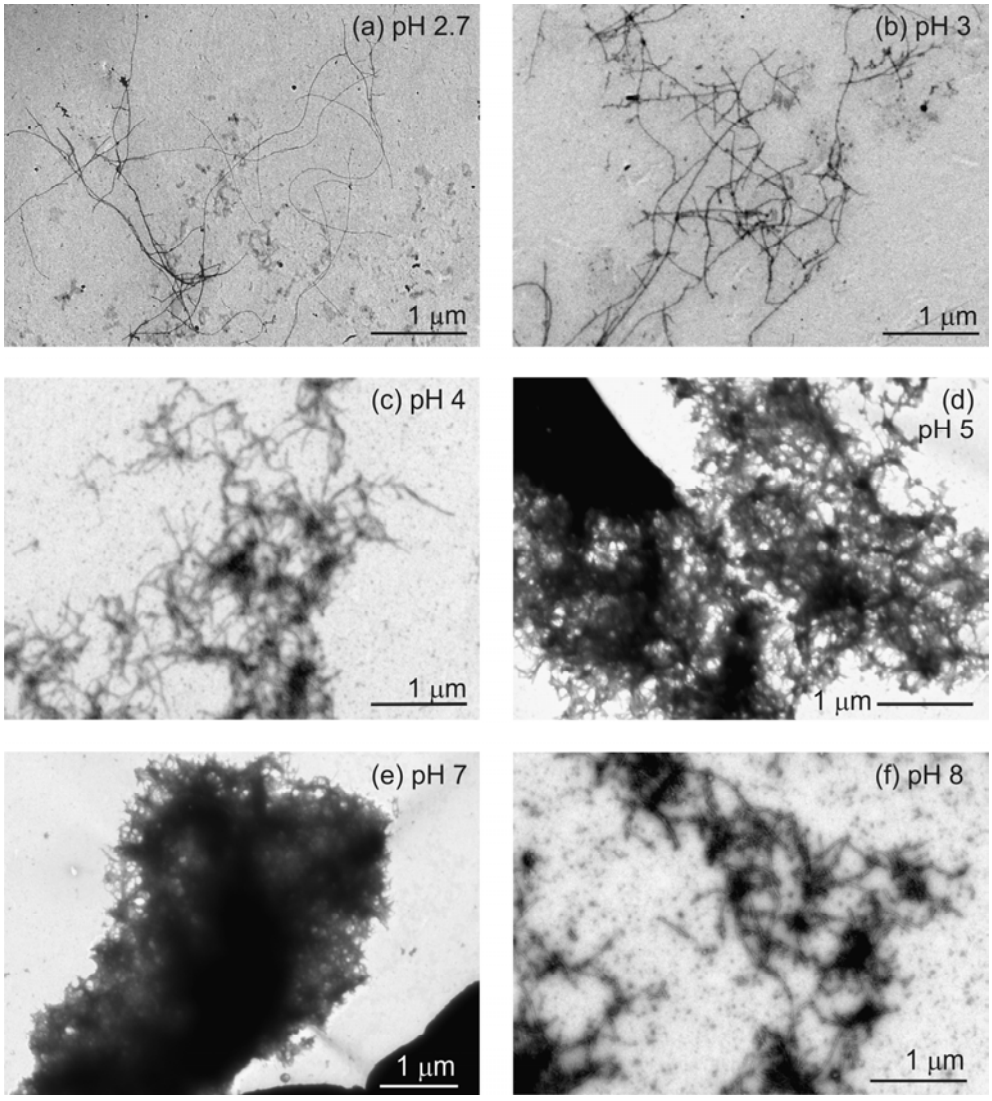

Figure 1. *TEM micrographs of the fibril solution (prepared by heating 2.8 wt% WPI for 20 hours at 90°C and pH 2) at different pH values: (a) pH 2.7, (b) pH 3, (c) pH 4, (d) pH 5, (e) pH 7 and (f) pH 8.*

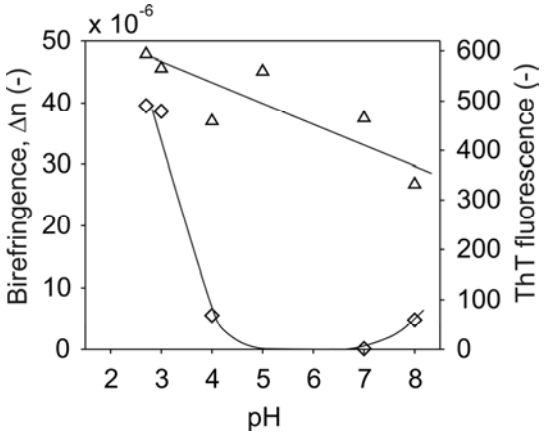

***Figure 2**. (◇)Birefringence (measured at a shear rate of 73 s^{-1}) and (Δ) ThT fluorescence (at 486 nm) of the fibril solution (prepared at pH 2) at different pH values (the lines are only meant to guide the eye).*

RESULTS

Properties of fibril solution at different pH values

Protein fibrils were prepared by heating a solution of WPI (2.8 wt%) at pH 2 and 90°C for 20 hours. During the heat treatment, the pH increased from 2 to 2.7. The properties of the fibril solution at different pH values were characterized by flow-induced birefringence, ThT fluorescence and TEM micrographs. Figure 1 shows TEM micrographs of the fibril solution at different pH values (pH 2.7, 3, 4, 5, 7 and 8). Long fibrillar aggregates with a length of a few micrometers are visible in the TEM micrograph of the original fibril solution (pH 2.7) and at pH 3. At pH 4 and 8, loose clusters of short (~0.5 μm) fibrils are visible, while at pH 5 and 7, dense clusters are visible. The latter solutions were turbid, while at other pH values, the solutions were transparent.

Figure 2 shows the birefringence and Thioflavin T fluorescence as a function of pH. Both measurements showed a decrease as a function of pH. The birefringence decreased very strongly, while the Thioflavin T fluorescence decreased more gradually. These measurements are in accordance with the observations of the TEM micrographs, because clustering of fibrils makes them less susceptible for flow-induced alignment. The gradual decrease of the Thioflavin T fluorescence

could be due to partial dissociation of the fibrils, which results in smaller fibrils as can be seen in the TEM micrographs. It is also possible that due to clustering, ThT binds less efficiently to the fibrils.

Effect of adding fibrils to WPI solutions

Table 2 shows the visual appearance of solutions containing only WPI (2.5 - 22.5 wt%), and solutions containing WPI (0 – 22.5 wt%) and fibrils. The pH of the solutions was 3.5 or 7. The solutions of pH 3.5 were transparent at low concentration and turbid at high concentrations. Upon increasing the protein concentration, the colour of the solutions became more beige. Adding fibrils to WPI solutions of pH 3.5, resulted in solutions containing birefringent domains. These domains were visible up to 7.5 wt% WPI. Above 7.5 wt% WPI, the solutions were turbid, which explains why birefringent domains were not observed anymore. The addition of fibrils at pH 3.5 resulted in an earlier transition from a transparent solution to a turbid solution; at a protein concentration of 7.5 wt%, the solution without fibrils was transparent, while the solution with fibrils was already slightly turbid. The solutions of pH 7 were transparent when no fibrils were present. Upon increasing the protein concentration, the colour became more yellow/ orange. Adding fibrils to WPI solutions of pH 7 resulted in turbid solutions for all protein concentrations, and the colour changed from white into beige upon increasing the protein concentration.

***Table 2**. Visual appearance of WPI solutions of different concentrations without or with fibrils at pH 3.5 and 7*

WPI	pH 3.5				pH 7		
(wt%)	- fibrils		+ fibrils		- fibrils		+ fibrils
0	transparent		transparent, birefringent		transparent	More yellow/orange ↓	turbid, white
2.5	transparent	More beige ↓	transparent, birefringent	More beige ↓	transparent		turbid, white
7.5	transparent		slightly turbid, birefringent		transparent		turbid, white
12.5	slightly turbid		Turbid		transparent		turbid, white
17.5	turbid		Turbid		transparent		turbid, beige
22.5	turbid		Turbid		transparent		turbid, beige

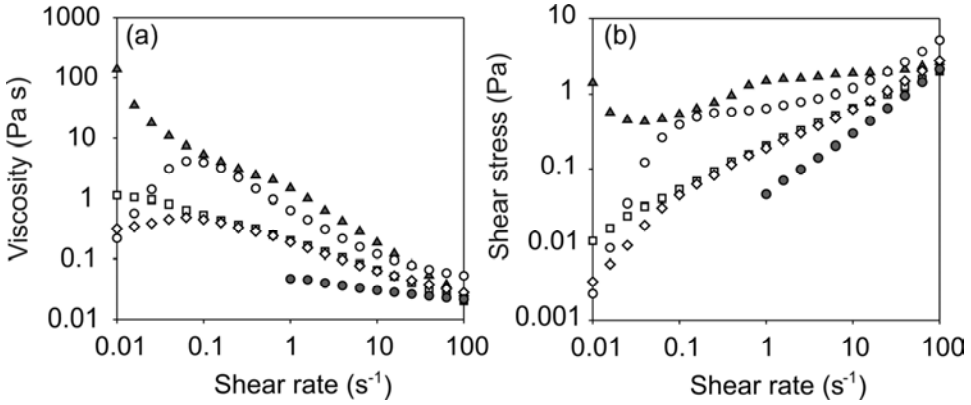

Figure 3. *Viscosity (a) and shear stress (b) curves for WPI/ fibril solutions of pH 3.5 of different WPI concentrations: (▲) 0 wt%, (□) 2.5 wt%, (◇) 12.5 wt%, (○) 22.5 wt%. The curves of a 22.5 wt% WPI solution without fibrils are also included (●).*

.

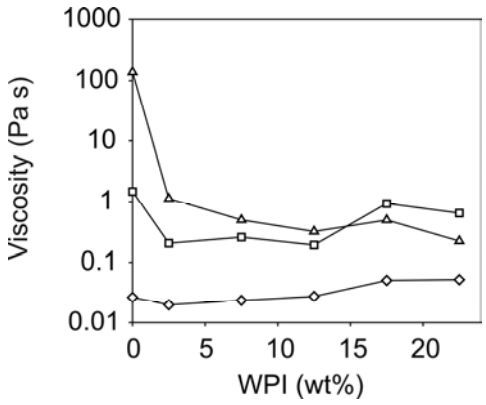

Figure 4. *Viscosities of WPI/ fibril solutions of pH 3.5 plotted versus WPI concentration, measured at 3 different shear rates: (△) 0.01 s^{-1}, (□) 1 s^{-1}, (◇) 100 s^{-1}.*

The flow behaviour of all WPI/ fibril solutions shown in Table 2 was measured, and the flow behaviour of the solution containing 22.5 wt% WPI without fibrils was also measured. Figure 3 shows a part of the flow curves of the pH 3.5 solutions. The flow curve of 7.5 wt% WPI/ fibril solution almost overlapped with the flow curve of 12.5 wt%, while the flow curve of 17.5 wt% almost overlapped with the flow curve of 22.5%. Therefore, the curves of these concentrations (7.5 and 17.5 wt%) are not shown in Figure 3.

The viscosity and degree of shear thinning of all WPI/ fibril solutions were higher than the viscosity and degree of shear thinning of 22.5 wt% WPI (without fibrils). Thus, combining fibrils and WPI at pH 3.5 resulted in a higher viscosity than only WPI. The flow curve of the solution to which no WPI was added (0 wt%) was for most shear rates above the flow curves of the WPI/ fibril solutions. Therefore, combining WPI and fibrils resulted in a lower viscosity (for most shear rates) than the fibril solution without WPI. Shear thickening behaviour, followed by shear thinning behaviour was observed in the flow curves of 12.5, 17.5 and 22.5 wt% WPI/ fibril solutions.

The stress curves in Figure 3b show interesting flow behaviour for a part of the solutions. First of all, an initial decrease in stress as a function of shear rate can be observed in the flow curve of the fibril solution (0 wt%) for low shear rates. This indicates that the system was unstable at these conditions. An explanation for this phenomenon could be phase separation, but this has to be on a microscopic scale because this solution was transparent (see Table 2). In the flow curves of 22.5 wt% and 17.5 wt%, a stress plateau was observed around a shear rate of 1 s^{-1}. This plateau could indicate that the system was also unstable due to phase separation.

Figure 4 shows the relation between the measured viscosities and the WPI concentration of the WPI/ fibril solutions at three different shear rates. For the lowest shear rate (0.01 s^{-1}), a decrease in viscosity was observed as a function of protein concentration. For a shear rate of 1 s^{-1}, the viscosity first decreased, then remained constant, and finally increased as a function of protein concentration. For the highest shear rate (100 s^{-1}), the viscosity increased as a function of protein concentration.

Figure 5 shows the flow curves of the WPI/ fibril solutions of pH 7, and the WPI solution containing 22.5 wt% WPI (without fibrils). The flow curves of 7.5 wt% and 17.5 wt% WPI/ fibril solutions are not included because they almost overlapped with the flow curves of 2.5 wt% and 22.5 wt%, respectively. All flow curves show shear thinning behaviour. The viscosities and shear stresses of all WPI/ fibril solutions were higher than the viscosity and shear stress of 22.5 wt% WPI (without fibrils). Thus, combining fibrils and WPI at pH 7 resulted in a higher viscosity than only WPI. The flow curve of the solution to which no WPI

was added (0 wt%) was also below the flow curves of the WPI/ fibril solutions. Therefore, combining WPI and fibrils resulted in a higher viscosity than the fibril solution without WPI. The stress curves of Figure 5b shown interesting flow behaviour for part of the solutions. Around a shear rate of 1 s^{-1}, a stress plateau was observed for the WPI/ fibril solutions of 12.5, 17.5 and 22.5 wt%. This stress plateau could again be caused by instabilities in the system due to phase separation.

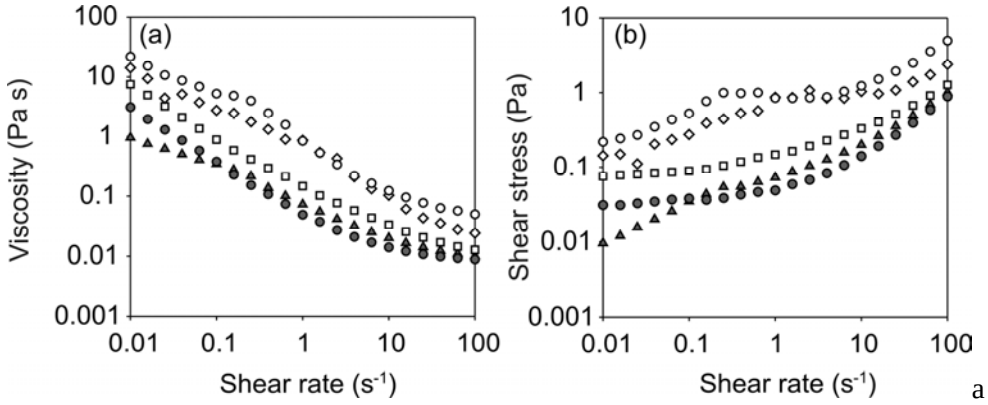

a

***Figure 5**. Viscosity (a) and shear stress curves (b) for WPI/ fibril solutions of pH 7 of different WPI concentrations: (▲) 0 wt%, (□) 2.5 wt%, (◇) 12.5 wt%, (○) 22.5 wt%. The curves of a 22.5 wt% WPI solution without fibrils are also included (●).*

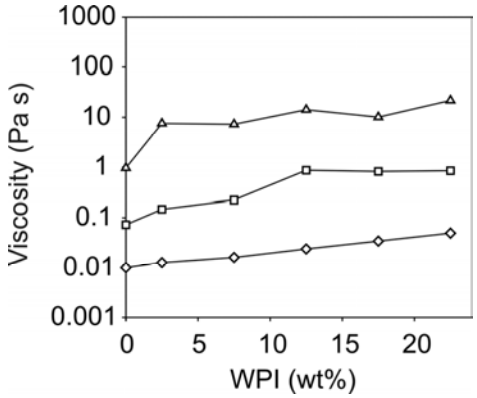

***Figure 6**. Viscosities of WPI/ fibril solutions of pH 7 plotted versus WPI concentration, measured at 3 different shear rates: (△) 0.01 s^{-1}, (□) 1 s^{-1}, (◇) 100 s^{-1}.*

Figure 6 shows the viscosities as a function of WPI concentrations of the WPI/ fibril solutions of pH 7. The general trend was an increase in viscosity for increasing protein concentration. At a shear rate of 1 s^{-1}, the viscosity was constant at the highest protein concentrations.

Effect of adding fibrils to WPI gels

WPI gels with and without fibrils were prepared by subjecting the solutions to a heating and shearing profile (see Material and Methods section for a description of the heating and shearing profile).

The gels of pH 3.5 and 7 prepared without fibrils were all transparent, while the gels of pH 7 prepared with fibrils were all white and turbid. This is in accordance with the appearance of the unheated solutions shown in Table 2. The gel of pH 3.5 prepared with fibrils and without shear flow was transparent, while the unheated solution was turbid (see Table 2). However, this is probably due to the smaller path length of light for the gel (~ 4 mm) than for the test tube (~ 10 mm). The gels prepared at pH 3.5 with fibrils under shear flow were turbid. This indicates that due to the shear treatment, larger structures were formed in the gels of pH 3.5 with fibrils compared to the gel that was not subjected to shear flow.

Figure 7 shows SEM micrographs of the gels of pH 3.5. For the gels without fibrils, micrographs were made from gels with a WPI concentration of 17.5 wt%. The gels all consisted of one phase, and there is no clear difference in structure visible for gels prepared with and without the addition of fibrils, or with or without shear flow. This is in contrast with the visual appearance, which indicated that the gels prepared with fibrils and with shear flow contained larger structures than the other gels. For the gels without fibrils, this lack of difference in structure could be due to the fact that these gels were prepared from a solution with a protein concentration of 17.5 wt%. At this protein concentration, the solution was already turbid, while the solution of 12.5 wt% is only slightly turbid (see Table 2).

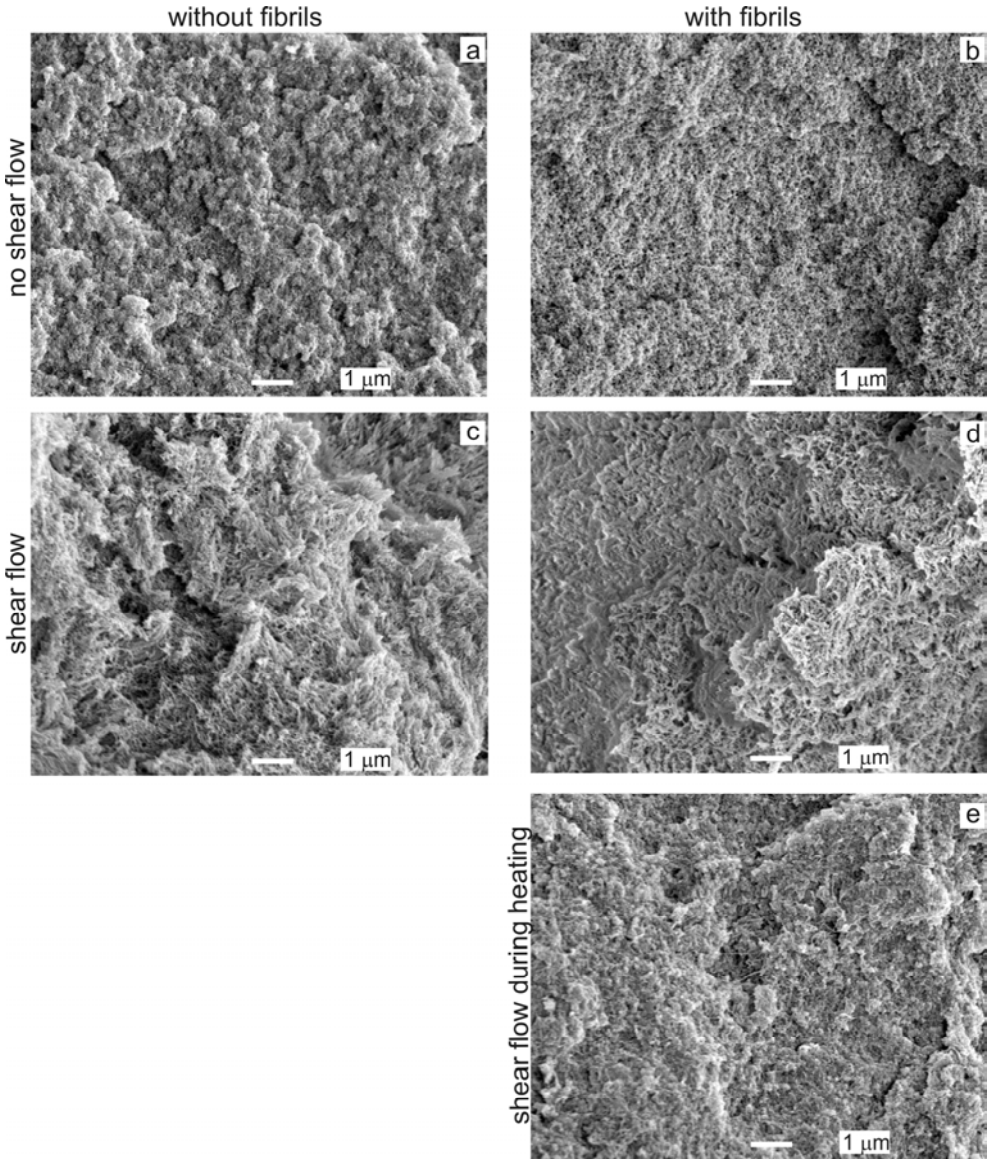

***Figure 7**. SEM micrographs of 17.5 wt% WPI (gels A1- and A2-) and WPI (12.5 wt%)/ fibril solutions (gels A1+, A2+, and A3+) of pH 3.5 (see Table 1 for the gel preparations).*

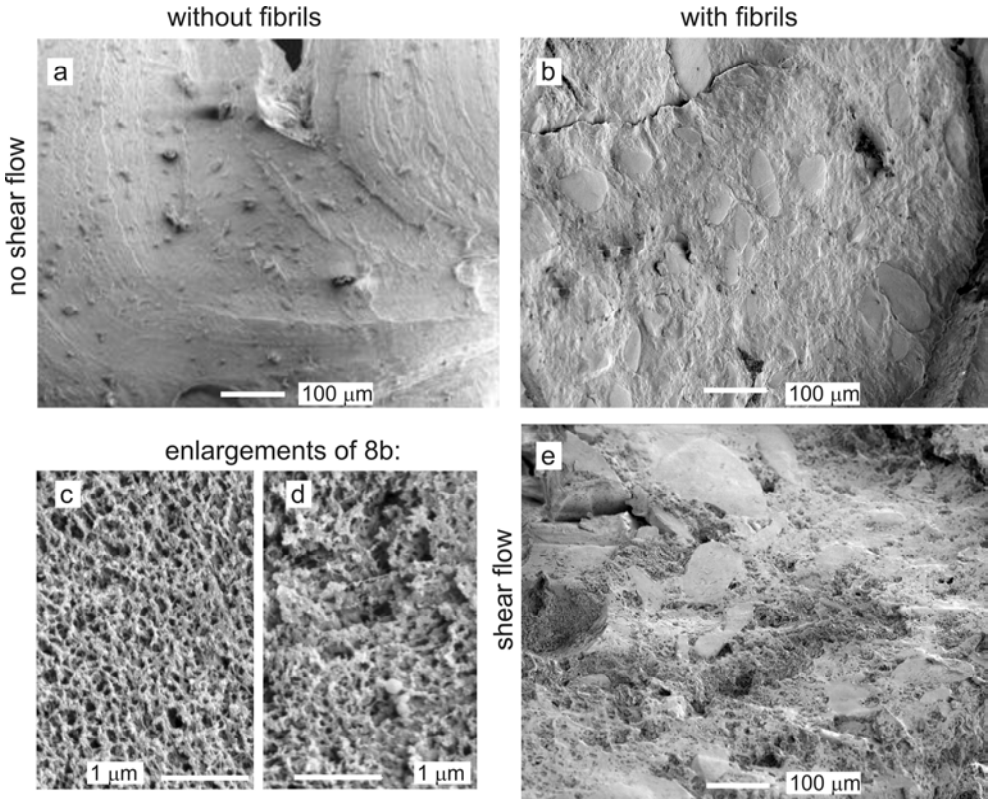

***Figure 8**. SEM micrographs of gels prepared at pH 7: (a) 17.5 wt% WPI (gel B1-), (b) gel of WPI (12.5 wt%)/ fibril solution (gel B1+), (c) enlargement of dispersed phase of 8b, (d) enlargement of continuous phase of 8b, and (e) gel of WPI (12.5 wt%)/ fibril solution (gel B2+).*

Figure 8 shows SEM micrographs of the gels of pH 7. The gel without fibrils consisted of one phase, while gels with fibrils consisted of two phases: a dispersed and continuous phase. Two enlargements of Figure 8b are shown in 8c (dispersed phase) and 8d (continuous phase). These micrographs show that the density of the dispersed phase was higher than the density of the continuous phase. Applying shear flow during the gel preparation resulted in a more porous network than not applying shear flow.

Figure 9 shows the elastic moduli and tan(δ) of the gels of pH 3.5, prepared without and with fibrils. The gels with fibrils were all more elastic than the gels

without fibrils. When shear flow was applied during the whole temperature profile, the elasticity of the WPI/ fibril gel was slightly lower than the WPI/ fibril gel without shear flow. However, when shear flow was only applied during the temperature increase, the gel was more elastic than without shear flow. This suggests that the structure is also influenced when shear flow is applied during the temperature decrease. At the highest strains applied, all gels started to fracture, which resulted in an increase of tan(δ).

Figure 10 shows the elastic moduli and tan(δ) of the gels of pH 7, prepared with and without fibrils. Again, gels with fibrils were more elastic than gels without fibrils. The gels without fibrils did not yield at the highest strain applied, which can be observed by the constant G' and tan(δ). The gels with fibrils started to yield around a strain of 50%. For the gels with fibrils, applying shear flow resulted in a higher elasticity than without applying shear flow. The increase in elasticity due to the addition of fibrils is more pronounced for gels of pH 7 (G' is a factor 100 higher) than for gels of pH 3.5 (G' is a factor 10 higher).

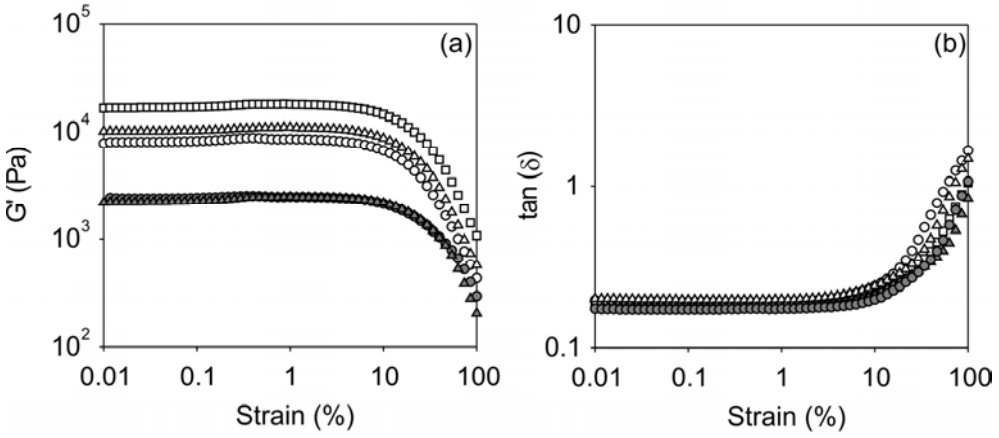

***Figure 9**. Elastic moduli (a) and tan (δ) (b) of WPI gels of pH 3.5: (▲) without fibrils, without shear flow (gel A1-), (●) without fibrils, with shear flow (gel A2-), (△) with fibrils, without shear flow (gel A1+), (○) with fibrils, with shear flow (gel A2+), (□) with fibrils, with shear flow during temperature increase (gel A3+).*

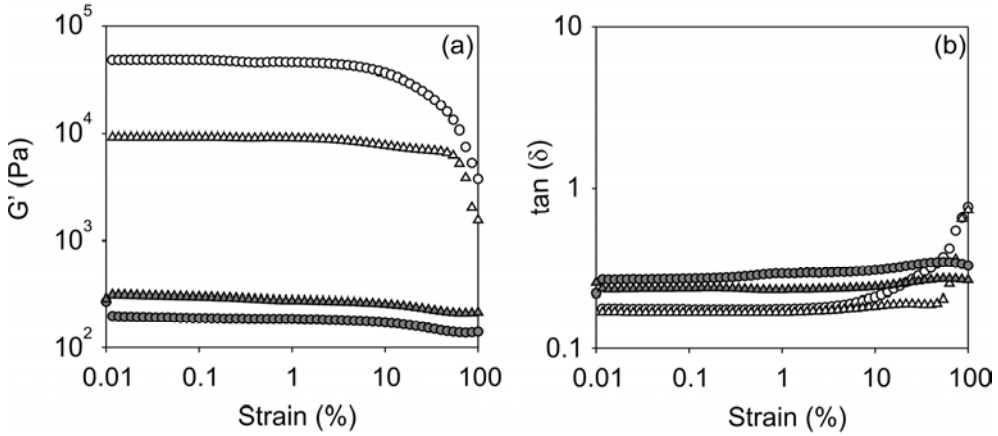

***Figure 10**. Elastic moduli (a) and tan(δ) (b) of WPI gels of pH 7: (▲) without fibrils, without shear flow (gel B1-), (●) without fibrils, with shear flow (gel B2-), (△) with fibrils, without shear flow (Gel B1+), (○) with fibrils, with shear flow (gel B2+).*

DISCUSSION

The properties of WPI fibrils are highly pH dependent. At low pH values, they are present as long non-clustered fibrils, while at higher pH values (5-7), clusters were present and the fibrils were shorter than at low pH. The properties of the fibrils can thus be influenced by modifying the pH. Although, pH modification might not be possible for all potential applications.

By adding fibrils to WPI solutions, we expected that the viscosity and gel strength would increase, and shear thinning behaviour would be induced. These phenomena were indeed observed, but phase separation and shear thickening behaviour were found as well. The occurrence of all these phenomena indicates that the system is highly complex when fibrils are added to whey proteins. Nevertheless, we tried to capture the phase behaviour and phenomena observed in a schematic overview (Figure 11).

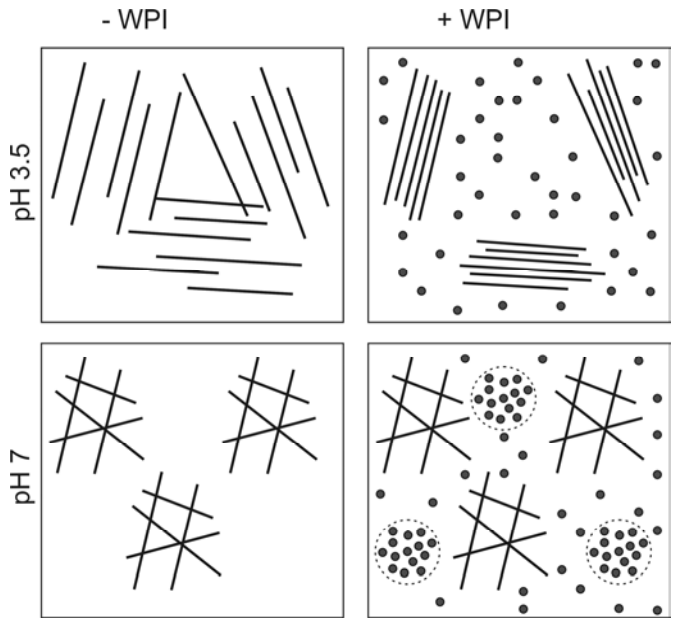

Figure 11. *Schematic overview of the microstructure of fibril solutions and WPI/ fibril solutions at pH 3.5 and 7 (lines = fibrils, and small spheres = WPI).*

At pH 3.5, the fibrils are present in birefringent domains, which was observed using polarized light (see Table 2). Therefore, we have depicted the fibrils in the scheme arranged parallel to each other in domains. When WPI was added to the fibrils, the viscosity decreased (Figure 3a and 4a). This can be explained by a denser packing of the fibrils in the domains due to depletion interactions. At pH 3.5, we observed shear thickening behaviour. Explaining this behaviour remains highly speculative, but it could be due to a rearrangement of the domains under flow, which results in an increase in viscosity. However, we only observed shear thickening at higher WPI concentrations (see Figure 3).

At pH 7, the fibrils are present in clusters, as was observed with TEM micrographs (Figure 1). In the scheme, we only depicted clusters of fibrils, but it is possible that non-aggregated proteins are also present inside the fibril clusters. The presence of these clusters resulted in a turbid solution. Upon adding WPI, the viscosity increased as a function of protein concentration. This means that the domains itself are not changed by adding WPI, and the increase in viscosity of the fibril solution

is due to the addition of WPI. In the gels, a dispersed phase was observed in a continuous matrix (Figure 8). As depicted in the scheme, we assume that the dispersed phase is composed of WPI. It is unlikely that the dispersed phase is composed of fibrils, because the contours of the dispersed domains are very smooth. Furthermore, the gels containing fibrils were ~100x stronger than the gels without fibrils. This drastic increase in gel strength indicates that the fibrils are present in the continuous phase.

At both pH values, instabilities in the flow behaviour were observed, which resulted in a plateau in the stress curves or a decrease in stress as a function of shear rate (see Figures 3b and 5b). These instabilities could be due to phase separation. For pH 7, we did indeed observe macroscopic phase separation in the gels. This phase separation could be due to the separation of fibrils and WPI domains. It is also possible that the fibrils itself arrange themselves into different phases, because the fibril length is polydisperse.[13,21]

As mentioned in the introduction, we also investigated the ability to form anisotropic macrostructures using these fibrils in combination with shear flow. For pH 7, shear flow resulted in a more porous structure and a more elastic gel, while at pH 3, no effect of shear flow was found. However, anisotropy was not observed in either one of these structures.

The results of previous studies on other structural ingredients (xanthan gum,[6] gelatin,[7] and whey protein polymers[8]) in combination with WPI and the results of our study show that different type of networks (e.g. phase separated, mixed, bi-continuous) can be obtained from WPI when mixed with different structuring agents, which makes it still a challenge to predict the structure formation in this system at this stage.

CONCLUSIONS

The results of this study show that the protein fibrils can be used to modify various properties of concentrated protein solutions and gels, which makes them interesting ingredients for various applications. The increase in viscosity and gel strength indicate that these fibrils are suitable to be used as thickening and gelling

agents. The shear thinning and thickening behaviour could be used to tune the flow behaviour during either processing or consumption. Furthermore, the phase separation observed could result in modified fracture properties of high protein foods. However, the properties of the system are highly dependent on the conditions (e.g. pH, protein concentration, and shear flow) used, which makes this system rather complex, and makes it difficult to understand all phenomena observed.

ACKNOWLEDGEMENTS

The authors thank K. Grabowska and J. Eisma for their contribution to a part of the experimental work, J. van Lent and H. Baptist (WUR) for their assistance with the TEM analysis, and J. Donkers (WUR) for her assistance with the SEM analysis. This research was financially supported by the Dutch graduate school VLAG, and the Dutch research program MicroNed.

REFERENCES

1. Westerterp-Plantenga, M.S.; Rolland, V.; Wilson, S. A.J.; Westerterp, K.R. Satiety related to 24 h diet-induced thermogenesis during high protein/ carbohydrate vs high fat diets measured in a respiration chamber. *European Journal of Clinical Nutrition* **1999**, 53, 495-502.
2. Anderson, G.H.; Moore, S.E. Dietary proteins in the regulation of food intake and body weight in humans. *The Journal of Nutrition* **2004**, 134, 974S-979S.
3. Pimentel, D.; Pimentel, M. Sustainability of meat-based and plant-based diets and the environment. *American Journal of Clinical Nutrition* **2003**, 78, 660S-663S.
4. White, T. Diet and the distribution of environmental impact. *Ecological Economics* **2000**, 34, 145-153.
5. Carlsson-Kanyama, A. Climate change and dietary choices - how can emissions of greenhouse gases from food consumption be reduced? *Food Policy* **1998**, 23, 277-293.
6. Bryant, C.M.; McClements, D.J. Influence of xanthan gum on physical characteristics of heat-denatured whey protein solutions and gels. *Food Hydrocolloids* **2000**, 14, 383-390.

7. Walkenström, P.; Hermansson, A.M. Fine-stranded mixed gels of whey protein and gelatin. *Food Hydrocolloids* **1996**, 10, 51-62.

8. Vardhanabhuti, B.; Foegeding, E.A.; McGuffey, M.K.; Daubert, C.R.; Swaisgood, H.E. Gelation properties of dispersions containing polymerized and native whey protein isolate. *Food Hydrocolloids* **2001**, 15, 165-175.

9. Gosal, W.S.; Clark, A.H.; Pudney, P.D.A.; Ross-Murphy, S.B. Novel amyloid fibrillar networks derived from a globular protein: β-lactoglobulin. *Langmuir* **2002**, 18, 7174-7181.

10. Durand, D.; Gimel, J.C.; Nicolai, T. Aggregation, gelation and phase separation of heat denatured globular proteins. *Physica A* **2002**, 304, 253 - 265.

11. Arnaudov, L.N.; De Vries, R.; Ippel, H.; Van Mierlo, C.P.M. Multiple steps during the formation of β-lactoglobulin fibrils. *Biomacromolecules* **2003**, 4, 1614-1622.

12. Bolder, S.G.; Sagis, L.M.C.; Venema, P.; Van der Linden, E. Effect of stirring and seeding on whey protein fibril formation. *Journal of Agricultural and Food Chemistry* **2007** 55, 5661-5669.

13. Akkermans, C.; Van der Goot, A.J.; Venema, P.; Van der Linden, E.; Boom, R.M. Formation of fibrillar whey protein aggregates: influence of heat- and shear treatment and resulting rheology. *Food Hydrocolloids* **2007**, doi: 10.1016/j.foodhyd.2007.07.001.

14. Akkermans, C.; Venema, P.; Van der Goot, A.J.; Gruppen, H.; Bakx, E.J.; Boom, R.M.; Van der Linden, E. Peptides are building blocks of heat induced fibrillar protein aggregates of β-lactoglobulin formed at pH 2. *Biomacromolecules*, in press.

15. Bolder, S.G.; Hendrickx, H.; Sagis, L.M.C.; Van der Linden, E. Ca^{2+}-induced cold-set gelation of whey protein isolate fibrils. *Applied Rheology* **2006**, 16, 258-264.

16. Manski, J.M.; Van der Goot, A.J.; Boom, R.M. Formation of fibrous materials from dense calcium caseinate dispersions. *Biomacromolecules* **2007**, 8, 1271-1279.

17. Peighambardoust, S.H.; Hamer, R.J.; Boom, R.M.; Van der Goot, A.J. Migration of gluten under shear flow as a novel mechanism for separating wheat flour into gluten and starch. *Journal of Cereal Science* **2008**, doi: 10.1016/j.jcs.2007.10.005.

18. Klein, C.; Venema, P.; Sagis, L.M.C.; Van Dusschoten, D.; Wilhelm, M.; Spies, H.W.; Van der Linden, E.; Rogers, S.S.; Donald, A.M. Rheo-optical measurements by Fast Fourier Transform and Oversampling. *Applied Rheology* **2007**, 17, 45210-1 - 45210-7.

19. Rogers, S.S.; Venema, P.; Sagis, L.M.C.; Van der Linden, E.; Donald, A.M. Measuring the length distribution of amyloid fibrils: a flow birefringence technique. *Macromolecules* **2005**, 38, 2948-2958.

20. Muller, W.H.; Van Aelst, A.C.; Humbel, B.M.; Van der Krift, T.P.; Boekhout, T. Field-emission scanning electron microscopy of the internal cellular organization of fungi. *Scanning* **2000**, 22, 295-303.

General discussion

Chapter 8

INTRODUCTION

The overall goal of this research project was to study the application possibilities of protein fibrils in food systems. A broad approach was used during this research, which expanded over the fields of food chemistry, physics and processing. Important results were obtained related to the *preparation*, *mechanism* and *application* of protein fibrils. In addition, requirements for the application were formulated in terms of the mechanistic and preparational findings. Chemical characterization of the system led to more knowledge on the mechanism, and as a result, a new processing method was developed. Regarding the preparation, the effect of flow on the fibril formation could be explained by physical processes, which led to a better understanding of the relevant process conditions for the fibril formation. In the last part of the research project, a first step was made towards the application of these fibrils as ingredients in relevant food systems. By adding the fibrils to concentrated protein solutions, an enriched phase behaviour was found.

PREPARATION

Mixing and stirring were known methods to enhance the fibril growth.[1,2] Before this project, it was not clear how the flow influences the fibril growth. During this research, it was observed that shear flow resulted in an earlier nucleation (Chapter 2) of the fibril formation. This behaviour shows similarities with a crystallization process where the system is in a meta-stable state, and nucleation can be induced by a mechanical disturbance.[3-5]

The results described in Chapter 3 showed that the shear rate can be used as a process parameter to control the fibril growth. The effect of shear flow on the fibril growth was explained as follows. First of all, the supply rate of monomers to the fibril tips was higher due to the flow field applied. Secondly, initial weak bonds between the monomers in the fibrils are probably broken at high shear rates (above 337 s^{-1}). The nucleating effect of shear was not observed anymore for the experiments described in Chapter 3, because fibril growth also took place when shear flow was not applied. An explanation could be the use of different heating

devices. In Chapter 3, a titanium shearing device was used, while in Chapter 2 heating was performed in glass tubes.

At high fibril concentrations, the flow behaviour of the fibril solutions remained unchanged as a function of fibril concentration when shear flow was applied during the fibril formation (Chapter 3). A possible explanation for this observation could be arrangement of the fibrils into so-called mesophasic domains that are characterized by an orientational ordering of the fibrils. For further investigation on this effect, it would be useful to analyze the fibril solution during the heat and shear treatment.

MECHANISM

Peptides in fibrils derived from β-lactoglobulin

At the start of this project, the general picture was that protein fibrils consist of intact protein monomers. However, it was not clear why a heat treatment at acidic pH led to the formation of fibrils from β-lactoglobulin. In addition, it was not clear why not all protein could be converted into the fibrils. Bolder et al.[6] explained the limited conversion of proteins into fibrils by considering the protein hydrolysis, because this hydrolysis reaction would reduce the availability of intact β-lactoglobulin to aggregate into fibrils. The results described in Chapter 5 shed a different light on the limited conversion and explain why a heat treatment at pH 2 leads to fibril formation.

Chapter 5 shows that the fibrils are composed of peptides derived from β-lactoglobulin. The hydrolysis into peptides takes place during heating at low pH and is very specific; peptide bonds before or after aspartic acid residues are preferably hydrolyzed.[7,8] The limited conversion of proteinaceous material into fibrils can be explained by the fact that not the whole sequence of β-lactoglobulin was found in the peptides present in the fibrils. The fibril formation will only start when a critical aggregation concentration of peptides is reached by hydrolysis, which explains why a lag time is generally observed during the process of fibril formation (see Figure 1 of Chapter 1).

Based on the results of Chapter 5, a new processing method was developed to

obtain fibril forming peptides which does not require a heat treatment at low pH. An enzyme (AspN endoproteinase) was used to cleave peptide bonds at the same position as the bonds cleaved during the heat induced acid hydrolysis. The enzymatic hydrolysis was performed at pH 8 and 37 °C. Those conditions did not lead to fibrillar aggregates, but only to random aggregates. When the pH was lowered to 2, fibrillar aggregates were observed. Obviously, acidic conditions were necessary to allow the peptides to arrange into fibrils. Optimization of this enzymatic method still needs to be done. Fibril forming peptides were possibly also present in these random aggregates, leading to a lower availability of peptides to be used for fibril formation.

The presence of certain peptides in the fibrils was related to their capacity to form β-sheets, their hydrophobicity, their low charge and charge distribution. In Chapter 5, it was shown that a positive charge of the peptides also plays a role, because fibrils were only obtained from the peptides at low pH values when the peptides are positively charged. Further research is necessary to observe which physical interactions are the most important ones for the fibril formation. To study these interactions, a more quantitative study on the peptides present in the fibrils will be necessary, for instance: HPLC in combination with mass spectrometry, and synthesis of the different peptide fragments.

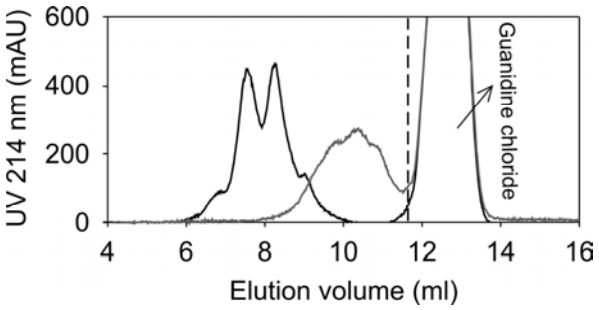

Figure 1. *HP-SEC elution profiles of soy glycinin unheated (black) and after heating for 20 h at pH 2 (grey). During the heat treatment, fibrils were formed. The elution was performed under fibril dissociation conditions (see Material and Methods section of Chapter 5).*

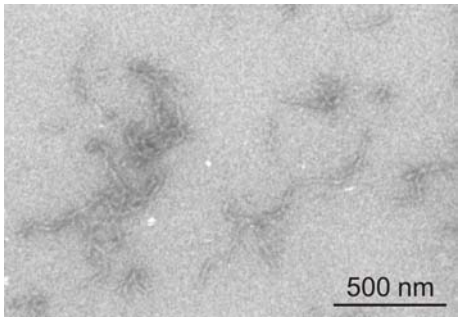

***Figure 2**. Fibrillar aggregates of the potato protein patatin, prepared by prolonged heating at pH 2.*

Peptides in fibrils from other proteins

The hydrolysis reaction that takes place during the heat treatment at low pH can play a role during the fibril formation of other proteins than β-lactoglobulin. For lysozyme, it was already shown that hydrolysis took places when the protein was heated at acidic pH. Lysozyme fibrils were found to consist of peptides and so called nicked proteins.[9-11] In Chapter 4, it was observed that fibrils could be obtained from soy proteins by heating at acidic pH. The soy protein glycinin is almost completely hydrolyzed into peptides during the heat treatment at pH 2. Figure 1 shows the HP-SEC elution profiles of soy glycinin before and after prolonged heating (20 h, 85 °C) at pH 2. The heated material eluted later than the unheated soy glycinin solution, which shows that the hydrolysis reaction took place. Since fibril dissociating conditions were applied during HP-SEC analysis, it seems that also the fibrils from soy protein were composed of peptides.

During this research, fibrils were also obtained from the potato protein patatin using the same treatment. These fibrils were shorter (~500 nm) and more flexible than fibrils formed from soy protein or β-lactoglobulin (Figure 2). The morphology of the patatin fibrils shows similarities with fibrils from BSA[12] and ovalbumin.[13] The reasons why different proteins form different fibril morphologies is not clarified yet. Studying the protein material present in protein fibrils from other protein sources could form a basis for the explanation of the different fibril morphologies.

APPLICATION

Structural properties

Previous research showed that protein fibril solutions have a high (zero-shear) viscosity and are shear thinning,[1] and that these solutions form gels on a weight efficient basis using Ca^{2+} to cross-link the fibrils.[14,15] However, it was not known how the fibrils behaved in the presence of other (food) ingredients. The results described in Chapter 7 show that adding fibrils to concentrated WPI solutions induced shear thinning behaviour, and increased the viscosity and gel strength. The fibrils can thus be used as thickening and gelling agents. Other phenomena that were observed were shear thickening and phase separation. The use of shear flow during gel formation resulted in more porous gels (observed with scanning electron microscopy). A higher porosity and phase separation can influence the fracture properties of high protein foods.

The results of previous studies on other structural ingredients (xanthan gum,[16] gelatin,[17] and whey protein polymers[18]) in combination with WPI and the results of our study show that different types of networks (e.g. phase separated, mixed, bi-continuous) can be obtained from WPI-dispersions when mixed with different structuring agents. Furthermore, the properties of the system are highly depended on the conditions applied (pH, concentration, shear rate). It is a challenge to explain all phenomena observed, but one way to start will be to thoroughly analyze the phase behaviour (also under flow).

Fibrous macrostructures

Protein fibrils could be used as nanoscale fibres in new meat-replacement products. Preparing these fibrils from plant proteins instead of animal based proteins will contribute to the development of more sustainable products. During this research, it was shown that protein fibrils could be obtained from soy and potato proteins. Other protein sources that could be studied for their capability to form fibrils are proteins from rapeseed or peas.

Although anisotropic macrostructures were not obtained in Chapter 7, it might be possible to obtain fibrous macrostructures using this system (fibrils in a

concentrated WPI solution). The shear thinning and shear thickening behaviour that was observed indicates that the structure of the fibril/ WPI dispersions can be modified using flow. This suggests that by optimizing the process conditions (pH, protein concentration, shear rate, heating time), fibrous macrostructures can be obtained using this system. For concentrated caseinate dispersions, it was already shown that the formation of anisotropic macrostructures was related to the susceptibility of the dispersion to flow.[19]

At high fibril concentrations and low pH, the fibrils arrange themselves into birefringent mesophasic domains (see Chapter 3). Fixation of the fibrils when they are arranged into these domains will also result in anisotropic macrostructures. Most cross-linking methods (e.g. adding calcium or using enzymes) can only be used at higher pH values. However, the results of Chapter 7 showed that upon increasing the pH, the fibrils become randomly clustered and not well-arranged in mesophasic domains. Therefore, a method needs to be sought to cross-link these fibrils at low pH. Alternatively, one can also think of adding another biopolymer that forms a gel around the fibrils when they are arranged into mesophasic domains.

REFERENCES

1. Bolder, S.G.; Sagis, L.M.C.; Venema, P.; Van der Linden, E. Effect of stirring and seeding on whey protein fibril formation. *Journal of Agricultural and Food Chemistry* **2007**, 55, 5661-5669.

2. Nielsen, L.; Khurana, R.; Coats, A.; Frokjear, S.; Brange, J.; Vyas, S.; Uversky, V.N.; Fink, A.L. Effect of environmental factors on the kinetics of insulin fibril formation: elucidation of the molecular mechanism. *Biochemistry* **2001**, 40, 6036-6046.

3. Young, S.W. Mechanical stimulus to crystallization in supercooled liquids. *Journal of the American Chemical Society* **1911**, 33, 148.

4. Mullin, J.W.; Raven, K.D. Influence of mechanical agitation on the nucleation of some aqueous salt solutions. *Nature* **1962**, 195, 35-38.

5. Mullin, J.W.; Raven, K.D. Nucleation in agitated solutions. *Nature* **1961**, 190, 251.

6. Bolder, S.G.; Vasbinder, A.J.; Sagis, L.M.C.; Van der Linden, E. Heat-induced whey protein isolate fibrils: conversion, hydrolysis and disulphide bond formation.

International Dairy Journal **2006**, 17, 846-853.

7. Inglis, A.S. Cleavage at aspartic acid. *Methods in Enzymology* **1983**, 91, 324-332.

8. Schultz, J. Cleavage at aspartic acid. *Methods in Enzymology* **1967**, 11, 255-263.

9. Frare, E.; Polverino de Laureto, P.; Zurdo, J.; Dobson, C.M.; Fontana, A. A highly amyloidogenic region of hen lysozyme. *Journal of Molecular Biology* **2004**, 340, 1153-1165.

10. Krebs, M.R.H.; Wilkins, D.K.; Chung, E.W.; Pitkeathly, M.C.; Chamberlain, A. K.; Zurdo, J.; Robinson, C.V.; Dobson, C.M. Formation and seeding of amyloid fibrils from wild-type hen lysozyme and a peptide fragment from the beta-domain. *Journal of Molecular Biology* **2000**, 300, 541-549.

11. Mishra, R.; Sorgjerd, K.; Nystrom, S.; Nordigarden, A.; Yu, Y.C.; Hammarstrom, P. Lysozyme amyloidogenesis is accelerated by specific nicking and fragmentation but decelerated by intact protein binding and conversion. *Journal of Molecular Biology* **2007**, 366, 1029-1044.

12. Veerman, C.; Sagis, L.M.C.; Heck, J.; Van der Linden, E. Mesostructure of fibrillar bovine serum albumin gels. *International Journal of Biological Macromolecules* **2003**, 31, 139-146.

13. Veerman, C.; De Schiffart, G.; Sagis, L.M.C.; Van der Linden, E. Irreversible self-assembly of ovalbumin into fibrils and the resulting network rheology. *International Journal of Biological Macromolecules* **2003**, 33, 121-127.

14. Veerman, C.; Baptist, H.; Sagis, L.M.C.; Van der Linden, E. A new multistep Ca^{2+}-induced cold gelation process for β-lactoglobulin. *Journal of Agricultural and Food Chemistry* **2003**, 51, 3880-3885.

15. Bolder, S.G.; Hendrickx, H.; Sagis, L.M.C.; Van der Linden, E. Ca^{2+}-induced cold-set gelation of whey protein isolate fibrils. *Applied Rheology* **2006**, 16, 258-264.

16. Bryant, C.M.; McClements, D.J. Influence of xanthan gum on physical characteristics of heat-denatured whey protein solutions and gels. *Food Hydrocolloids* **2000**, 14, 383-390.

17. Walkenström, P.; Hermansson, A.M. Fine-stranded mixed gels of whey protein and gelatin. *Food Hydrocolloids* **1996**, 10, 51-62.

18. Vardhanabhuti, B.; Foegeding, E.A.; McGuffey, M.K.; Daubert, C.R.; Swaisgood, H.E. Gelation properties of dispersions containing polymerized and native whey protein isolate. *Food Hydrocolloids* **2001**, 15, 165-175.

19. Manski, J.M.; Van Riemsdijk, L.E.; Van der Goot, A.J.; Boom, R.M. Importance of intrinsic properties of dense caseinate dispersions for structure formation. *Biomacromolecules* **2007**, 8, 3540-3547.

Summary

Protein fibrils are anisotropic aggregates with a length in the order of 1 μm and a diameter of a few nanometers. These dimensions make these fibrils interesting to be used as food ingredients (e.g. high protein foods, meat replacement products, and low-calorie products) to increase the viscosity and gel strength, to induce shear thinning behaviour, or to modify the structure. As protein sources, β-lactoglobulin and WPI were mainly used during this study, because β-lactoglobulin has been the subject of many previous studies, and WPI is an industrially relevant protein mixture. Fibrils from β-lactoglobulin or whey protein isolate (WPI) can be obtained by heating the protein at acidic pH and low ionic strength. The overall goal of this project was to study the application possibilities of protein fibrils in food systems by obtaining more knowledge about the preparation and mechanism of fibril formation, and studying the behaviour of these fibrils in the presence of other proteins. Therefore, the research can be divided into different objectives, related to *preparation*, *mechanism* and *application*.

Preparation

The first objective was to gain more insight into the preparation of fibrils, and more specifically, the effect of shear flow on the fibril formation. **Chapter 2** describes the effect of shear flow on the nucleation of the fibril formation of β-lactoglobulin. After a short heat treatment, fibril growth could be initiated at room temperature by using either continuous shear flow or short shear pulses, while no fibril growth occurred if no flow was applied. This behaviour shows similarities with a crystallization process in which the system is in a meta-stable state and nucleation can be induced by a mechanical disturbance.

In **Chapter 3**, shear flow was applied during heating to observe the effect of shear flow on the fibril growth of WPI fibrils. This study showed that shear flow can result in a higher fibril concentration, and that the shear rate can be used as a process parameter to control the fibril properties. The fibril concentration initially

increased as a function of the shear rate, which could be explained by an enhanced supply rate of monomers towards the fibril tips. At higher shear rates, the fibril concentration decreased as a function of shear rate, which could be caused by breakage of non-mature bonds inside the fibrils. By applying shear flow, higher fibril concentrations could be established, but these high fibril concentrations did not automatically result in a different flow behaviour. Above a critical fibril concentration, the flow behaviour remained unchanged as a function of fibril concentration, which could be caused by the presence of mesophasic domains of fibrils.

Preparing these fibrils from proteins that are plant based instead of animal based contributes to the development of more sustainable products. Therefore, the ability of soy proteins to aggregate into long, thin fibrils was studied, and the results are presented in **Chapter 4**. Fibrils could be formed from soy protein by heating the protein at acidic pH and low ionic strength. Many physical properties (length, thickness, rigidity, flow behaviour) of soy protein fibrils were similar to fibrils of β-lactoglobulin and WPI. However, unlike WPI/β-lactoglobulin fibrils, soy protein fibrils were branched, and the degree of branching was different for the different soy protein isolates used.

Mechanism

The proteinaceous material present in β-lactoglobulin fibrils was invesigated to explain the necessity of the heat treatment at pH 2, and the limited conversion of β-lactoglobulin into fibrils. The results of this study are shown in **Chapter 5**. During prolonged heating at pH 2, β-lactoglobulin was hydrolyzed into peptides. The hydrolysis was found to be highly specific; mainly peptide bonds before or after aspartic acid residues were cleaved. The fibrils are composed of these peptides, and not of intact β-lactoglobulin. The limited conversion of protein into fibrils is due to the fact that not all peptides are present in the fibrils. One region of the sequence of β-lactoglobulin is completely absent inside the fibrils. This region contains many amino-acid residues that are positively charged at low pH. Explanations for the frequent presence of other regions of the protein in the fibrils

can be found in the capacity to form β-sheets, hydrophobicity, low charge, and charge distribution.

Based on the results of the study shown in Chapter 5, an alternative route was developed to obtain β-lactoglobulin fibrils (**Chapter 6**). First, β-lactoglobulin was hydrolyzed into peptides with the enzyme AspN endoproteinase, which cleaves the peptide bonds N-terminal to aspartic acid residues. During this hydrolysis, random aggregates were formed. After hydrolysis, the pH was lowered to 2, and besides random aggregates, long fibrillar aggregates were found to be present at this pH. This study confirms that the fibrils are composed of peptides. Furthermore, a heat treatment at pH 2, which is a rather extreme processing condition, is not necessary to obtain fibril forming peptides. Nevertheless, this route needs to be optimized, because non-fibrillar aggregates were also formed.

Application

In **Chapter 7**, the application possibilities of protein fibrils were studied in order to modify structural properties of concentrated WPI solutions. The first step was to study the properties of WPI fibrils at different pH values. The properties were highly pH dependent; at low pH values, long non-clustered fibrils were observed, while upon increasing the pH, clusters were present. The next step was to study the effect of fibrils on the properties of WPI solutions. Rheological measurements showed that the presence of fibrils resulted in an increase in viscosity, gel strength and induced shear thinning behaviour. These results show that the fibrils can be used as gelling and thickening agents. Other observations were that adding fibrils could sometimes result in shear thickening behaviour and phase separation, and in combination with shear flow, more porous structures could be obtained. Phase separation and porosity could be used to modify the fracture properties of high protein foods. However, the properties of the system are highly depended on the conditions (e.g. pH, protein concentration, and shear flow) used, which makes this system rather complex, and makes it difficult to understand all phenomena observed.

Based on the previous chapters, several topics for further research were discussed in Chapter 8 (‘General Discussion’). The main topics were the formation of fibrous macrostructures using protein fibrils, characterization of the proteinacous material present in fibrils from other proteins, and obtaining fibrils from other plant proteins (e.g. peas and rapeseed).

Samenvatting

Eiwitfibrillen zijn aggregaten van globulaire eiwitten met een lengte van ongeveer 1 micrometer en een dikte van een paar nanometer. Deze afmetingen maken deze fibrillen interessant om gebruikt te worden als ingrediënt in levensmiddelen, bijvoorbeeld voor producten met een hoog eiwitgehalte, vleesvervangers en light-producten. Hun aanwezigheid in levensmiddelen kan zorgen voor een hogere viscositeit en een sterkere gel. Verder kunnen ze pseudo-plastisch gedrag (daling van viscositeit onder stroming) induceren en de macrostructuur veranderen. Tijdens dit onderzoek zijn met name β-lactoglobuline (één van de belangrijkste wei-eiwitten) en wei-eiwit isolaat (WPI) als eiwitbronnen gebruikt. Over fibrillen van β-lactoglobuline is al veel bekend, terwijl WPI een relevant eiwitmengsel is voor de levensmiddelenindustrie. Fibrillen van β-lactoglobuline en WPI kunnen gemaakt worden door de eiwitten te verhitten in een zure oplossing.
Het doel van dit promotieonderzoek was het onderzoeken van de toepassingsmogelijkheden van eiwitfibrillen in levensmiddelen. Hiervoor was meer kennis nodig over het maken van fibrillen (productie) en het mechanisme van de fibrilvorming. Daarnaast is het gedrag van deze fibrillen in aanwezigheid van andere eiwitten bestudeerd. Dit onderzoek kan dus onderverdeeld worden in drie aspecten: de *productie*, het *mechanisme* en de *toepassing*.

Productie

Het eerste subdoel was om meer inzicht te verkrijgen in de productie van fibrillen. In dit deel van het promotieonderzoek is met name het effect van afschuifstroming op de fibrilvorming bekeken. In **Hoofdstuk 2** wordt het effect van afschuifstroming op de nucleatie van de fibrilvorming van β-lactoglobuline beschreven. Hieruit bleek dat na een korte verhittingsstap de fibrilvorming geïnitieerd kan worden door het toepassen van afschuifstroming, zowel continu als in de vorm van korte pulsen. Het systeem vertoont hierdoor vergelijkbaar gedrag met een kristallisatieproces; het systeem bevindt zich in een metastabiele toestand

en de nucleatie van het proces vindt plaats door een mechanische verstoring, zoals stroming.

In **Hoofdstuk 3** is het effect van afschuifstroming tijdens verhitting onderzocht. Hiervoor is een speciale 'shear cell' ontwikkeld waarmee afschuifstroming en verhitting tegelijkertijd toegepast konden worden. Het gebruik van afschuifstroming tijdens de fibrilvorming beïnvloedde de fibrileigenschappen. Bij lage afschuifsnelheden steeg de fibrilconcentratie als functie van afschuifsnelheid. Deze stijging kan verklaard worden door een sneller transport van eiwitten naar de fibriluiteinden. De fibrilconcentratie daalde wanneer de afschuifsnelheid verder verhoogd werd. Deze daling wordt waarschijnlijk veroorzaakt door het verbreken van bindingen tussen de eiwitten in de fibrillen, die in het begin nog zwak zijn. Een hogere fibrilconcentratie resulteerde niet automatisch in een ander stromingsgedrag. Boven een bepaalde fibrilconcentratie was het stromingsgedrag van de verkregen vloeistof namelijk hetzelfde terwijl de fibrilconcentratie varieerde. Waarschijnlijk werd dit veroorzaakt door ordening van de fibrillen in mesoscopische domeinen.

Het maken van soortgelijke fibrillen van plantaardig in plaats van dierlijk eiwit draagt bij aan de ontwikkeling van meer duurzame producten. **Hoofdstuk 4** laat zien dat het mogelijk is om fibrillen van soja-eiwit te maken door verhitting in een zure oplossing. Veel fysische eigenschappen van deze fibrillen (zoals de lengte, dikte, rigiditeit en het gedrag onder stroming) waren vergelijkbaar met de eigenschappen van fibrillen van β-lactoglobuline en wei-eiwit. Er waren echter ook verschillen. In tegenstelling tot fibrillen van β-lactoglobuline en wei-eiwit waren de fibrillen van soja-eiwit vertakt en de mate van vertakking verschilde wanneer er een ander soja-eiwit isolaat gebruikt werd.

Mechanisme

De samenstelling van de fibrillen van β-lactoglobuline is onderzocht om te verklaren waarom verhitting in een zure oplossing tot fibrilvorming leidt en waarom er maar een beperkte hoeveelheid eiwitmateriaal ingebouwd wordt in de fibrillen. De resultaten van dit onderzoek staan beschreven in **Hoofdstuk 5**. De verhittingstap bij lage pH blijkt te zorgen voor een gedeeltelijke hydrolyse van het

eiwit. Hierdoor ontstaan eiwitfragmenten (peptiden). De fibrillen blijken te bestaan uit deze peptiden en niet uit intact β-lactoglobuline. De hydrolyse is zeer specifiek, want er worden voornamelijk peptide-bindingen verbroken voor of na het aminozuur asparaginezuur. Een deel van de sequentie van β-lactoglobuline was afwezig in de peptiden die in de fibrillen zaten, hetgeen verklaart waarom niet al het eiwitmateriaal ingebouwd wordt in de fibrillen. Dit deel van de sequentie bevat veel aminozuren die positief geladen zijn bij lage pH. Andere delen van de sequentie van β-lactoglobuline waren wel vaak aanwezig in de fibrillen. Hun aanwezigheid in de fibrillen kan verklaard worden door hun capaciteit om β-sheets te vormen, de hydrophobiciteit, de lage ladingsdichtheid en de ladingsverdeling.
Op basis van de resultaten van Hoofdstuk 5 is een alternatieve methode ontwikkeld om fibrillen van β-lactoglobuline te maken (**Hoofdstuk 6**). Als eerste stap werd β-lactoglobuline bij pH 8 gehydrolyseerd in peptiden met het enzym Asp-N endoproteinase. Dit enzym knipt de peptidebindingen tussen asparaginezuur en ieder ander aminozuur. Tijdens de hydrolyse bij pH 8 werden niet-fibrillaire aggregaten gevormd. Na de hydrolyse werd de pH verlaagd naar 2, waardoor naast de niet-fibrillaire aggregaten ook lange fibrillen gevormd werden. Dit onderzoek bevestigt dat de fibrillen inderdaad bestaan uit peptiden. Verder blijkt hieruit dat extreme procesomstandigheden als een hittebehandeling in zure oplossing niet noodzakelijk zijn om de fibrilvormende peptiden te verkrijgen. Desalniettemin zal deze enzymatische methode verder geoptimaliseerd moeten worden, omdat naast fibrillen ook andere aggregaten gevormd worden.

Toepassing

In **Hoofdstuk 7** is onderzocht hoe de eiwitfibrillen de structurele eigenschappen van geconcentreerde WPI oplossingen kunnen veranderen. Een eerste stap in dit onderzoek was het bestuderen van de eigenschappen van de eiwitfibrillen bij verschillende pH waarden. Bij lage pH werden lange, losse fibrillen waargenomen, terwijl bij hogere pH (5-7) clusters aanwezig waren. Vervolgens werd het effect van toevoeging van de fibrillen aan WPI oplossingen onderzocht. Uit reologische metingen bleek dat de aanwezigheid van de fibrillen in geconcentreerde WPI oplossingen zorgde voor een stijging van de viscositeit en gelsterkte. Deze

resultaten geven aan dat de fibrillen gebruikt kunnen worden als verdikkings- of geleringsmiddel. Daarnaast zorgde de aanwezigheid van de fibrillen ook voor fasescheiding en pseudo-plastisch en dilitant gedrag. Het toepassen van afschuifstroming tijdens de gelering zorgde voor een meer poreuze structuur van het gel-netwerk. Fasescheiding en een hogere porositeit kunnen het breukgedrag beïnvloeden van producten. De eigenschappen van dit systeem bleken echter wel sterk afhankelijk van de opgelegde condities (pH, eiwitconcentratie en stroming).

Op basis van de eerdere hoofdstukken is in **Hoofdstuk 8** (‘General Discussion’) een aantal onderwerpen voor verder onderzoek besproken. De belangrijkste onderwerpen zijn het gebruik van eiwitfibrillen om vezelachtige macrostructuren te maken, karakterisering van de samenstelling van fibrillen van andere eiwitten, en het maken van fibrillen van andere planteneiwitten (zoals eiwitten van erwten en koolzaad).

Publications

Akkermans, C.; Van der Goot, A.J.; Venema, P.; Van der Linden, E.; Boom, R.M. Properties of protein fibrils in whey protein isolate solutions: microstructure, flow behaviour and gelation. *Submitted for publication.*

Akkermans, C.; Venema, P.; Van der Goot, A.J.; Boom, R.M.; Van der Linden, E. Enzyme induced formation of β-lactoglobulin fibrils by AspN endoproteinase. *Submitted for publication*.

Van der Goot, A.J.; Peighambardoust, S.H.; Akkermans, C.; Manski, J.M. Creation of novel structures in food materials: the role of well-defined shear flow. *Food Biophysics* **2008**, doi:10.1007/s11483-008-9081-8.

Akkermans, C.; Venema, P.; Van der Goot, A.J.; Gruppen, H.; Bakx, E.J.; Boom, R.M.; Van der Linden, E. Peptides are building blocks of heat induced fibrillar protein aggregates of β-lactoglobulin formed at pH 2. *Biomacromolecules* **2008**, doi:10.1021/bm7014224.

Akkermans, C.; Van der Goot, A.J.; Venema, P.; Van der Linden, E.; Boom, R.M. Formation of fibrillar whey protein aggregates: influence of heat- and shear treatment and resulting rheology. *Food Hydrocolloids* **2007**, doi:10.1016/j.foodhyd.2007.07.001.

Akkermans, C.; Van der Goot, A.J.; Venema, P.; Gruppen, H.; Vereijken, J.M.; Van der Linden, E.; Boom, R.M. Micrometer-sized fibrillar protein aggregates from soy glycinin and soy protein isolate. *Journal of Agricultural and Food Chemistry* **2007**, 55, 9877-9882.

Akkermans, C.; Venema, P.; Rogers, S.S.; Van der Goot, A.J.; Boom, R.M.; Van der Linden, E. Shear pulses nucleate fibril aggregation. *Food Biophyisics* **2006**, 1, 144-150.

Van den Einde, R.M.; Akkermans, C.; Van der Goot, A.J.; Boom, R.M. Molecular breakdown of corn starch by thermal and mechanical effects. *Carbohydrate Polymers* **2004**, 56, 415-422.

Proceedings
Akkermans, C.; Venema, P.; Rogers, S.S.; Van der Goot, A.J.; Boom, R.M.; Van der Linden, E. Formation of β-lactoglobulin fibrils at low temperature due to a short shear treatment, *Proceedings 4th International Symposium on Food Rheology and Structure (ISFRS)*, **2006**, 235-237.

Patent
Akkermans et al., Composition and fibrils from whey protein peptides. **2007**, 2001123.

The research presented in this PhD dissertation was financially supported by the Graduate School VLAG, and the Dutch research program MicroNed.